PLOS ONE

RESEARCH ARTICLE

Pancreatic Beta Cell G-Protein Coupled Receptors and Second Messenger Interactions: A Systems Biology Computational Analysis

Leonid E. Fridlyand*, Louis H. Philipson

Departments of Medicine and Pediatrics, the Kovler Diabetes Center, The University of Chicago, Chicago, IL, 60637, United States of America

* lfridlia@medicine.bsd.uchicago.edu

OPEN ACCESS

Citation: Fridlyand LE, Philipson LH (2016) Pancreatic Beta Cell G-Protein Coupled Receptors and Second Messenger Interactions: A Systems Biology Computational Analysis. PLoS ONE 11(5): e0152869. doi:10.1371/journal.pone.0152869

Editor: Tao Cai, NIDCR/NIH, UNITED STATES

Received: December 4, 2015

Accepted: March 21, 2016

Published: May 3, 2016

Data Availability Statement: All relevant data are within the paper.

Funding: This work was supported by grants from the National Institutes of Health to LHP (DK063493 and DK092616), and by University of Chicago Diabetes Research and Training Center funding from the NIH (DK020595) to LHP. The Virtual Cell is supported by NIH Grant Number P41 GM103313 from the National Institute for General Medical Sciences.

Competing Interests: The authors have declared that no competing interests exist.

Abstract

Insulin secretory in pancreatic beta-cells responses to nutrient stimuli and hormonal modulators include multiple messengers and signaling pathways with complex interdependencies. Here we present a computational model that incorporates recent data on glucose metabolism, plasma membrane potential, G-protein-coupled-receptors (GPCR), cytoplasmic and endoplasmic reticulum calcium dynamics, cAMP and phospholipase C pathways that regulate interactions between second messengers in pancreatic beta-cells. The values of key model parameters were inferred from published experimental data. The model gives a reasonable fit to important aspects of experimentally measured metabolic and second messenger concentrations and provides a framework for analyzing the role of metabolic, hormones and neurotransmitters changes on insulin secretion. Our analysis of the dynamic data provides support for the hypothesis that activation of Ca^{2+}-dependent adenylyl cyclases play a critical role in modulating the effects of glucagon-like peptide 1 (GLP-1), glucose-dependent insulinotropic polypeptide (GIP) and catecholamines. The regulatory properties of adenylyl cyclase isoforms determine fluctuations in cytoplasmic cAMP concentration and reveal a synergistic action of glucose, GLP-1 and GIP on insulin secretion. On the other hand, the regulatory properties of phospholipase C isoforms determine the interaction of glucose, acetylcholine and free fatty acids (FFA) (that act through the FFA receptors) on insulin secretion. We found that a combination of GPCR agonists activating different messenger pathways can stimulate insulin secretion more effectively than a combination of GPCR agonists for a single pathway. This analysis also suggests that the activators of GLP-1, GIP and FFA receptors may have a relatively low risk of hypoglycemia in fasting conditions whereas an activator of muscarinic receptors can increase this risk. This computational analysis demonstrates that study of second messenger pathway interactions will improve understanding of critical regulatory sites, how different GPCRs interact and pharmacological targets for modulating insulin secretion in type 2 diabetes.

Abbreviations: AC, adenylyl cyclase; AC_P, PM bound AC; AC_c, soluble cytoplasmic AC; AdR, adrenergic receptors; ER, endoplasmic reticulum; CAM, calmodulin; CM, computational model; CRA, Ca^{2+} release-activated nonselective cation channel; $[Ca^{2+}]_c$, cytoplasmic free Ca^{2+} concentration; $[Ca^{2+}]_{ER}$, Ca^{2+} concentration inside of endoplasmic reticulum; DAG, diacylglycerol; Epac, guanyl exchange protein directly activated by cAMP; ER, endoplasmic reticulum; GIP, glucose-dependent insulinotropic polypeptide; GLP-1, glucagon-like peptide-1; GIPR, glucose-dependent insulinotropic polypeptide receptor; GLP-1R, glucagon-like peptide-1 receptor; GPCR, G-protein-coupled receptor; GPR40, G-protein-coupled receptor 40; GSIS, glucose-stimulated insulin secretion; FFA, free fatty acid; FFAR1/GPR40, free fatty acid receptor; IP_3, inositol 1,4,5-trisphosphate; IP_3R, IP_3 receptor; K_{ATP} channels, ATP-sensitive K^+ channels; MR, muscarinic acetylcholine receptor; NALCN, nonselective cation channels; PDE, phosphodiesterase; PI, phosphatidylinositol; PIP, phosphatidylinositol 4-phosphate; PIP_2, phosphatidylinositol 4,5-bisphosphate; PKA, protein kinase A; PKD, protein kinase D; PKC, protein kinase C; PLC, phospholipase C; PLC_P, G-protein-coupled PLC localized on PM; PLC_c, cytoplasmic PLC; PM, plasma membrane; P4P, phosphatidylinositol-4-phosphate; SERCA, sarco-(endo)plasmic reticulum Ca^{2+}-ATPase; SOC, store operated-current; T2D, type 2 diabetes; VGCC, voltage-gated Ca^{2+} channel; V_p, plasma membrane potential.

Introduction

Insulin release from the pancreatic β-cells must respond acutely to meet the insulin demands of the organism. However, in type 2 diabetes (T2D) pancreatic β-cells fail to compensate for an increase in blood glucose concentration with sufficient insulin secretion, leading to progressive hyperglycemia [1]. T2D is a chronic metabolic illness with dramatic increasing medical and financial costs but prevention and effective treatments remain suboptimal. Numerous studies have been published on the regulation of β-cell function. A general reaction network diagram for the β-cell is shown in Fig 1.

Glucose is the major physiologic regulator of insulin release. Glucose-stimulated insulin secretion (GSIS) includes an increase in ATP/ADP ratio leading to a closure of ATP sensitive potassium (K_{ATP}) channels, plasma membrane (PM) depolarization, opening of voltage-gated calcium channels(VGCC) with corresponding calcium influx and an increased cytosolic Ca^{2+}. The rise in intracellular free calcium concentration ($[Ca^{2+}]_c$) is an important signal in the initiation of β-cell insulin secretion [2–4]. The β-cell has numerous G protein coupled receptors (GPCRs) that can activate or inhibit β-cell insulin secretion [5]. Therefore a better understanding of how activation of GPCRs regulate β-cell function might illuminate approaches to help β-cell compensation and lead to better approaches to treatment of T2D.

Additional regulation of insulin release is provided by circulating metabolic secretagogues and by stimuli such as hormones and neurotransmitters. This permits close regulation of islet hormone secretion. For example, non-metabolic stimulation of insulin release occurs during the first phase of feeding and precedes any increase in blood glucose (termed the "cephalic phase"). This is largely mediated by the release of acetylcholine from nerves innervating pancreatic islets and the cholinergic stimulation of the muscarinic acetylcholine receptors [3, 6–8]. Incretin hormones released from gastrointestinal L-cells in response to food intake also stimulate insulin secretion [9]. On the other hand the neurotransmitters such as noradrenaline inhibit insulin secretion to increase glucose availability during times of stress [10]. These signals are mediated by a variety of GPCRs that have complimentary or antagonistic actions on insulin secretion [5, 11]. Interestingly, signaling networks must convert a large variety of extracellular stimuli onto a limited number of intracellular second messenger pathways. This includes intracellular free Ca^{2+} concentration and the two main signals of activated GPCRs: cyclic AMP (cAMP) on the one hand and inositol 1,4,5-trisphosphate (IP_3) and diacylglycerol (DAG) on the other [3, 12, 13]. Group of third pathways through adhesion class GPCR was also found in islets [14]. However, these pathways were only beginning to be studied in β-cells and there is not enough data to include them here. There is therefore considerable interest in understanding how GPCRs in β-cells integrate second messenger signaling.

Despite the recent increase in our knowledge of β-cell physiology and biochemistry, we still lack a coherent model of how second messengers and their interactions regulate β-cell secretion. The complex nature of the receptors and second messenger interactions makes it extremely difficult to understand how they are regulated and which parameters determine their dynamics. However, systems biology has emerged to provide a systematic approach to integrate the complexity of cellular signaling combining dynamic experiments with a computational biology approach [15–17]. Mathematical modeling has been used extensively and with great success to study metabolic and signaling networks [16, 18, 19]. This approach is useful for describing experimental data, deducing regulatory principles, and understanding complex dynamic phenomena such as oscillations. Integrated complex models of signal transduction pathways were published recently for synaptic input studies [20], mouse hepatocytes [21], cardiac myocytes [22] and liver metabolism [15]. However, this approach has not been as well

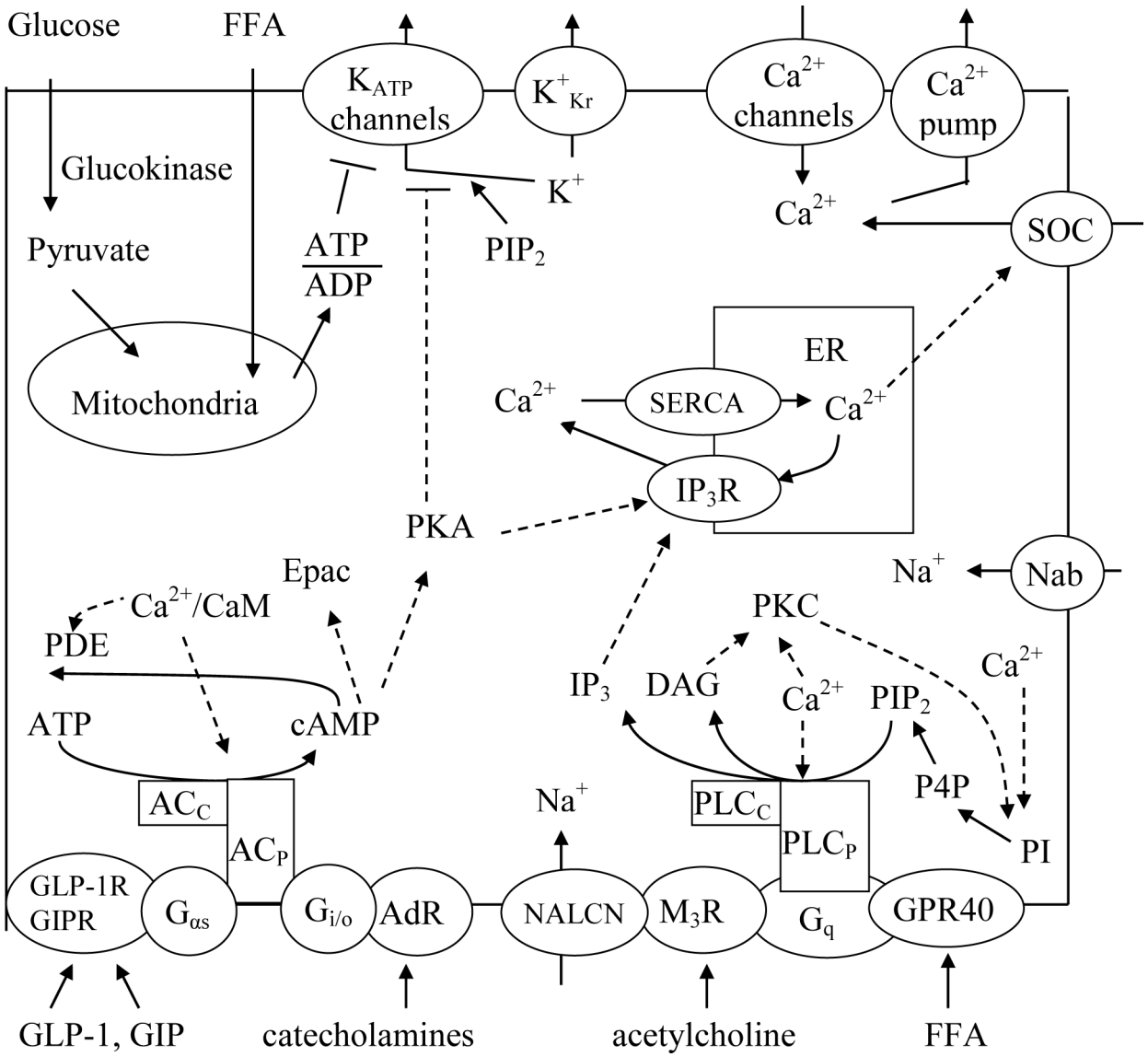

Fig 1. A schematic model of the main signaling pathways that regulate insulin secretion. Glucose enters the cell through its glucose transporter, and is phosphorylated and metabolized in the mitochondrion as well free fatty acids (FFA). Glucose and FFA metabolism leads to an increase in the ATP/ADP ratio, closure of the ATP-sensitive potassium (K_{ATP}) channels leading to plasma membrane (PM) depolarization that increase a calcium influx through the voltage-gated calcium channels and an increase in cytoplasmic Ca^{2+}. Other transmembrane channels can also regulate PM potential: K^+_{Kr} is the voltage gated K^+ channel, SOC is the store operating channels, Nab is the Na^+ background current, NALCN is the specific nonselective cation channel that can be modulated by acetylcholine through activation of M_3 muscarinic receptors (M_3R). Increase in cytoplasmic Ca^{2+} leads to the activation of several calcium dependent enzymes including adenylyl cyclase (AC) and phospholipase C (PLC). Phosphoinositides pathway: phosphatidylinositol-4-phosphate (P4P) is synthesized from phosphatidylinositol (PI) by phosphatidylinositol 4-kinases and its synthesis activates by PKC and Ca^{2+}. Phosphotidylinositol-4,5-bisphosphate (PIP_2) in turn is primarily formed from P4P by phosphatidylinositol-4-phosphate 5-kinase I. cAMP pathway: Ca^{2+}/CaM is Ca^{2+}-bound calmodulin, Synthesis and degradation of cAMP are catalyzed by adenylyl cyclase and phosphodiesterase (PDE), respectively. AC_c is the soluble AC, AC_P is the G-protein controlled AC on plasmalemma that can be activated by stimulatory $G_{\alpha s}$ type G-protein and Ca^{2+}/CaM and deactivated by inhibitory $G_{i/o}$ type G-protein. PDE activity can be enhanced by Ca^{2+}/CaM, cAMP activates protein kinase A (PKA) and exchange protein (Epac). The incretins glucagon-like peptide-1 (GLP-1) and glucose-dependent insulinotropic polypeptide (GIP) bind to their respective receptors (GLP-1R and GIPR), activate AC_P and increase intracellular levels of cAMP. Endogenous catecholamines adrenaline (epinephrine) and noradrenaline (norepinephrine) bound with G-protein-coupled α_{2A}-adrenergic receptors (AdR) on plasma membrane and inhibit AC_P. Phospholipase C (PLC) pathway. PLC_C is the cytoplasmic calcium activated PLC and PLC_P is plasma membrane bound PLC that can be activated by G_q type G-protein. Acetylcholine and FFA can bind to their respective receptors (M_3R and FFAR1/GPR40) expressed at the cell surface and trigger a Ga_q-mediated activation of PLC_P. PLC_C and PLC_P generate inositol-3-phosphate (IP_3) and diacylglycerol (DAG) by hydrolyzing membrane PIP_2. DAG activates protein kinase C (PKC). Endoplasmic

reticulum (ER): SERCA is the endoplasmic reticulum Ca^{2+}ATPase, IP_3R is the IP_3 receptor; that can be activated by IP_3 and PKA. Solid lines indicate fluxes, and dashed lines indicate inhibitory or stimulatory influences on currents or fluxes.

doi:10.1371/journal.pone.0152869.g001

developed for pancreatic β cells. Indeed only GLP-1 receptor coupled G-protein regulated cAMP signaling has been modeled previously [23–28].

We have previously focused on applying this mathematical modeling approach to mechanisms of glucose sensing of insulin secretion, Ca^{2+} and cAMP dynamics, electrophysiology events and exocytosis in pancreatic β-cells [23, 25, 29–34]. Here the objective is to evaluate the effect of interactions of metabolites, hormones, GPCRs and second messengers in regulation of insulin secretion in the pancreatic β-cell. For this aim we have constructed an integrated mathematical model of interaction of these components based on the framework developed in our previous models. In this work we focus on those cellular signaling pathways that appear essential for relatively rapid β-cell responses. We have estimated individual reaction rates and model parameters by fitting the theoretical reaction scheme to a variety of key experimental findings published to date in both β-cells and insulinoma cell lines. The model gives a reasonable fit to important aspects of experimentally measured metabolic, plasma membrane potential and second messenger concentrations and provides a framework for analyzing the role of metabolic, hormones and neurotransmitters changes on insulin secretion. This allowed us to refine the model to test hypotheses and conclusions about interacting pathways to design *in silico* experiments.

We analyzed interactions of clinically relevant GPCR agonists. We included those responding to the neurotransmitters acetylcholine and catecholamines with stimulation and inhibition of insulin secretion, respectively, to the incretin hormones GLP-1 and GIP with potentiation of GSIS, and the agonists for the free fatty acid (FFA) receptor (e.g., FFAR1/GPR40) and determined how combinations of different agonists affect second messenger dynamics in β-cell.

Defective regulation of messenger pathways clearly contributes to T2D in a variety of ways (see below). For this reason new anti-diabetic drugs in use and in development exploit several β-cell stimulating GPCR pathways in order to combat the growing health and economic costs of T2D. However, the effects of agonist combinations on the tightly coupled metabolic and signaling pathways of β-cells as well as on insulin secretion in diabetic states have not been carefully studied. We have attempted to analyze these processes and evaluate how particular impairments in the mechanisms of β-cell regulations sensing can lead to insulin release changes in T2D. Here we also examined the hypothesis that simultaneous stimulation of multiple signaling pathways is potentially is inhibitory for β-cell function and insulin secretion, but instead found that for the most part that combined stimulation can be synergistic.

Models and Methods

Here we will briefly outline the different parts of the regulatory mechanisms in β-cell. Fig 1 shows a schematic diagram of the biochemical steps, Ca^{2+} handling, channels, G-protein-coupled-receptors and mechanisms of second messenger regulation that were used for our mathematical modeling. Details of modeling are described below in the section "Computational model" (CM).

Metabolic regulation

The cellular metabolic mechanisms leading to insulin secretion in pancreatic β-cells are fairly well understood. Glucose-dependent signal transduction begins with uptake of glucose into β-cells via the glucose facilitative transporter. Glucose molecules are rapidly phosphorylated by

glucokinase and converted to pyruvate in the cytosol via the glycolytic pathway, and pyruvate and FFA are oxidized within the mitochondria producing ATP. Blocking K_{ATP} channels by an ATP/ADP-dependent mechanism initiates plasma membrane depolarization to the threshold potential for leading to Ca^{2+} influx through VGCCs and increases free cytosolic calcium concentration ($[Ca^{2+}]_c$). The rise in $[Ca^{2+}]_c$ is a key signal in the initiation of -cell insulin secretion (for reviews, see [2, 3, 32]). Other metabolic cofactors such as NADH or NAD(P)H have also been considered as possible coupling candidates as well [32, 35]. We used a simplified coarse-grained mathematical model of these mechanisms for pancreatic β-cells that is based on previous results [31, 32] (see CM).

The effects of FFAs on insulin secretion can also due to simply supplying fuel for cell metabolism [36] and we include this role for FFAs in our model as an increase in ATP/ADP ratio following FFA challenge (see CM). However, we do not consider this mechanism in detail here, because in physiological conditions FFA concentration in blood is low so that FFA acts mainly through FFA activated GPCRs [37] and only this signaling FFA effect is considered here.

Channels and regulation of plasma membrane potential

Plasma membrane potential (V_p) regulates Ca^{2+} influx through VGCCs in β-cells. On other hand V_p is regulated by ion channels and pumps. A schematic diagram of the principle β-cell channels (Fig 1) includes the more completely characterized channels and pumps. Additional actions such as activation of ion channels by second messengers also have been described [38, 39] and considered in our model (see CM).

β-cells display spike activity in response to glucose, an effect that has been modeled previously [29, 30, 40]. However, changes in PM potential and their corresponding voltage-dependent currents are considerably faster during spikes (milliseconds) than the changes in second messenger concentrations (minutes). For this reason, we excluded fast changes of PM potential here and for simplicity we did not describe ionic spike activity, modeling the time-dependent gating variables for currents as the stationary voltage dependences.

K^+ channels

We have included the ATP-sensitive potassium (K_{ATP}) channel and the voltage gated K^+ (K^+_{Kr}) channel. Messengers can affect K^+ channel dynamics in various ways. We have taken into account that protein kinase A (PKA) activation and a decrease in phosphatidylinositol 4,5-bisphosphate (PIP_2) concentration can lead to block of K_{ATP} channels [38, 41, 42] (see CM for details). Several studies suggest that voltage-gated K^+ channels might be also regulated by PIP_2 [43, 44]. However, $K_v2.1$ channels, that are the main voltage-gated K^+ channels in β-cells [2, 4] are not sensitive to PIP_2 depletion [43]. For this reason we excluded the influence of PIP_2 on voltage-gated K^+ channels.

Ca^{2+} channels and pumps

PM depolarization potentiates glucose-induced Ca^{2+} influx through voltage-gated Ca^{2+} channel (VDCCs). Depletion of intracellular Ca^{2+} stores in β-cells activates a special Ca^{2+}-release activated current (or store operating current (SOC)). While the detailed mechanism for coupling of ER Ca^{2+} store depletion with these PM channels activation is uncertain, it likely involves translocation of STIM1 and STIM2 proteins from the ER calcium stores to the PM where they interact with ORAI1 and related proteins associated with cation influx channels [45, 46]. Plasma membrane Ca^{2+} pumps provide an outward Ca^{2+} current.

Na^+ channels

Voltage-gated Na^+ current is likely inactivated in mouse β-cells [47] due to the relatively high resting V_p, so it is not considered, although it may play a role in human beta cells (see [30]). Non-selective PM cation channels permeable to Na^+ and Ca^{2+} have been described in pancreatic β-

cells, and the transient receptor potential ion channels were proposed for this role [48, 49]. Specific nonselective cation channels (NALCN) are expressed in pancreatic islets and can also be modulated by acetylcholine through activation of M_3 muscarinic receptors [39, 50]. We modeled these currents as Na^+ background current (I_{Nab}) through specific channels on PM (see CM).

Receptors, G-proteins and messenger regulation

Regulating signals from hormones and neurotransmitters are mediated by a variety of G-protein-coupled-receptors (GPCRs) that bind ligands from the extracellular space. GPCRs couple to stimulatory and inhibitory membrane-bound heterotrimeric G-proteins, mediating regulation of insulin secretion by the second messenger pathways. Activation of most GPCRs occurs in a similar time frame, but downstream effects may decay with a slower time course and may also effect gene expression.

Two main types of activation were found for different receptors: 1. Collision coupling, where a ligand binds to the free receptor and then the ligand-receptor complex "collides" with the free G-protein. 2. Pre-coupling, where stable receptor/G-protein complexes pre-exist and a ligand can bind with these complexes. There is accumulating evidence for both collision coupling and pre-coupling of GPCRs [51, 52].

Although there are many different GPCRs for the specific type of receptors there is a shared mechanism of activation. Following interaction with activated receptor the heterotrimeric G-proteins catalyze the exchange of GDP for GTP on the α-subunit. This event triggers conformational and/or dissociation events between the α-subunit and βγ-subunit. Both Gα-GDP and Gβγ subunits then activate (or inhibit) downstream signaling molecules (enzymes, kinases and ion channels) and thereby elicit cellular responses. The activation cycle is terminated by the Gα intrinsic GTPase activity which allows GTP hydrolysis and the reassociation of Gα-GDP with Gβγ subunits so to restore the inactive basal state. Then the G-protein system initiates a new cycle [53](see CM).

Desensitization is an important mechanism of regulation of receptor activity. At the receptor level several processes of desensitization have been shown to play a role in limiting signal duration and intensity [54]. Desensitization of GPCRs occurs with three phases: the phosphorylation of the receptor bound to ligand (activated receptor) by G-protein-coupled receptor kinases, sequestration/internalization and down-regulation or return to the surface [55]. We will consider the processes of desensitization for each receptor. However, we do not consider how specific processes result in desensitization, such as the SUMOylation of the GLP-1 receptor in response to glucose we have previously described [56] or phosphorylation [57]. We also did not consider synthesis, degradation or irreversible translocation of receptors in the model. The multiple dephosphorylation/recycling steps were shortened into one single reaction (for details see CM).

Constitutive receptor activity has been observed to occur in many different GPCRs ("tonic receptor activation") and can be explained by different mechanisms [58–60]. On other hand, islet α-cells can also secrete GLP-1 [61] and it may be that the neurotransmitter acetylcholine can be secreted by human alpha cells [62]. FFAs that activate FFAR1/GPR40 are present in blood and vary following meals. All these data provide reason enough to suggest that some activation of GPCRs takes place even without an additional GPCR agonist. For simplification, we have employed low concentrations of receptor ligands in modeling of experiments even where no specific GPCR agonists were used (for details see CM).

cAMP pathway

Signal routing to cAMP involves multiple GPCRs that regulate activity of several isoforms of AC and phosphodiesterases leading to production and hydrolysis of cAMP (Fig 1). cAMP

activates both PKA and the cAMP-regulated guanine nucleotide exchange factor (Epac). We previously developed a computational model of the pancreatic β-cell cAMP pathway [23, 25] that was used in the construction of the general model here (see CM).

Incretin hormones and receptors in β-cells. Glucagon-like-peptide-1 (GLP-1) is one potent incretin hormone coupled primarily to the specific α_s-G-protein-coupled receptor (GLP-1R). The GLP-1R belongs to the class B family of GPCRs. The GLP-1R couples to the G-protein complex and facilitates the release of the activated $G\alpha_s$ subunit of the complex, which activates plasma membrane-bound adenylyl cyclase (AC_P) to produce cAMP [12, 63, 64]. Following agonist-induced receptor activation, GLP-1R is probably internalized [65]. Small ubiquitin-related modifier protein (SUMO) can covalently modify GLP-1R and thereby desensitize GLP-1 signaling [56].

In islets, GLP-1R is expressed predominantly on β-cells [66]. A mathematical model for GLP-1R signal transduction was published recently [24]. However, this model lacks components such as a complex of G-protein with AC_P. To address this we used our general model for GPCR effects (for details see CM).

Another important incretin hormone is glucose-dependent insulinotropic polypeptide or gastric inhibitory polypeptide (GIP). GIP is a 42-amino-acid hormone, secreted from the enteroendocrine K cells and one of the major mediators in the regulation of nutrient-dependent insulin release from the pancreas [67]. Hyperglycemic clamp studies or GIP infusion established that GIP was insulinotropic at physiological concentrations [68]. GIP exerts its effects through binding to a specific α_s-G-protein-coupled receptor (GIPR) that also belongs to the B-family class of GPCRs of the glucagon–secretin family of peptides [68, 69].

The GIPR undergoes rapid and reversible homologous desensitization following binding of GIP [68, 70]. Regulator of G-protein signaling-2, G-protein receptor kinase 2, and β-arrestin 1 all have been implicated in GIPR desensitization [71].

Interestingly, class B GPCRs are characterized by a common topology of the ligand-receptor complex, and by their ability to couple multiple G-proteins. Biochemical and structural studies have led to a model of class B1 GPCR activation by peptide hormones including GLP-1 and GIP, referred to as the "two-step" mechanism [72]. This corresponds to collision coupling, where an agonist binds to the free receptor and then the agonist-receptor complex "collides" with the free G-protein. Corresponding models were developed for GLP-1R and GIPR (see CM).

Adrenergic receptors. Adrenergic agonists, the endogenous catecholamines adrenaline (epinephrine) and noradrenaline (norepinephrine), as well as agonists such as clonidine, all inhibit insulin secretion [10, 73, 74]. G-protein-coupled α_{2A}-adrenergic receptors (AdR) are responsible for these effects for adrenaline/noradrenaline, and they are mediated by the pertussis toxin-sensitive heterotrimeric G_i and G_o proteins, that inhibit AC [10, 73]. The mRNAs encoding the α_{2A} adrenoceptor are expressed at relatively high levels in human islets [5].

Co-immunoprecipitation studies showed pre-coupling of a_{2A}-adrenergic receptors with $G_{i/o}$ proteins [75]. However, no evidence for a_{2A}-adrenergic receptor and G_i-protein precoupling was found in resonance energy transfer studies and it was suggested that a_{2A}-adrenergic receptors and G-proteins interact by rapid collision coupling [76]. For this reason we also used the collision coupling mechanism for α_{2A}-adrenergic receptor (see CM). Desensitization mechanisms have not been specifically studied in pancreatic β-cells for these receptors, however, these receptors recycle rapidly in COS-7 and HEK-293 cells [77].

We modeled the processes of desensitization of GLP-1R, GIPR and AdR as a simplified mechanism that includes only one step for the active state (where a receptor is bound with ligand) pass off or recirculation of GPCRs (see CM), because these mechanisms are not well studied.

Adenylyl cyclases and phosphodiesterases. Activated adenylcyclase (AC) synthesizes cAMP from the substrate $Mg^{2+}ATP$. Rodent and human β-cells and insulinoma cell lines express different AC isoforms, including the Ca^{2+} and calmodulin-activated isoforms AC1, AC3, and AC8 [78–81]. Interestingly, among the cloned and characterized members of the mammalian AC family, two isoforms, AC1 and AC8, are synergistically activated by Ca^{2+}-calmodulin and $G_{s\alpha}$ [82, 83]. Both receptors for GIP and GLP-1 activate the α subunit ($G_{s\alpha}$) of the G-protein leading to an activation of AC in pancreatic cell lines and isolated pancreatic islets [67, 84]. The activation of AC by the α subunit ($G_{s\alpha}$) of the G-protein may be associated with formation of their complex with PM bound AC (AC_p) [85, 86].

GLP-1 resulting in increments in G_{sa} has been proposed to regulate calmodulin-activated AC8 that is central to GLP-1 signaling in rodent and human β-cells [78, 79, 87]. Our previous kinetic analysis supports this conclusion [23]. Similar interactions with AC8 was suggested for GIPR [68]. Catecholamines inhibit AC, however it is not known which isoform of AC in the β-cell is inhibited [10]. Activation of G_i by catecholamines may block AC_P mediated cAMP synthesis thus preventing the augmentation of insulin release stimulated by GLP-1 and GIP [10]. Acute activation of $G_{i/o}$-coupled receptors leads to inhibition of AC8 isoform [88]. Therefore we suggest that this G_i binds to the same AC isoform as G-proteins activated by GLP-1 or GIP, but AC bound with G_i has no catalytic activity. We found that these mechanisms of interaction between G-proteins and target enzymes (represented for AC_p in Fig 2) can play an important role in the regulation of messenger pathways (see Results and discussion).

Some soluble cytoplasmic adenylate cyclases (AC_c) can also contribute to cAMP synthesis that are not controlled by G-proteins and forskolin but rather by calcium, ATP and bicarbonate [89]. Therefore alongside G-protein activated or inhibited AC_p we modeled a cytoplasmic AC_c that is insensitive to G-protein and can be activated by glucose and/or Ca^{2+} (see for detals CM).

Some resting cAMP concentration exists in the absence of agonists (see below). Mechanisms of AC activation were not studied in this case for β–cells. We suggest that AC activity in this case can be a consequence of basal activity of AC_c and constitutive G-protein dependent receptor for AC_P that is observed in other GPCRs.

Phosphodiesterases (PDEs) hydrolyze cAMP and cyclic GMP. There are eleven known PDE families that differ in primary structures, responses to specific effectors and sensitivities to specific inhibitors, cellular expression and intracellular location and may modulate distinct regulatory pathways within the cell [90, 91]. In β-cells, it has been suggested that several PDE isoforms (1C, 3B, 4, 8B, and 10A) are involved in regulation of insulin secretion [91, 92]. In our model we consider both Ca^{2+} bound calmodulin activated and constitutive PDE activity as in a previous model [23] (see CM).

PKA and Epac. The two primary downstream effectors of cAMP are PKA and the cAMP-regulated guanine nucleotide exchange factors (Epac) that play a critical role in insulin release [64, 93]. PKA is a holoenzyme composed of catalytic and regulatory subunits. The catalytic subunits release when cAMP binds to the regulatory subunits and then act to phosphorylate downstream substrates. Epac is similarly activated by cAMP [64, 93]. We have used a simple mathematical model of these events [25]. There are multiple phosphorylation targets of PKA and Epac that are related to their effects on exocytosis. PKA and Epac pathways can have different physiological relevance based on differences in cAMP binding constants and downstream targets [94]. However, in the present model, downstream targets of PKA and Epac include only PKA blocking of K_{ATP} channels (see Eq 13, CM) and regulation of the IP_3 receptors in the ER (see CM).

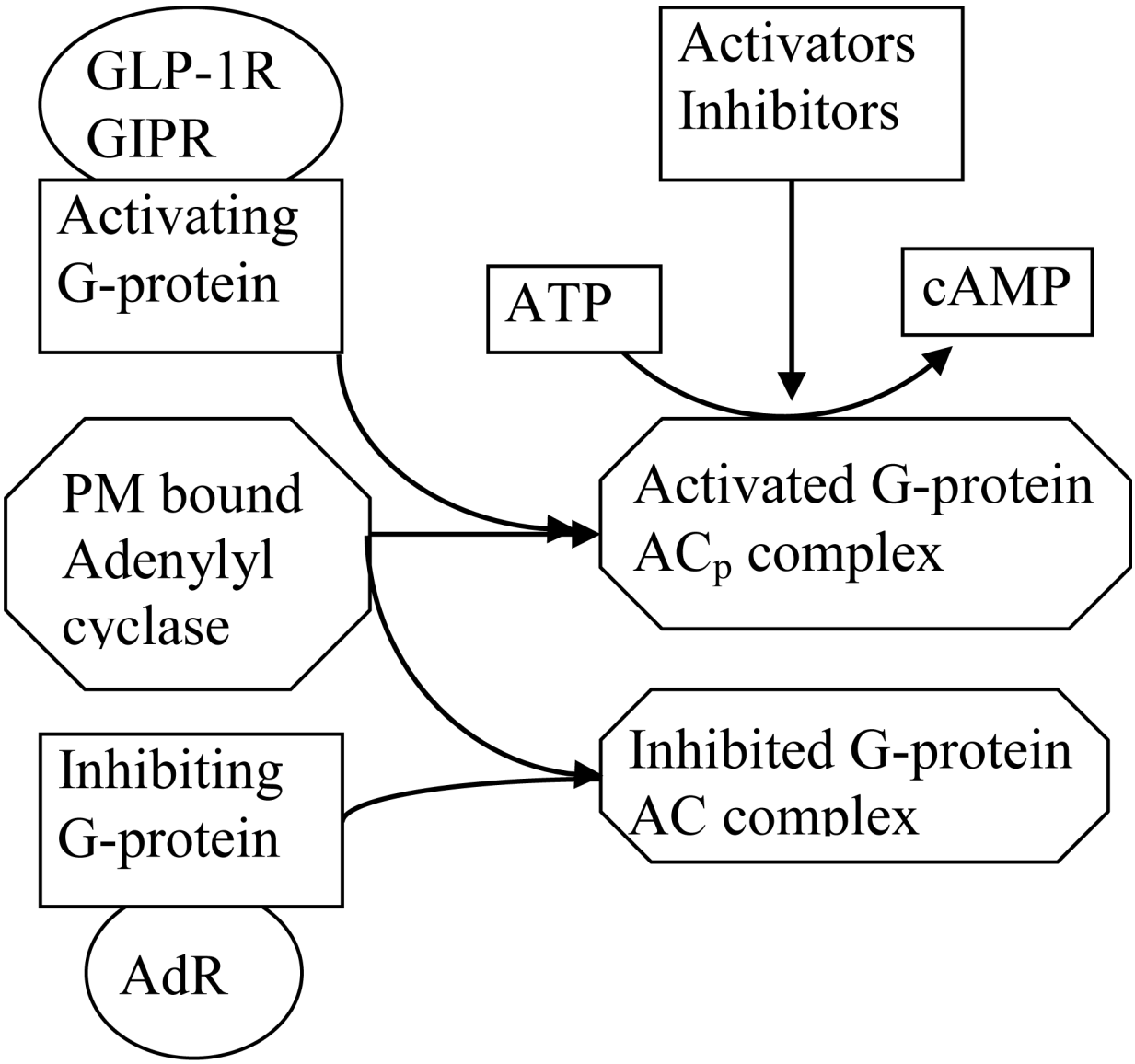

Fig 2. A schematic model of interaction of G-proteins activated by receptors with PM bound adenylyl cyclase (AC_p). Activating G-protein can bind with AC_p and their complex can accelerate cAMP production. AC_p complex bounded with inhibiting G-protein cannot catalyze cAMP production.

doi:10.1371/journal.pone.0152869.g002

Phosphoinositides

Numerous phosphoinositides are now accepted as independent signaling molecules [95]. We will consider here phosphoinositides for β-cell physiology (see CM). Phosphatidylinositol-4-phosphate (P4P) is synthesized from phosphatidylinositol (PI) by phosphatidylinositol 4-kinases (PI4Ks) and its synthesis activates by PKC and Ca^{2+} [96]. Phosphotidylinositol-4,5-bisphosphate (PIP_2) in turn is primarily formed from P4P by phosphatidylinositol-4-phosphate 5-kinase I [97] (Fig 1).

Despite being a small component of the plasma membrane, PIP_2 has many diverse and critical roles in β-cell physiology. PIP_2 serves as a precursor for the messenger molecules inositol-1,4,5-trisphosphate (IP_3) and diacylglycerol (DAG) generated following activation of PLC.

Membrane content of phospholipids, in particular PIP_2, can also determine the sensitivity of the K_{ATP} channels. Particularly, the K_{ATP} channels became more resistant to ATP-induced closure as the membrane content of PIP_2 was increased [98, 99]. A decrease in the PM PIP_2 concentration may lead to K_{ATP} channels closure and corresponding PM depolarization [41]. We have developed a mathematical model for phosphoinositide dynamics where PIP_2 can activate K_{ATP} channels (see Eq 10 in CM) and serves as a precursor for IP_3 and DAG (see CM).

Phospholipase C pathway

An important component of islet cell signal transduction and the control of islet function is innervation. Importantly, the modulators of insulin secretion include acetylcholine released from pancreatic parasympathetic nerve endings or possibly from alpha cells that activates phospholipase C (PLC) [3, 62, 100]. In general, over 50 hormone receptors can couple to the specific PLC-coupled G-proteins and some receptor tyrosine kinases can also stimulate PLCs that catalyze the formation of DAG and IP_3 from PIP_2 [101–103].

PLC pathway receptors. Pancreatic β cells express various G_q-coupled receptors, including the muscarinic receptors, FFAR1/GPR40, GPR120 and different P2Y receptor subtypes, that can regulate PLC activity [67]. However, here we included only what seem to be the most important for the β-cell: muscarinic acetylcholine receptor (MR) and FFAR1/GPR40. Others of this class seem to be expressed at lower levels [5, 104].

Muscarinic acetylcholine receptor (MR). Acetylcholine binds to MRs in the β-cell membrane coupled to $G\alpha_{q/11}$ to activate PLC [3]. mRNA encoding the type 3 MR is the most abundant in human islets but other isofroms are expressed in β-cells [5].

Initially, it was thought that MR and G-proteins interact freely with each other on the cell membrane [105]. However, type 3 MRs can pre-couple with their preferential classes of G-proteins [51] and here we used a pre-coupled model (see CM). Agonist-bound MR are phosphorylated by G-protein-coupled receptor kinases that leads to receptor internalization and recycling (or down regulation) [55].

Free fatty acid receptor (FFAR1/GPR40). The class A G-protein-coupled receptor GPR40, now also known as free fatty acid receptor 1 (FFAR1) is predominantly expressed in mouse, rat and human pancreatic β-cells and plays a major part in fatty acid amplification of GSIS [106]. FFAR1/GPR40 is activated by medium- to long-chain fatty acids and it is predominantly coupled to $G\alpha_q$ that typically signals through PLC-mediated hydrolysis of membrane phospholipids and is coupled to the formation of IP_3 and DAG [5, 106]. A collision coupling mechanism was suggested as the predominant mechanism for FFAR1/GPR40 (see [107]). Interestingly, investigations of β cell-specific inactivation of the genes encoding the $G\alpha_{q/11}$-coupled receptor have shown that glucose does not directly activate this receptor [108]. In stably transfected HEK-293 cells, FFAR1/GPR40 receptors underwent rapid agonist-induced internalization [109]. However, in the absence of specific data we used a general mechaism for modeling the processes of desensitization for MR and FFAR1/GPR40 in β-cells (see CM).

Phospholipase C (PLC). At least thirteen different PLC family members have been identified in various mammalian tissues and the consensus is that PIP_2 is the major substrate of PLC yielding DAG and IP_3 [110, 111]. Mouse and rat islets have been reported to express members of the three major phospholipase (PLC) subfamilies; PLC-β1,—β2,—β3,—β4, PLC-γ1, PLC-δ1 and PLC-δ2 [112, 113]. These enzymes appear to be activated by different mechanisms. It is likely that PLC-β isoforms, activated by carbachol, are localized on the PM and are regulated by the $G\alpha_q$ subfamily of G-proteins [114]. On other hand PLCδ1 is localized in the cytoplasm and regulated by nutrients including glucose [115]. PLC-γ1 is entirely cytoplasmic in MIN6 cells [116]. Interestingly, PLC-γ is directly phosphorylated and activated by tyrosine kinase

[114]. Therefore we modeled the two main PLC forms in β-cells as a nutrient (glucose) activated cytoplasmic PLC form (PLC_C) and as a G-protein-coupled PLC that is activated by specific G_q-type G-proteins in the PM (PLC_P) (Fig 1).

PLC- β and $G\alpha_q$ can form a complex mediating PLC activity [114]. We therefore suggested that the PLC_P can be activated only when this G-protein binds with its corresponding PLC (see CM). Interestingly, all the PLC isoforms discussed here can be activated by Ca^{2+} [110, 111]. However, the cytoplasmic PLC isoform activated by glucose is more strongly controlled by Ca^{2+} availability than the isoform that is activated by agonists [115, 117]. We thus considered the constant for $[Ca^{2+}]_c$ activation for PLC_p to be higher (0.4 μM) in comparison with the PLC_C (0.2 μM) (see CM).

IP_3 and DAG handling. The dynamic intracellular concentrations of IP_3 and DAG are determined by the rates of synthesis and degradation. We used our simple model [33] for modeling IP_3 synthesis and degradation. The DAG model was developed similarly to the IP_3 model (see CM). However, DAG remains bound within the PM and it was simulated as a concentration closely associated with the PM.

Regulation of PKC activation. DAG promotes membrane recruitment and activation of protein kinase C (PKC), an enzyme linked to the regulation of many cellular processes [118]. Several PKC isoenzymes are expressed in pancreatic β-cells and it is known that PKC phosphorylates and activates the components of the exocytotic machinery in β-cell that is important for the regulation of insulin secretion. However, the precise role of PKC-family proteins in β-cell physiology is still controversial and the phosphorylation targets that mediate the enhancement of exocytosis by PKC are not well known [119]. For this reason in our quantitative model of messenger interactions we consider only activation of P4P synthesis from PI by activated PKC (see Fig 1).

DAG can also activate PDK1 in mouse islets [120] and this kinase is also responsible for stimulating insulin release [121]. However, activated PDK1 does not seem to directly regulate the processes that we consider here and its regulation is not further considered.

Regulation of Ca^{2+} dynamics

Calcium is a ubiquitous second messenger that regulates many biological processes, such as cell signaling and transport, membrane excitability and substance secretion. In the β-cell Ca^{2+} homeostasis is controlled by transmembrane ion flux and involves coordinated interplay between multiple ion transport mechanisms and organelles. Ca^{2+} enters the β-cells primarily through voltage-gated Ca^{2+} channels. Additionally, Ca^{2+} store-operated current (SOC) increases $[Ca^{2}]_c$ (see CM). The plasma membrane of β-cells contains P-type ATPases that pump Ca^{2+} out of the cytosol to the extracellular environment [122, 123].

Ca^{2+} enters the endoplasmic reticulum (ER) via P-type ATPases (SERCA pumps, primarily SERCA2 and 3 in β-cells) using ATP and leaves predominantly through intracellular ER Ca^{2+} channels. The type III inositol 1,4,5 triphosphate receptor (IP_3R) is the main calcium release channel in the β-cell ER. When IP_3 binds to IP_3R, Ca^{2+} passes from the lumen of ER into the cytosol [3, 122–124]. An additional regulatory control of IP_3R is possible through phosphorylation of IP_3R or through the associated proteins that bind to the regulatory domain. PKA activation leads to an opening of IP_3R [125–127] (Fig 1). We have included models of IP_3R in our general model (see CM).

Developing and simulation an integrated computational system of β-cell GPCR signal transduction and metabolic signaling

We were able to construct an integrated kinetic mathematical model of second messenger pathways. The model is described by mass action kinetics and is formulated as a system of

ordinary differential equations (see CM). To handle the model equations from a numerical viewpoint, we need to know the dimensions and ranges of both variables and parameters so as to confine output values within physiological limits. However, precise determination of the model coefficients is limited due to a lack of adequate experimental data. Therefore, the model parameters were taken from the literature when possible and evaluated manually to best reproduce the experimental results that were found in available literature. All parameters and constants were fitted to be in their physiological ranges.

Equations, parameters, coefficients and outputs are represented below in the "Computational Model" and contain all the information necessary to carry out the simulations presented in this paper. They are pointed out in the text as a simulation at basal levels, and all simulations used the same set of parameters except where noted in the text or in the corresponding figure legends. Our simulations give time-dependent changes of cellular parameters. This allows a comparison with the corresponding experimental time-dependent data. To calculate persistent cellular parameters, the model was allowed to run up to steady-state values without changes in coefficients.

The model consists of a system of nonlinear ordinary differential equations describing the time rate of change in parameters. We developed the mathematical submodels of regulation process in the β-cell using web-based modeling resources of "The National Resource for Cell Analysis and Modeling (NRCAM)" This system was solved using the Virtual Cell simulation framework (University of Connecticut Health Center). The entire model and simulated results is publicly available for direct simulation on the website "Virtual Cell" (www.nrcam.uchc.edu) in "Math-Model Database" on the "math workspace" in the library "Fridlyand" with name "Messengers interaction". Free registration and corresponding instructions are available on that website. It is easy to copy, change and simulate this model with other parameters directly on the Virtual Cell platform on their website. Visualization and graphical analysis were performed using "Excel".

Results and Discussion

In this section we use computational simulations to critically review and analyze the experimental observations of intracellular regulatory mechanisms. Increases in the intracellular concentrations of Ca^{2+}, cAMP and DAG contribute to increased insulin secretion [3, 93, 123]. This allows us to compare data on insulin secretion with simulated results of second messenger pathway activation dynamics.

Simulation of glucose action (Fig 3, left part)

At low glucose concentrations (defined here as 3 mM) the simulated resting PM potential is approximately -62 mV and $[Ca^{2+}]_c$ is approximately 0.1 μM, corresponding to experimental data [122, 128]. The constitutive concentrations of activators for each specific G-protein coupled receptors were chosen to obtain 1/10 activity of the corresponding PM bound enzymes.

A simulation of increasing extracellular glucose would produce a rise in the ATP/ADP ratio that blocks K_{ATP} channels. This inhibition would allow the PM depolarization that activates the voltage-gated Ca^{2+} channels and increases cytoplasmic Ca^{2+} (Fig 3). Increased $[Ca^{2+}]_c$ activates constitutive PM bound and G-protein independent PLC activity and thereby increases IP_3 and DAG concentrations. DAG activates PKC. PKC and Ca^{2+} also activate phosphatidylinositol 4-kinases leading to an increase in P4P concentration and corresponding acceleration of IP_3 and DAG production. cAMP dynamics is considered later.

Increased $[Ca^{2+}]_c$ accelerates Ca^{2+} entry into the ER by SERCA pumps that can increase $[Ca^{2+}]_{ER}$. Simulated increase in $[Ca^{2+}]_{ER}$ (Fig 3B) corresponds to the experimental data that

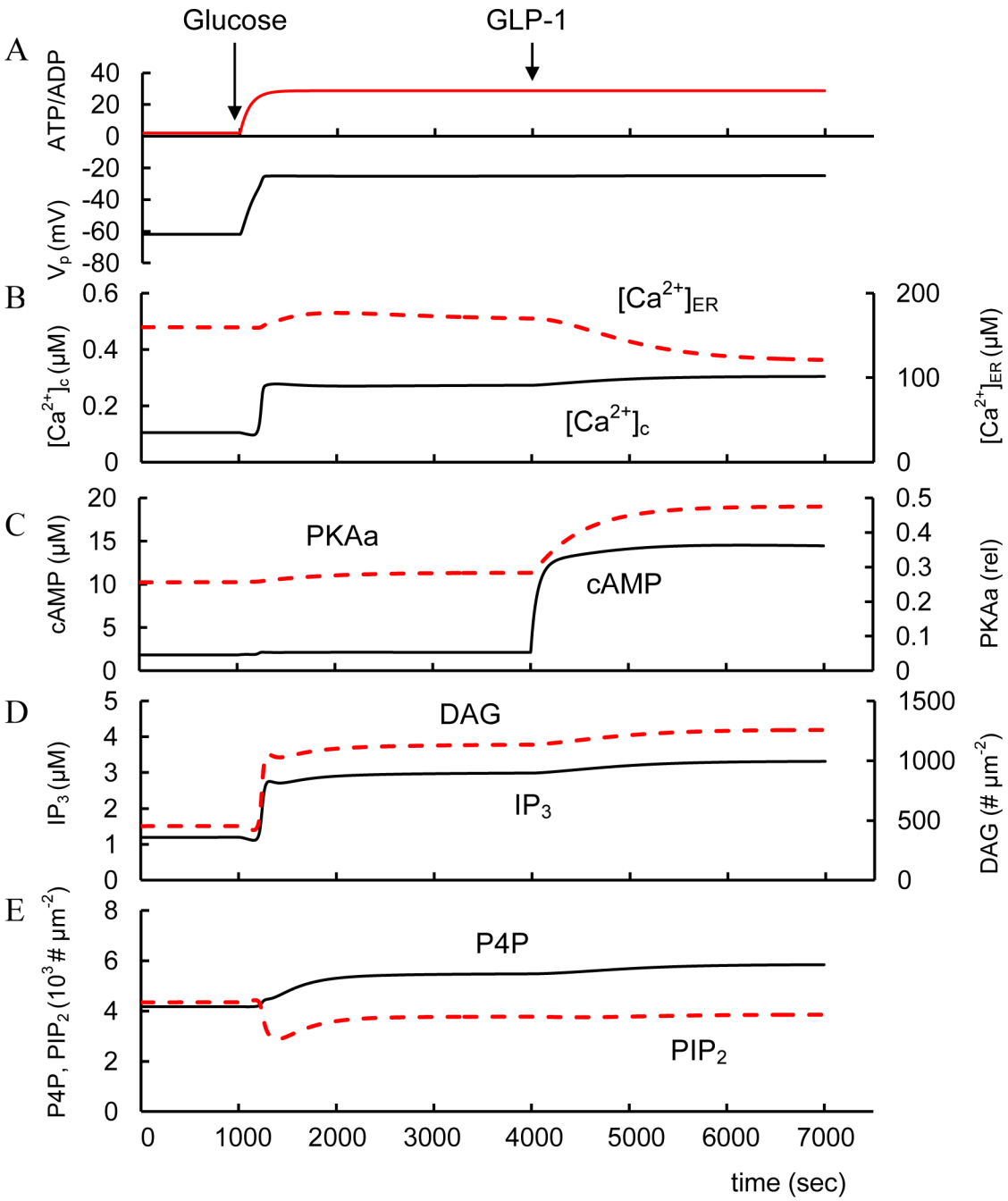

Fig 3. Modeling of spontaneous glucose-and GLP-1 stimulated changes of intracellular parameters. (A) ATP/ADP and PM potentials (V_p); (B) Free cytoplasmic Ca^{2+} concentration ($[Ca^{2+}]_c$) and free Ca^{2+} concentration in ER ($[Ca^{2+}]_{ER}$); (C) Cytoplasmic cAMP and relative activated PKA (PKAa). (D) IP_3 and DAG concentrations. (E) Concentrations of P4P and PIP_2 on PM. Initially all coefficients were on basal level (see Tables in CM). Low glucose concentration (3 mM) was simulated initially (left part). An increased extracellular glucose level at 1000 sec (from 3 to 8 mM) stimulates ATP/ADP increase that blocks K_{ATP} channels. This inhibition allows the PM depolarization (Fig 3A) that activates the voltage-gated Ca^{2+} channels and increases cytoplasmic Ca^{2+}. This activate SERCA and increase Ca^{2+} in the endoplasmic reticulum ($[Ca^{2+}]_{ER}$). Increased $[Ca^{2+}]_c$ activates also PLC and correspondently increases IP_3 and DAG, decreases PIP_2 and increases P4P concentrations. Increase in GLP-1 (from 3.1e-7 μM to 6.2e-4 μM) with corresponding AC_P activation was simulated at 4000 sec. This leads to a fast increase in cAMP concentration and PKA activation (Fig 3C). Rise in PKA activity increases Ca^{2+} discharge from the ER through the inositol 1,4,5 triphosphate receptor (IP_3R) and decreases $[Ca^{2+}]_{ER}$ (Fig 3B).

doi:10.1371/journal.pone.0152869.g003

have shown an increased $[Ca^{2+}]_{ER}$ with increased glucose [129–131]. The half-time for increased $[Ca^{2+}]_{ER}$ after increased glucose was about 10 min [129] matched by our simulations (Fig 3B).

In at least some islets from patients with T2D, althought data is extrememly limited, there seems to be a limited glucose-stimulated ATP production in β-cells so that glucose is not fully capable of closing K_{ATP} channels in order to stimulate Ca^{2+} influx [132–134]. Under these pathophysiological conditions, glucose alone fails to generate the critically important cytosolic Ca^{2+} signal that initiates insulin exocytosis. By facilitating glucose-dependent K_{ATP} channel closure, sulfonylureas can restore the Ca^{2+} signal, thereby allowing glucose-stimulated insulin secretion (GSIS) to occur [135]. We were able to simulate this mechanism. For example, we simulated the decrease of the glucose dependent saturated ATP/ADP ratio that leads to decreased PM potential and a failure to increase $[Ca^{2+}]_c$ in GSIS. Additional closure of K_{ATP} channels can depolarize the PM and restore increased $[Ca^{2+}]_c$ in GSIS (Fig 4).

cAMP pathway regulation

Cellular cAMP level is determined by the relative activities of AC and phosphodiesterases (PDEs). The association of cAMP effectors with signaling complexes and PM bound AC (AC_p) that regulate cAMP concentration (Fig 2) explains the differential signaling initiated by members of the G_s-and G_i-protein receptor families.

Glucose stimulation alone has led to either unchanged [136] or insignificantly increased cAMP levels [137–139]. Our simulation (Fig 3C) explains the insignificant increase in cAMP levels due to low activity of G-protein dependent PM bound AC (AC_p) when the specific hormone is absent, closely reflecting the corresponding experimental data. For example, according to [78] cAMP concentration in rat β-cells corresponds to 2.6 fmol 10^3 $cells^{-1}$ at low glucose levels (1.4 mM) and 3.6 fmol 10^3 $cells^{-1}$ at high glucose (20 mM). We converted these units in 1.81 μM and 2.51 μM for cAMP concentration in cell using volume of single β-cell. Our simulated cAMP concentrations were 1.83 μM at low and 2.104 μM at high glucose similar to the experimental data (Fig 3C). In this case cAMP dynamics are determined by constitutively active G-proteins that activate AC_p and soluble AC (AC_c) (both can be activated by Ca^{2+}/CaM) and Ca^{2+}-dependent PDE isoforms. The insignificant increase in cAMP concentration may result from offsetting events: calcium-stimulated phosphodiesterase activity may offset increased AC activity.

Even a low cAMP level may be necessary for insulin secretion because decreasing cAMP inhibits GSIS. For example phosphodiesterase 3β (PDE3B) negatively regulates insulin secretion during GSIS through its cAMP-hydrolyzing activity [140].

Incretin hormones. GIP is secreted in the same time and concentration frame as GLP-1 and these concentrations are sufficient to activate GLP-1R or GIPR in humans [141, 142]. GLP-1 and GIP receptor activation on β-cells leads to increased cAMP and intracellular Ca^{2+} that result in exocytosis of insulin-granules as a late response to oral glucose (20–120 min) [143]. GLP-1 and GIP have insulinotropic action in healthy humans [141, 144, 145].

We modeled the actions of incretin hormones and the resulting activation of AC_p that increases cAMP synthesis and PKA activation. To do this we set up a simulation with GLP-1 and GIP levels 20 times higher than the Michaelis constant for GLP-1 or GIP receptor binding (coefficient K_{GLP1}, or K_{GIP}, Eqs 46 and 47). As illustrated in Figs 1 and 3 simulation of increased cAMP leads to dual activation of the PKA and Epac branches of the cAMP pathway. Indeed it was found that GLP-1 and GIP lead to additional glucose-dependent closure of K_{ATP} channels and an increase in Ca^{2+} release from ER leading to $[Ca^{2+}]_c$ increase, that accelerates Ca^{2+} dependent insulin secretion [64, 68, 93, 146]. We were able to simulate increased $[Ca^{2+}]_c$

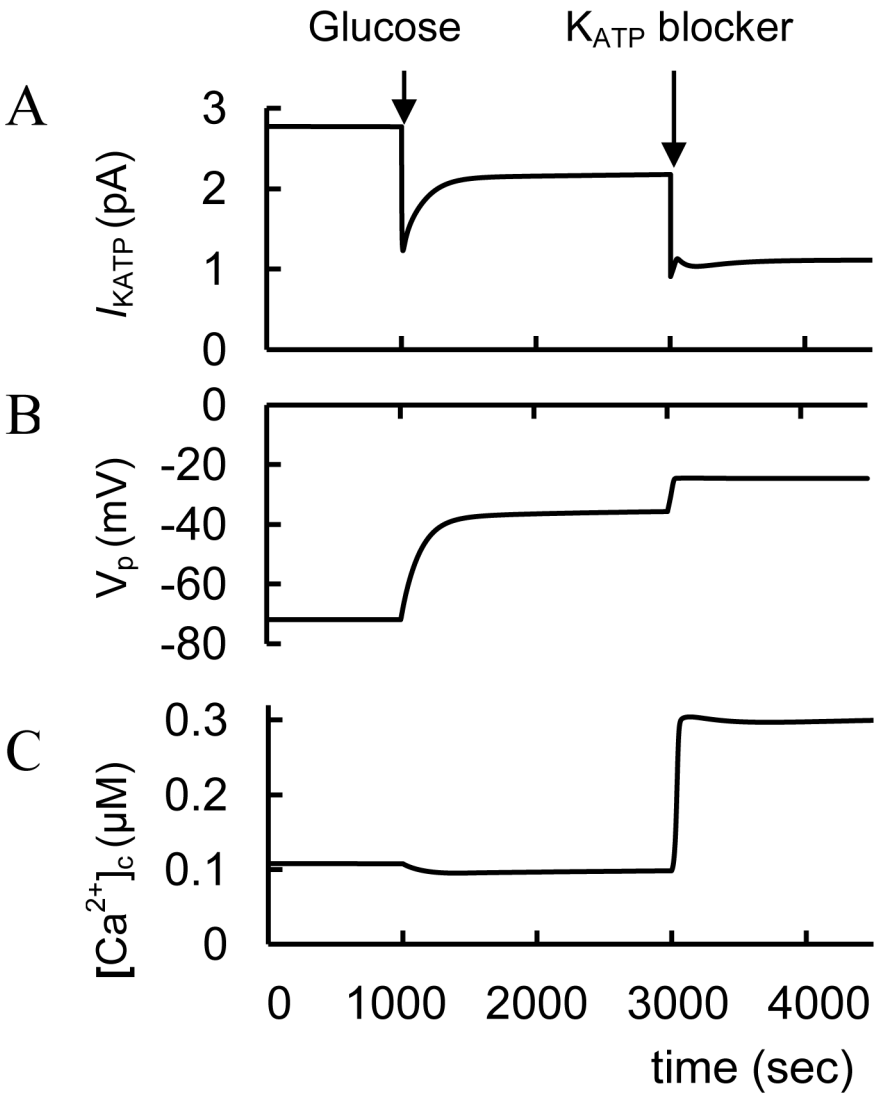

Fig 4. Simulated response to block of K_{ATP} channel in type 2 diabetes (T2D). (A) K_{ATP} channel current (I_{KATP}), (B) PM potential (V_p); (C) $[Ca^{2+}]_c$. T2D conditions were simulated by a decrease of the coefficient that is responsible for glucose dependent saturated ATP/ADP ratio (ATD_m, Eq 4). ATD_m was decreased from 32 (basal level) to 15. In this case PM membrane potential does not increase up to the nessesary threshold and does not lead to $[Ca^{2+}]_c$ increase as glucose is increased from 3 mM to 8 mM at 1000 sec. For simulation of K_{ATP} channel blocking the maximal conductance (g_{mKATP}, Eq 9) was decreased from 24 nS (basal level) to 9 nS at 3000 sec. This induces additional PM depolarization and fast $[Ca^{2+}]_c$ increase.

doi:10.1371/journal.pone.0152869.g004

(and a corresponding fall in $[Ca^{2+}]_{ER}$) by GLP-1R activation as a consequence of IP_3R stimulation through PKA activation (Fig 3).

However, in low glucose concentrations treatment of pancreatic β-cells with agents that increase cAMP- alone has little or no effect on insulin secretion. Only a combination of GLP-1 or GIP and high glucose potentiates GSIS [84, 147]. This important feature reduces the chance of producing hypoglycemia in patients with T2D with GLP-1 agonists [148]. Our computational model agrees with this behavior (see Fig 5, left part). At low glucose when $[Ca^{2+}]_c$ is low, activation of GLP-1R significantly increases AC_P (Fig 5B), however this does not lead to increased cAMP because increased $[Ca^{2+}]_c$ is required for ACp activation. On the other hand the model predicts that a facilitation of cAMP production by AC_P by GLP-1R agonists can be

stimulated if glucose increases the concentration of Ca^{2+}-dependent calmodulin that can activate PM bound AC in β-cells (see Figs 3 and 5). A small effect of GLP-1 on increased cAMP at low glucose was also simulated in our previous model of AC activation and of cAMP dynamics [23] becouse this effect can be explained by the sensitivity of AC_P to $[Ca^{2+}]_c$ changes rather than by the properties of GLP-1R. (A similar simulation of GLP-1 effects via AC activation was reported [24]). This and our previous analysis [23] provides support for a pivotal role of Ca^{2+}/CaM-dependent AC activation (possibly the AC8 isoform) in GLP-1 effects. The potentiating effect of cAMP on insulin secretion requires synergism between the cAMP pathway and the Ca^{2+} signal. Our model of cAMP dynamic regulation may also help to explain the mechanism responsible for the pattern of cAMP changes that take place during phases changes and oscillations in intracellular Ca^{2+} [23].

This model also provides an explanation for the observed clinical interaction between GLP-1R agonists and K_{ATP} channel blockers. Several human clinical trials have demonstrated that patients using GLP-1R agonists and K_{ATP} channel blockers therapies have a greater incidence of hypoglycaemia than those not using K_{ATP} channel blockers [148]. K_{ATP} channel blockers have also been shown to abrogate the glucose dependence of GLP-1R agonist activity in the rat pancreas [149].

Although the mechanism of this proposed uncoupling event has not been fully elucidated experimentally, our simulation suggests that K_{ATP} channel blockers may lead to modest PM depolarization and increased Ca^{2+} concentration even in low glucose (not shown) leading to activation of Ca^{2+} dependent AC on PM and an increased cAMP (and corresponding insulin secretion) in the presence of GLP-1R agonists. Thus, block of K_{ATP} channels independently of glucose may allow GLP-1R agonists to bypass their inherent glucose requirement by stimulating the downstream effects ordinarily associated with increased glucose. Our simulation shows also that similar behavior may also occur for GIPR activators in the presence of K_{ATP} channel blockers (not shown).

GLP-1 and GIP interaction. In rodent and healthy human subjects the insulinotropic effectiveness of GLP-1 and GIP may be additive [141]. We were able to simulate an additional increase in cAMP concentration following GIPR activation with GLP-1 administration (Fig 5B). This synergetic GIP effect takes place because GLP-1R cannot fully activate AC_p and GIPR administration leads to additional AC_p activation in our model, i.e. a sum of AC_p activated by GLP-1R (AC_{GLP}) and GIPR (AC_{GIP}) was higher than AC_{GLP} with GLP-1 activation only.

However, investigations in mice have shown a less protracted action of GIP vs GLP-1 that would suggest a more prolonged activation of the GLP-1 receptor than that of GIPR [150]. One hypothesis, is that GIP provokes accelerated desensitization of the GIPR [150]. Ligand-induced desensitization and trafficking of GPCRs have been implicated as critical mechanisms for modulating response duration *in vivo* [151]. A naturally occurring variant of the GIP receptor underwent enhanced agonist-induced desensitization in adipocytes, which impaired GIP control of adipose insulin sensitivity [152]. We have exploited our mathematical model to examine the influence of receptor desensitization in cAMP dynamics. According to results of our modeling an increase in the rate constant for desensitization and/or a decrease of rate of return to surface for GIPR can actually decrease AC_p activity bound with GIPR to compare with AC bound with GLP-1R (not shown). However, we were not able to find any data where a signaling desensitization in response to these two hormones has been compared under the same experimental setting in pancreatic β-cells.

Incretin hormones and T2D. GLP-1 may be able restore a Ca^{2+} signal by facilitating glucose-dependent K_{ATP} channel closure and by enhancing SOC allowing normal GSIS [64]. We were able to simulate this mechanism (Fig 6). In Fig 4 we suggested that in T2D glucose leads

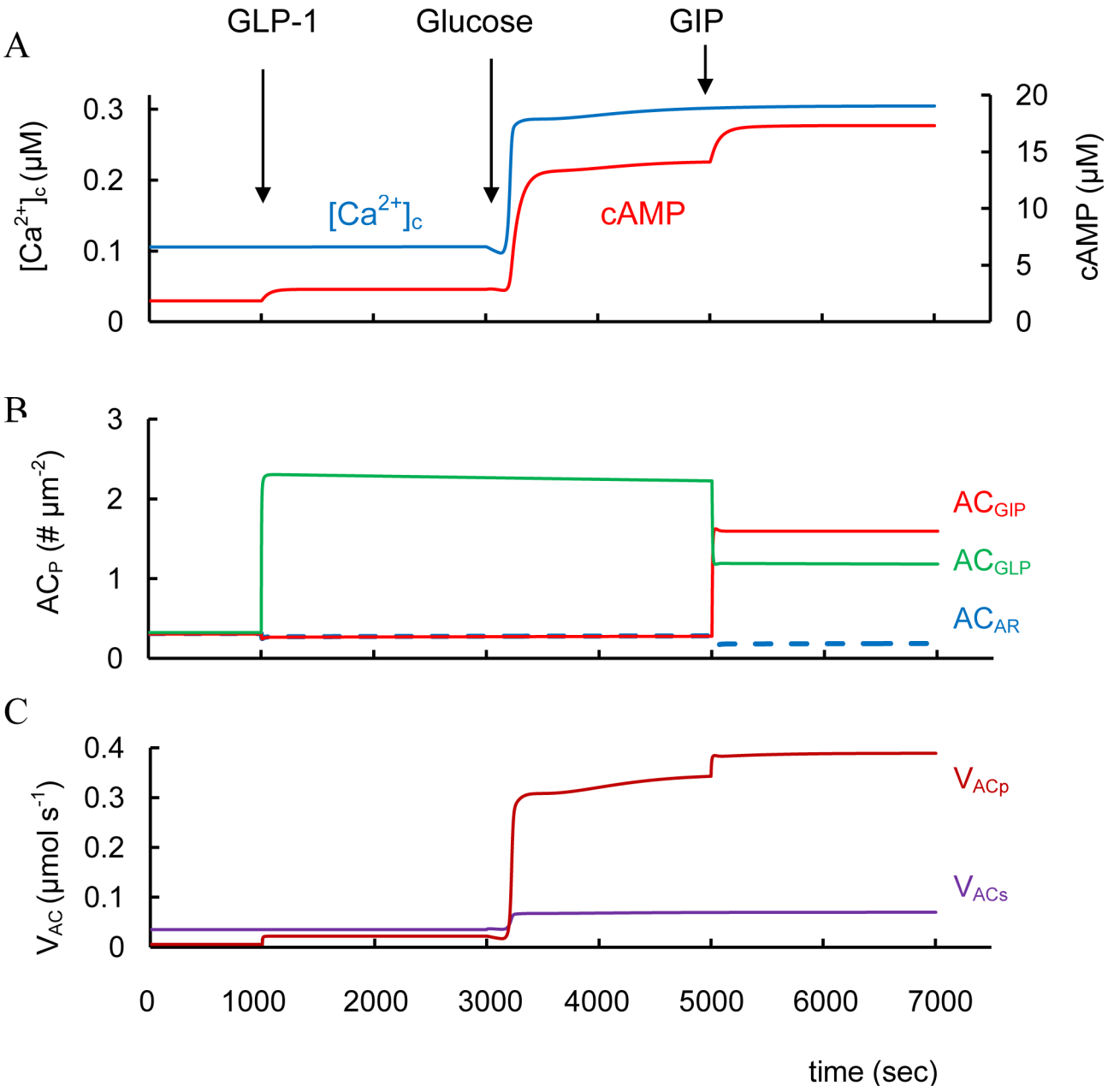

Fig 5. Simulation of GLP-1 and GIP action at low and high glucose levels. (A) Cytoplasmic $[Ca^{2+}]_c$ and cAMP dynamics. (B) AC_{GLP}, AC_{GIP} and AC_{AR} are the concentrations of complexes of AC on PM (AC_P) bound with corresponding G-proteins activated by GLP-1R, GIPR and α_{2A} adrenergic receptors. (C) V_{ACp} is G-protein and Ca^{2+} dependent AC activity on PM, V_{ACc} is the glucose and Ca^{2+}-activated soluble AC activity that is independent on G-protein. At low glucose concentrations (3 mM) (left part) GLP-1 was increased from basal level (3.1e-7 μM) to 6.2e-4 μM at 1000 sec. Increased extracellular glucose level was simulated at 3000 sec (from 3 mM to 8 mM). Than GIP administration was modeled as the increased GIP from basal level (1.37e-6 μM) to 3.42e-3 μM at 5000 sec.

doi:10.1371/journal.pone.0152869.g005

to an insufficiently increased ATP/ADP ratio (as a consequence of some unspecified dysfunction). We simulate the initial T2D conditions in Fig 6 (as well as in Fig 4) as decreased glucose dependent saturated ATP/ADP ratio that leads to a inability to increase $[Ca^{2+}]_c$ during GSIS. However, GLP-1 administration then leads to additional depolarization and $[Ca^{2+}]_c$ increase in our model (Fig 6). This additional depolarization is a consequence of increased I_{SOC} due to

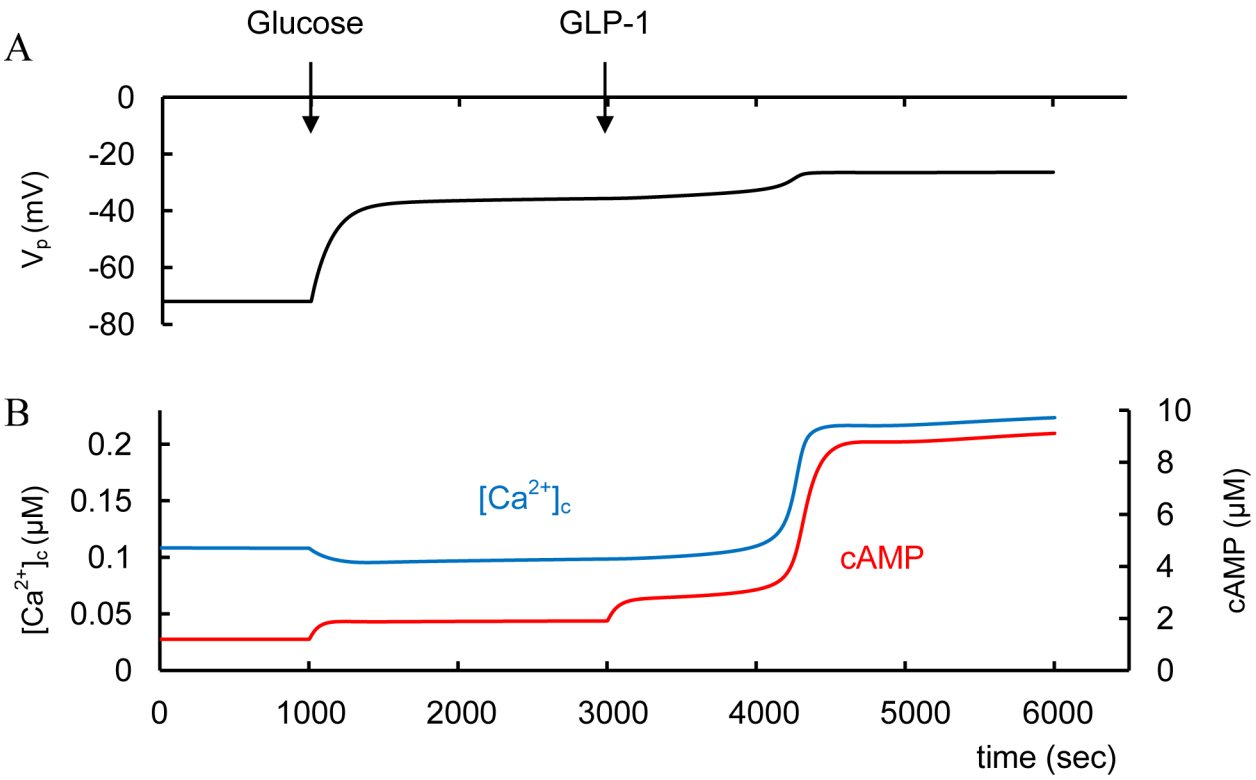

Fig 6. Simulated response of GLP-1 action in T2D conditions. T2D conditions were simulated by decreasing the glucose dependent saturated ATP/ADP ratio (ATD_m, Eq 4). ATD_m was decreased from 32 (basal level) to 15 as in Fig 4. In this case PM membrane potential is decreased and does not lead to $[Ca^{2+}]_c$ increase as glucose increases from 3 mM to 8 mM at 1000 sec as well as in Fig 4. GLP-1 administration was simulated at 3000 sec ([GLP-1] was increased from 3.1e-7 μM to 6.2e-4 μM. This induces cAMP increase with additional PM depolarization and Ca^{2+} influx into cell. Corresponding PKA activation also increases Ca^{2+} flow from ER. These effects lead to significant $[Ca^{2+}]_c$ and cAMP increase.

doi:10.1371/journal.pone.0152869.g006

decreased $[Ca^{2+}]_{ER}$ after IP_3R activation by PKAa, that also leads to increased Ca^{2+} flux from ER to cytosol. PKA activation also decreases the conductance of K_{ATP}.

Patients with T2D can have preserved GLP-1 and GIP secretion [142, 153]. However, the insulinotropic effect of incretins is diminished in T2D patients, due in part to reduced expression of incretin receptors as a consequence of perhaps glucotoxicity or lipotoxicity. For example, GLP-1R and GIPR levels were decreased in islets from mouse and rat model of diabetes and from T2D patients [57, 154, 155]. Elevated non-esterified fatty acids lead to a decreased GLP-1R expression and downregulation of GLP-1 receptor signaling in β-cell lines and mouse islets from db/db mice [156]. On other hand the transgenic expression of GLP-1R was able to restore GLP-1R-dependent stimulation of cAMP in isolated islets from mouse and in insulinoma cell lines [156, 157]. It was also shown that at high glucose levels GLP1-R can also be covalently modified in mouse islets by small ubiquitin-related modifier protein (SUMO) reducing its ability to be stimulated by GLP-1R agonist [56]. We have exploited our model to analyze these results. Proportional loss of cell surface GLP-1R and GIPR leads to a decreased cAMP and Ca^{2+} level even in the presence of high GLP-1 and GIP stimulation because the total receptor number is a limiting factor for activation of G-protein bound AC in our model. For example, a decrease in the total GLP-1R by 2-fold leads to a decrease of cAMP from 10.5 to 4.5 μM in a simulation of GLP-1 administration (if the calculations were made similar to Fig 3).

In summary, the results in this section suggest that the concentration of incretin hormone receptors on the PM can be a limiting factor in incretin function in rodent, normal human and T2D patients.

Catecholamines. Catecholamines (epinephrine and norepinephrine), the agonists of alpha adrenergic receptors, inhibit insulin secretion by decreasing cAMP content in β-cell as a result of inhibition of AC activity [10]. Our simulation also shows a catecholamine inhibition of cAMP concentration that can reduce GSIS (Fig 7A). This is a consequence of block of PM bound AC (AC_P) activity because this AC isoform following catecholamine-receptor binding cannot produce cAMP (see Fig 7B). AC_P plays a role in maintaining low levels of cAMP at GSIS in our model even without GPCR agonists activating the cAMP pathway. This is a consequence of constitutive activity of GPCRs that activate AC_p. Even low cAMP levels may be necessary for insulin secretion (see above). Therefore, activation of catecholamine receptors decreasing AC_p activity further suppresses GSIS even though cAMP content may already be low.

Subthreshold α_2-adrenergic activation with clonidine counteracts GLP-1 potentiation of GSIS [158]. Our simulation also shows that activated adrenergic receptors can block an increased cAMP concentration by incretin hormones because a significant part of PM bound AC is bound with G_i-proteins activated by catecholamine receptors. It blocks the ability of AC_P to be activated by G α_s-protein-coupled receptors. In this case the increase in cAMP concentration after simulation of GLP-1 was reduced (~6 μM, Fig 7A) in comparison with simulation in the absence of α_2-adrenergic activation (~15 μM, Fig 3C).

α_{2A} receptor antagonists have been proposed as T2D therapeutic agents [159]. We used our model to evaluate this possibility. Our simulation showed that a decrease in the number of α_{2A} receptors does not lead to a significantly increased cAMP concentration during GSIS, when we assume that α_{2A} receptor number is small (to reflect basal levels of this receptor accepted in our model). For example, with glucose stimulation (as in Fig 3) the increase in cAMP concentration is insignificant (from 2.104 to 2.106 μM) if the α_{2A} receptor content (Re_{ARt} in Eq 48) is lowered 10-fold. This happens because constitutive catecholamine activity blocks only a small fraction of the PM bound AC in the absence of specific activators (see Fig 5B). Block of this fraction cannot significantly effect activation of the remaining fraction of AC_P by incretins (not shown). Consequently, α_{2A} receptor antagonists are unlikely to be useful in T2D if the activity of α_{2A} receptors is insignificant.

However, T2D diabetes risk can be associated with increased expression of α_{2A} receptors and a concomitant reduction in insulin secretion [160]. Our simulation of cAMP dynamics with an increased α_{2A} receptor expression level (even without their agonists being present) gives a result that is indeed similar to α_2-adrenergic activation shown in Fig 7, i.e. to significant decrease in cAMP. This shows that increased α_{2A} receptor expression should lead to decreased cAMP production during GSIS without and with the incretin hormones (under physiological conditions). AC_P activity is reduced since a significant part of PM bound AC may be inhibited (bound with G_i-proteins) and cannot be activated during GSIS or by incretin receptors. In this case α_{2A} receptor antagonists might be useful in increase insulin secretion. It does seem that this effect is limited to situations where this is significantly increased expression of α_{2A} receptors over control situations.

Regulation of AC and PDE activity. Regulation of intracellular cAMP concentration during GSIS is also possible using AC activators such as forskolin or a PDE inhibitor (e.g., IBMX) [139]. For example, β-cell PDE3B can be activated by insulin, IGF-1 and leptin that inhibit insulin secretion [140]. Interestingly, PDE4 inhibitors may increase insulin secretion in humans [161].

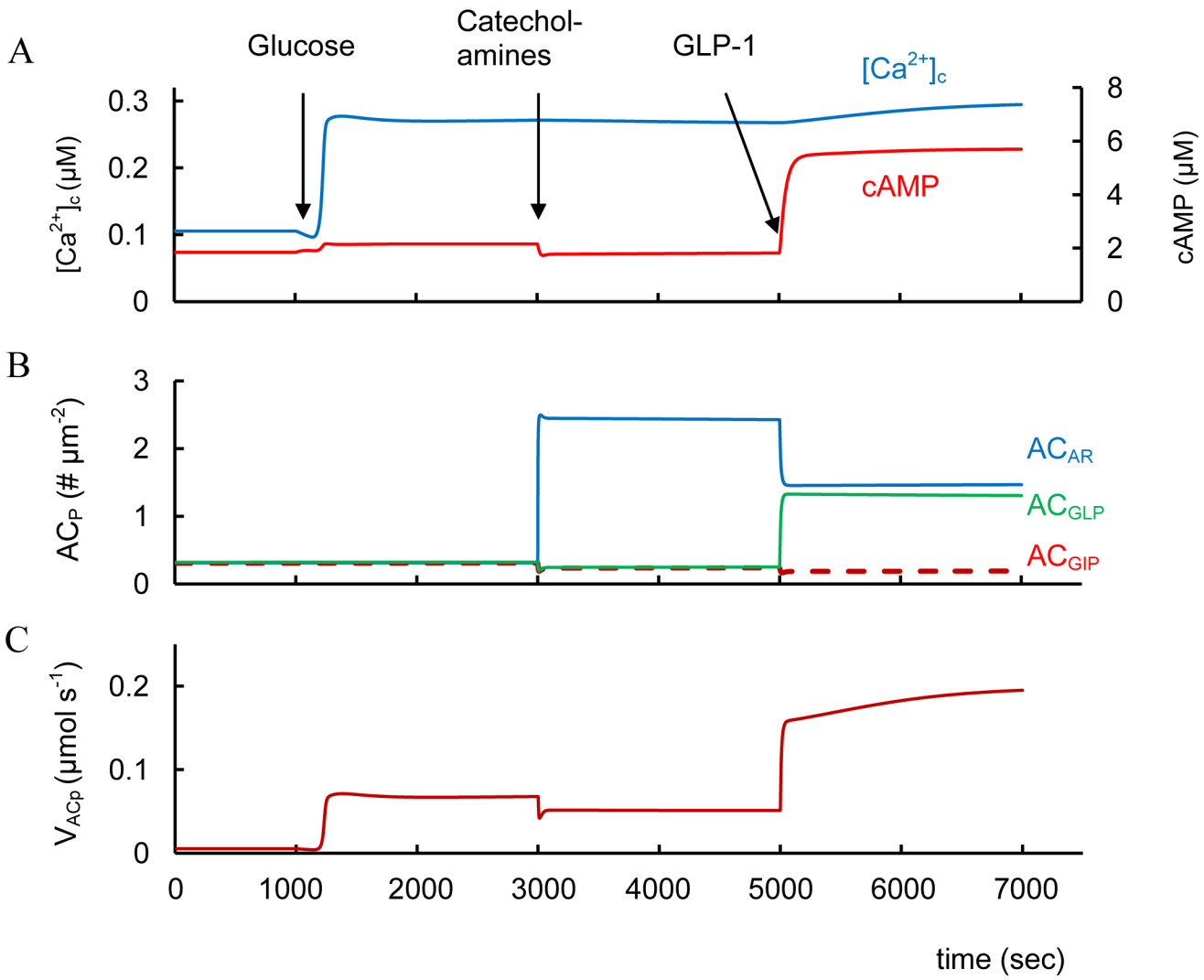

Fig 7. Simulation of catecholamines and GLP-1 interaction at high glucose levels. (A) Cytoplasmic cAMP and $[Ca^{2+}]_c$ dynamics. (B) AC_{GLP}, AC_{GIP} and AC_{AR} are the concentrations of complexes of AC on PM (AC_P) bound with corresponding G-proteins activated by GLP-1R, GIPR and α_{2A} adrenergic receptors. (C) V_{ACp} is G-protein and Ca^{2+} dependent AC activity on PM. The initial simulation was with low glucose (3 mM) as in Fig 3. Increase of glucose (8 mM at 1000 sec) induced changes of intracellular parameters. Catecholamine concentration (AR_3) was increased from basal level (0.002 μM) to 3 μM at 3000 sec. Than GLP-1 was increased from basal level (3.1e-7 μM) to 6.2e-4 μM at 5000 sec.

doi:10.1371/journal.pone.0152869.g007

Increased cAMP by AC activation or PDE inhibition causes various events, including Ca^{2+} mobilization from internal Ca^{2+} stores and activation of non-selective cation channels [80, 84]. In our model, activation of AC or PDE inhibition increased cAMP concentration, similar to the above for GLP-1 or GIP stimulation (see below for a special case of expression of different PDE isoforms). Then increased cAMP leads to PKA activation and block of K_{ATP} channels, activation of Ca^{2+} release from ER and additional PM depolarization (see Figs 1 and 6). Notice that dual activation of the PKA and Epac branches of the cAMP signaling mechanism can act directly on the exocytotic machinery [68, 146].

PLC pathway regulation

PLC activation increases insulin secretion in mouse and rat islets [3, 100, 115]. Drug-mediated, chronic, and selective activation of β-cell G_q signaling greatly improves β-cell function and glucose homeostasis in mice [162].

Constitutuve PLC activity occurs at low glucose levels. Increased glucose can activate the PLC pathway and significantly increase IP_3 and DAG concentration in conditions when PLC pathway GPCRs are not activated [95, 124, 163]. We simulated this process (Fig 3D) and found that the increases in IP_3 and DAG following glucose stimulation occur through cytoplasmic Ca^{2+} activation of both G-protein dependent and independent forms of PLC. In this case the degradation rate for IP_3 or DAG does not increase with increased $[Ca^{2+}]_c$. This is in contrast to cAMP degradation where Ca^{2+} activates phosphodiesterases. Additionally, PLC activation during GSIS and the corresponding decrease in PIP_2 concentration can simulate K_{ATP} channels closure and increased Ca^{2+} influx through voltage-activated Ca^{2+} channels (see Figs 1 and 3E).

FFAR1/GPR40 receptops. FFAR1/GPR40 agonists enhance insulin secretion. They markedly enhance cytoplasmic and mitochondrial Ca^{2+} in insulinoma cells and increased IP_3 and ATP levels in islets normal and diabetic rats [164]. GSIS (i.e. at high glucose level) was also augmented in pancreatic β-cells in normal and diabetic mice that overexpressed FFAR1/GPR40 [165, 166].

We simulated the effect of FFAR1/GPR40 activation via $G\alpha_q$-proteins leading to PLC (PLC_p) pathway activation (Fig 8). However, this effect was insignificant for Ca^{2+} and IP_3 at low glucose levels and only increased glucose levels (that can increase $[Ca^{2+}]_c$) can significantly activate PLC_p (Fig 8D). This leads to an additional rise in IP_3 and DAG concentrations. Increased IP_3 also results in decreased $[Ca^{2+}]_{ER}$ and an increase in $[Ca^{2+}]_c$ as a result of IP_3-dependent release of Ca^{2+} from the ER. Decreased $[Ca^{2+}]_{ER}$ also opens store-operated channels (SOC) accelerating Ca^{2+} and possibly other cations into the cytoplasm through these channels. PLC_p activation decreases PIP_2 that can also lead to additional K_{ATP} channels inhibition (see Fig 8E). All these processes enhance PM depolarization, increasing Ca^{2+} influx (Fig 8A). Formation of DAG also activates PKC, resulting in increased efficiency of Ca^{2+} on exocytosis during GSIS (Fig 1).

These simulations reflect experimental data. Unbound FFAs in plasma in the physiological range can activate FFAR1/GPR40 in the presence of glucose and eventually amplifies GSIS in short-term exposure [106, 167]. FFA action on FFAR1/GPR40 caused PLC activation and a rise in $[Ca^{2+}]_c$ both in primary mouse and rat β-cells and in INS-1 cells with increased glucose [168–170]. Palmitate also markedly reduced the calcium storage capacity of the ER measured by thapsigargin-induced Ca^{2+} release, suggesting that ER calcium stores may participate in raising $[Ca^{2+}]_c$ in isolated mouse islets [37]. These events are consistent with a decrease in $[Ca^{2+}]_{ER}$ following FFAR1/GPR40 activation in our simulation (Fig 8B).

We evaluated the effect of FFAR1/GPR40 potentiation at low glucose in more detail to evaluate possible enhanced risks of hyperglycemia. At low glucose concentrations, activating FFAR1/GPR40 does not increase $[Ca^{2+}]_c$ in pancreatic rat β-cells [170] nor does it stimulate insulin secretion in mouse islets [166]. Interestingly, mouse pancreatic β-cells expressing increased FFAR1/GPR40 do not show increased insulin secretion in low glucose [165]. PLC activity is unaffected in our model (Fig 8D left part), because increased cytosolic Ca^{2+} is required to increase G-protein dependent PLC activity. This is an advantageous feature that should reduce the chance of producing hyperinsulinemia and hypoglycemia in T2D patients given FFAR1/GPR40 agonists. Indeed, selective pharmacological activation of FFAR1/GPR40 by TAK-875 significantly improved glycemic control in T2D patients with only a modest risk of hypoglycemia [171]. This result resembles our analysis of GSIS stimulated by GLP-1, where

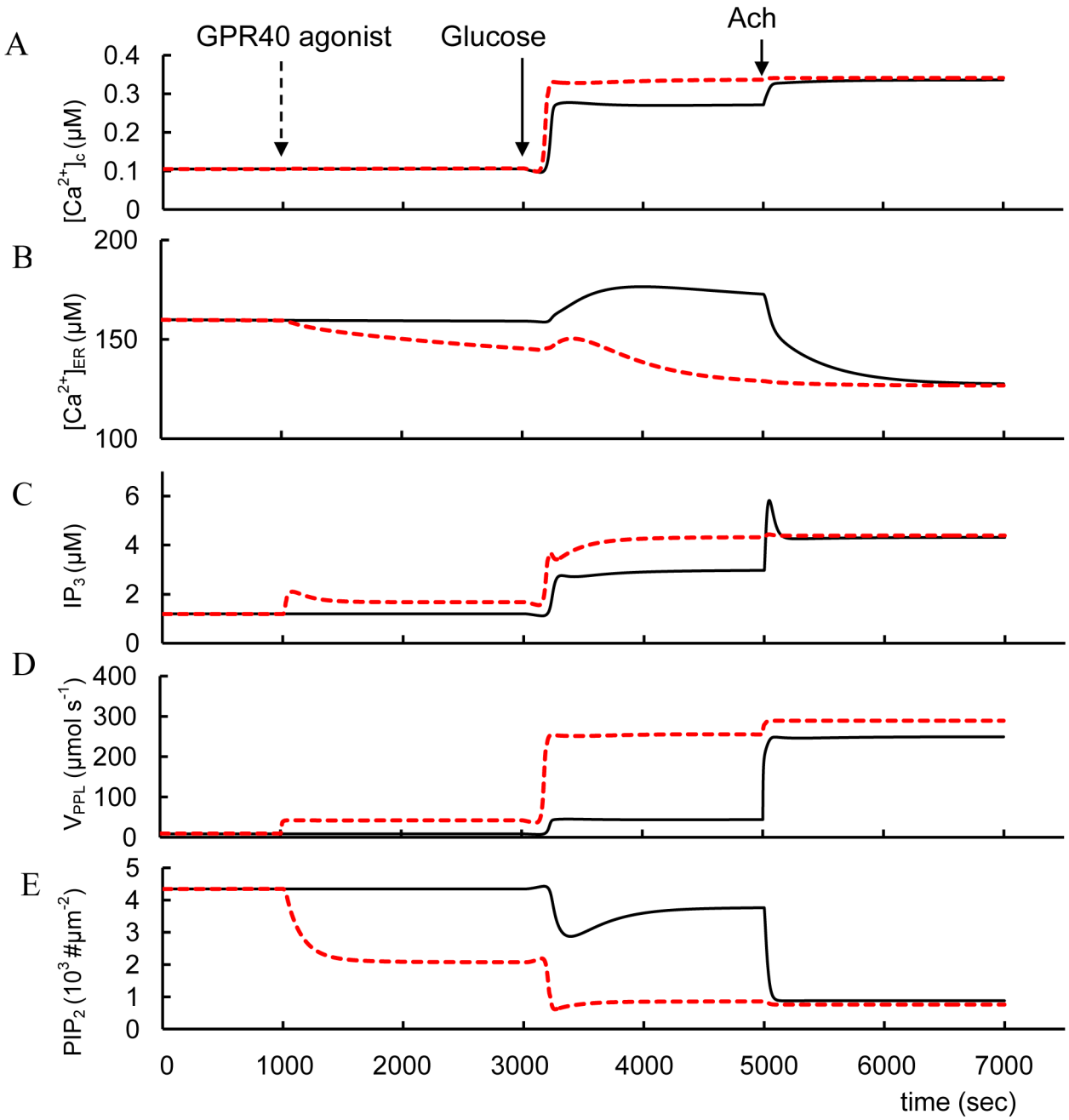

Fig 8. Effects of FFAR1/GPR40 activators and acetylcholine (Ach) on changes of intracellular parameters. Two protocols were stimulated: 1. (—) glucose was increase from 3 mM to 8 mM at 3000 sec, than acetylcholine, M_3R activator, (AM_3 concentration in model) was added at 5000 sec (AM_3 was increased from basal level 0.0022 μM to 2.2 μM) and 2. (- - - -) FFAR1/GPR40 agonist was added at 1000 sec (AR_7 was increased from basal level 0.0506 μM to 82 μM), than glucose (3000 sec) and acetylcholine were added (5000 sec). (A) Free cytoplasmic Ca^{2+} concentration ($[Ca^{2+}]_c$. (B) Free Ca^{2+} concentration in ER ($[Ca^{2+}]_{ER}$); (C) IP_3 concentration. (D) V_{PLP} is the activity of PM bound PLC (Eq 78). (E) Concentrations of PIP_2 on PM.

doi:10.1371/journal.pone.0152869.g008

GLP-1 action alone (i.e. at low glucose) has little or no effect on insulin secretion. Only a combination of GLP-1 and high glucose potentiates insulin secretion. We explained this effect also through the dependence of increased $[Ca^{2+}]_c$ to increase G-protein dependent AC activity.

We can also predict that using FFAR1/GPR40 agonists simultaneously with K_{ATP} channel blockers can lead to increased incidence of hypoglycemia similar to employing GLP-1R agonists and K_{ATP} channel blockers together. Both of these effects are associated with an increase in $[Ca^{2+}]_c$ due to sulfonylureas or similar K_{ATP} inhbiting drugs that can activate PLC or AC even in low glucose levels. Indeed, FFAR1/GPR40 activation increased insulin secretion in the presence of sulfonylurea under low glucose conditions through enhancement of PKC signaling in insulinoma cells [172].

Activation of FFAR1/GPR40 may be a viable therapeutic approach for treatment of type 2 diabetes [173]. Our simulations suggest that FFAR1/GPR40 should increase insulin secretion in the presence of elevated glucose, because FFAR1/GPR40 agonists should increase $[Ca^{2+}]_c$ and DAG during GSIS, supporting the evidence that these agonists may be useful as novel insulin secretagogues with low risk of hypoglycemia. However, the simulations also indicate that using FFAR1/GPR40 activators together with sulfonylureas could increase the incidence of insulin secretion overshoot and thereby increase hypoglycemia, as it was discussed for incretin hormones.

Activation of muscarinic receptors. Cholinergic muscarinic agonists, including the endogenous neurotransmitter acetylcholine and its synthetic nonhydrolyzable analog carbachol, increase $[Ca^{2+}]_c$ and GSIS in normal β-cells [3]. Stimulation of the MR activates $G\alpha_q$-proteins leading to PLC_p activation in our model (Fig 1) Modeling of MR activation is shown in Fig 8 (right) for high glucose levels for two cases, with and without preliminary FFAR1/GPR40 activation. This simulation (without preliminary FFAR1/GPR40 activation) corresponds to experimental evidence that at high glucose level, stimulation with the muscarinic receptor agonists (for example, carbachol), induces a rapid and sustained PLC activation [124, 174], depolarizes PM and enhances glucose-induced electrical activity [175]. Several studies have also suggested that acetylcholine can regulate $[Ca^{2+}]_c$ dynamics leading to $[Ca^{2+}]_c$ increase and $[Ca^{2+}]_{ER}$ decrease [129, 176]. Our model also takes into account a suggestion that the depolarizing effects of the muscarinic receptor agonists can be attributed partially to a store-operated current (SOC) that activates following IP_3-dependent release of Ca^{2+} from the ER.

β-cell specific inactivation of genes encoding $G\alpha_{q/11}$ in mice leads to decreased PM depolarization with increased glucose [108]. According to our simulations this result seems to be a consequence of decreased SOC because (1) $[Ca^{2+}]_{ER}$ does not decrease significantly without IP_3 and (2) K_{ATP} channels remain open because PIP_2 concentration does not decrease markedly without PLC activation.

The effect of glucose and carbachol on GSIS is at least additive in rat islets [115]. Based on our model this effect can be explained by significant independence of PLC pathway that increases IP_3 and DAG (DAG content changes proportionally IP_3 in our model) (Fig 8C) and glucose activation of GSIS through PM depolarization and $[Ca^{2+}]_c$ increase (Fig 8A).

Moderate levels of acetylcholine have little effect on PM depolarization or on sustained cytosolic Ca^{2+} in mouse islets at low glucose [124, 176–178]. We simulated activation of muscarinic receptors (MR) at low glucose levels. In this case, activation of MR evoked only a small increase in $[Ca^{2+}]_c$ similar to modeling of FFAR1/GPR40 activation (for example, see Fig 8, left) if conductivity of specific nonselective cation channels (NALCN) (that can be activated by MR) was insignificant (not shown). This can be explained as well as for FFAR1/GPR40 activation (see Fig 8) so that increased cytosolic Ca^{2+} is necessary for activation of membrane bound PLC.

A different scenario was found for rat or human islets. Acetylcholine increased $[Ca^{2+}]_c$ in isolated islets from Wistar rats at low glucose (2.8 mM) [179] and in human β–cells [62]. These results can be explained by activation of the MR dependent NALCN channels that lead to transient PM depolarization and increased $[Ca^{2+}]_c$ even with the simulation conducted in low glucose (Fig 9). Likewise, our simulation of electrophysiological events in human β-cells showed

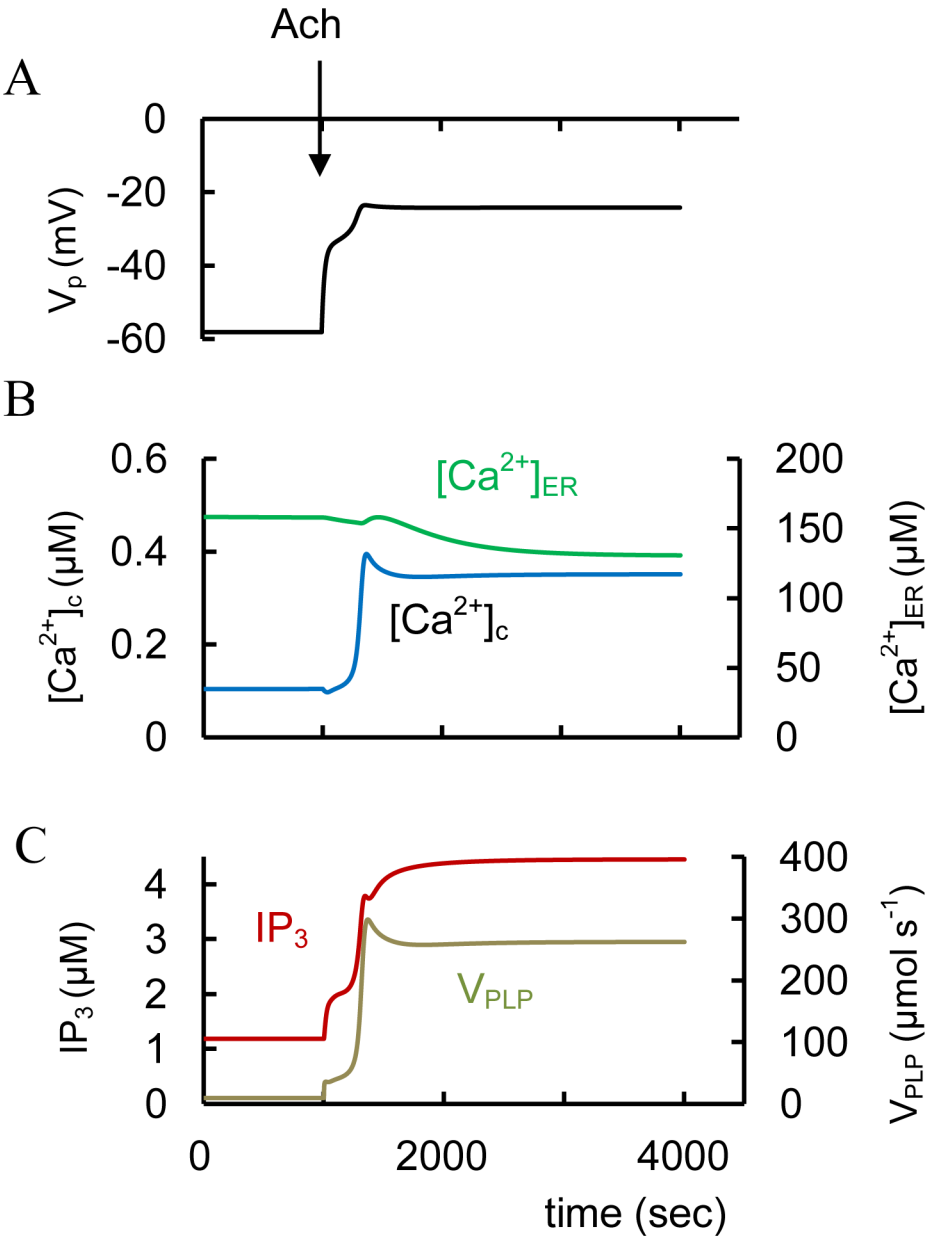

Fig 9. Effects of Ach on changes of intracellular parameters at activated NALCN channels at low glucose. (A) PM potential (V_p); (B) $[Ca^{2+}]_c$ and $[Ca^{2+}]_{ER}$; (C) Cytoplasmic IP_3 concentration and the activity of PM bound PLC (V_{PLP}). For simulation of NALCN channel activity the maximal conductance (g_{mNM3}, Eq 25, CM) was initially increased from 0 nS (basal level), to 35 nS. Addition of acetylcholine that opens NALCN channel was simulated at 1000 sec at the arrow (AM_3 was increased from basal level 0.0022 μM to 2.2 μM). All simulations were performed at low glucose (3 mM).

doi:10.1371/journal.pone.0152869.g009

that activation of NALCN channels can lead to additional PM depolarization and increased insulin secretion at high glucose. This can also decrease the threshold for glucose-induced spike activity and also lead to increased $[Ca^{2+}]_c$ [30].

Acetylcholine activates Na^+ influx by an activation of NALCN permeable to Na^+ [3], i.e. an increased Na^+ inward current through NALCN leading to PM depolarization (see [30, 50])

that corresponds to mechanisms considered in our model, where opening of NALCN lead to increase in Na^+ influx (see Eq 25, CM).

Activation of MR dependent NALCN channels in low glucose could be a mechanism by which acetylcholine increases human insulin secretion during first phase of feeding where an increase in insulin secretion precedes an increase in blood glucose. This increase, termed "cephalic phase", is thought to be largely mediated by the release of acetylcholine from nerves innervating pancreatic islets or from the alpha cells [6, 62, 180]. In this case activation of MRs may increase the capability for insulin secretion even while still in sub-threshold glucose levels.

Zawalich and colleagues [115] showed that the failure of PLC activation resulted in impairment of insulin secretion under sustained glucose exposure in rats. It was also found that mice that selectively lacked MRs in pancreatic β-cells showed decreased insulin release and impaired glucose tolerance. Consistent with this concept, transgenic mice that selectively overexpressed type 3 MRs in pancreatic β-cells exhibited increased insulin release and improved glucose tolerance [181]. Our simulation with a decreased number of MRs leads to decreased $[Ca^{2+}]_c$ and DAG concentration at high glucose because constitutive MR activity takes part in IP_3 and DAG production. For example, our simulation with 10x reduced MR abundance (to compare with the example in Fig 3) shows a significant decrease in $[Ca^{2+}]_c$ (from 272 to 250 nM) and DAG concentration (from 1131 to 926 #/μm^{-2}) at high glucose. The "cephalic phase" should also be blocked in these conditions. This should lead to decreased insulin secretion. These experimental data and our simulations suggest that optimal acetylcholine receptor stimulation is essential for β-cell insulin secretion.

Approaches aimed at enhancing signaling through β-cell MRs (or downstream) might become therapeutically useful for the treatment of T2D (see [104, 182]). However, our consideration shows that MR activation could conceivably lead to hypoglycemia at relatively low glucose concentrations as a consequence of NALCN channel activation leading to PM depolarization and increased $[Ca^{2+}]_c$.

FFAR1/GPR40 and muscarinic receptor interactions. The temporal interplay between FFAR1/GPR40 and muscarinic receptors was investigated [37]. Palmitic acid at physiological levels could acutely inhibit subsequent acetylcholine-stimulated insulin secretion (through activation of FFAR1/GPR40) and the rise of intracellular Ca^{2+} production in isolated mouse islets during GSIS. According to these authors the mechanism of such effect could be a Ca^{2+} release from the ER during FFAR1/GPR40 activation that prevents subsequent acetylcholine induced Ca^{2+} release. Our simulation shows that this effect can take place, i.e. FFAR1/GPR40 activation can prevent additional $[Ca^{2+}]_{ER}$ decrease and Ca^{2+} release at acetylcholine administration (Fig 8A and 8B). However, there is also competition at the level of PLC such that activation of FFAR1/GPR40 leads to G-proteins binding to PLC_p that decreases the ability of PLC_p to bind with G-proteins, activated by acetylcholine (Fig 8D). Consequently, simultaneous use of activators for FFAR1/GPR40 and the muscarinic receptor may not lead to significant additive effects on insulin secretion.

Role of phosphoinositides

The rate of phosphoinositide metabolism is increased in glucose-stimulated islets. This effect is due to PLC-mediated hydrolysis of PIP_2 and leads to a decrease in PIP_2 content and an increase in P4P [183]. Increased glucose leads also to activation of PLC and decreased PIP_2. An increase in P4P in our model is a consequence of PKC and Ca^{2+} mediated activation of phosphatidylinositol 4-kinase (see Fig 1 and Fig 3E).

We modeled block of K_{ATP} channels due to decreased PIP_2 (see Eq 10, CM). This can cause additional PM depolarization and an elevated level of $[Ca^{2+}]_c$ thogether increasing the insulin

secretion rate. These simulations reflect data that shows disrupting the interaction between K_{ATP} channels and PIP_2 by overexpressing Kir6.2 in mutants with decreased sensitivity to PIP_2 causes persistent membrane depolarization and elevated basal level insulin secretion [184]. Additionally, PLC activation can also simulate closure of K_{ATP} channel as a consequence of a decreased PIP_2 concentration [41, 42].

Glucose-induced P4P elevation required voltage-gated Ca^{2+} entry and was mimicked by membrane-depolarizing stimuli. P4P elevation was also sensitive to PKC inhibition and mimicked by phorbol ester stimulation [96]. We were able to simulate these results because P4P synthesis is activated by PKC (see Eq 74 in CM and Figs 1 and 8E). Our model confirms that PIP_2 levels in β cells are regulated for proper insulin exocytosis [96, 183].

Interaction of pathways

Activation of the GLP-1R, GIPR, MR and FFAR1/GPR40 receptors following meal ingestion could be simultaneous, very closely timed or even sequential. For this reason it is important to evaluate cross talk between GPCR agonists, comparing and combining those that function via the $G_{\alpha s}$ pathway (e.g., GLP-1 and GIP) with those that function via the $G\alpha_{q/11}$ pathway (e.g. acetylcholine and FFA or FFAR1/GPR40 agonists).

Interestingly, activation of the cAMP pathway can activate the PLC pathway. For example, GLP-1 can activate PKC through Ca^{2+}-dependent activation of PLC in the insulin-secreting rat β-cell line INS-1 [185]. Indeed, according to our calculations an activation of the cAMP pathway (such as GLP-1 addition) leads to PKA activation and corresponding closure of the K_{ATP} channels and opening of IP_3R leading to an significant increase in $[Ca^{2+}]_c$ (from 0.272 to 0.302 μM) (Fig 10A). This activates Ca^{2+}-dependent PLC leading to an increase of IP_3 (and DAG) concentrations (see Fig 10B).

On other hand, if FFAR1/GPR40 activators are employed first, to activate the PLC pathway, this does not lead to an increase in cAMP concentration (see Fig 11B). In this case FFAR1/GPR40 activation significantly increases $[Ca^{2+}]_c$, IP_3 and DAG but it does not effect cAMP concentration. According to our model (that was constructed mainly from mouse islets data) cAMP concentrationis not increased because this would occur only by activation of PM bound AC by specific G-protein coupled receptors (such as GLP-1R or GIPR). Indeed agonist activation of the $G_{q/11}$ receptor (i.e. an activation of PLC pathway) has no significant effect on intracellular cAMP level in mouse islets [186, 187].

However, the effect of activation of the PLC pathway on the cAMP pathway may be species dependent. For example, a different behavior was found in rat β-cells. In isolated rat islets the MR agonist carbamylcholine chloride (CCh) evoked a concentration-dependent increase in cAMP generation with a maximum at least 4.5-fold above control even at basal 2.8 mmol/l glucose. However, in this case activation of the PLC pathway may only partially activate the cAMP pathway. This was "partial" because forskolin and GLP-1 increased cAMP accumulation 10-fold and 23-fold, respectively [188], i.e. G-protein dependent AC activity plays a significant role in rat β-cells. Interestingly, acetylcholine acts predominately through activation of the cAMP/PKA pathway alone (no increase in the IP3 pathway) to enhance Ca^{2+}-stimulated insulin release islets in the Goto-Kakizaki β-cell, a spontaneous rat model of T2D [189] although this finding has not been replicated.

We used our model to propose a hypothesis that can explain these experimental data. For example, our simulation showed that increased cAMP following activation of the PLC pathway may be due to the presence in rat of mainly PDE forms that are not activated by $[Ca^{2+}]_c$ (Fig 12). In this case increased $[Ca^{2+}]_c$ following acetylcholine MR activation (for example by activation of NALCN channels at low glucose accelerates the rate of cAMP production but not

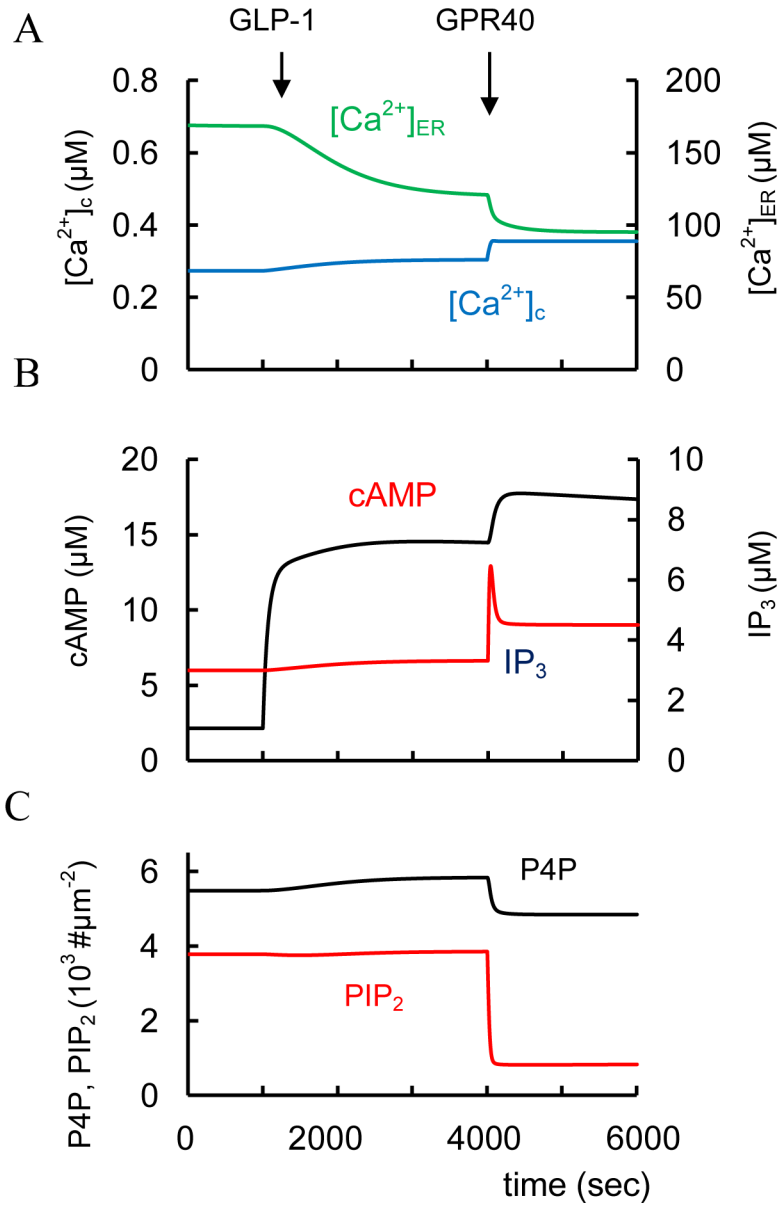

Fig 10. Simulated responses to GLP-1 and FFAR1/GPR40 activator at high glucose. (A) $[Ca^{2+}]_c$ and $[Ca^{2+}]_{ER}$; (B) Cytoplasmic cAMP and IP_3 concentrations; (C) Concentrations of P4P and PIP_2 on PM. Glucose (8 mM) induced changes of intracellular parameters were initially simulated as in Fig 3 up to steady state (left part). GLP-1 was simulated at 1000 sec as an increased GLP-1 from basal level (3.1e-7 μM) to 6.2e-4 μM. After that FFAR1/GPR40 activation was simulated at 4000 sec as increased AR_7 from basal level (0.0506 μM) to 82 μM.

doi:10.1371/journal.pone.0152869.g010

degradation, because the maximal activity in Ca^{2+}/CaM activated PDE was decreased, leading to a significant increase in cAMP. cAMP increases 4.8 fold following simulation of the MR receptor activation and 24-fold with additional GLP-1 administration, compared to cAMP levels without agonists (Fig 12C), that corresponds to experimental data [188]. We could not find any information about the behavior of cAMP and IP_3 in human β-cells related to possible interactions of the cAMP and PLC pathways. This question demands further investigation.

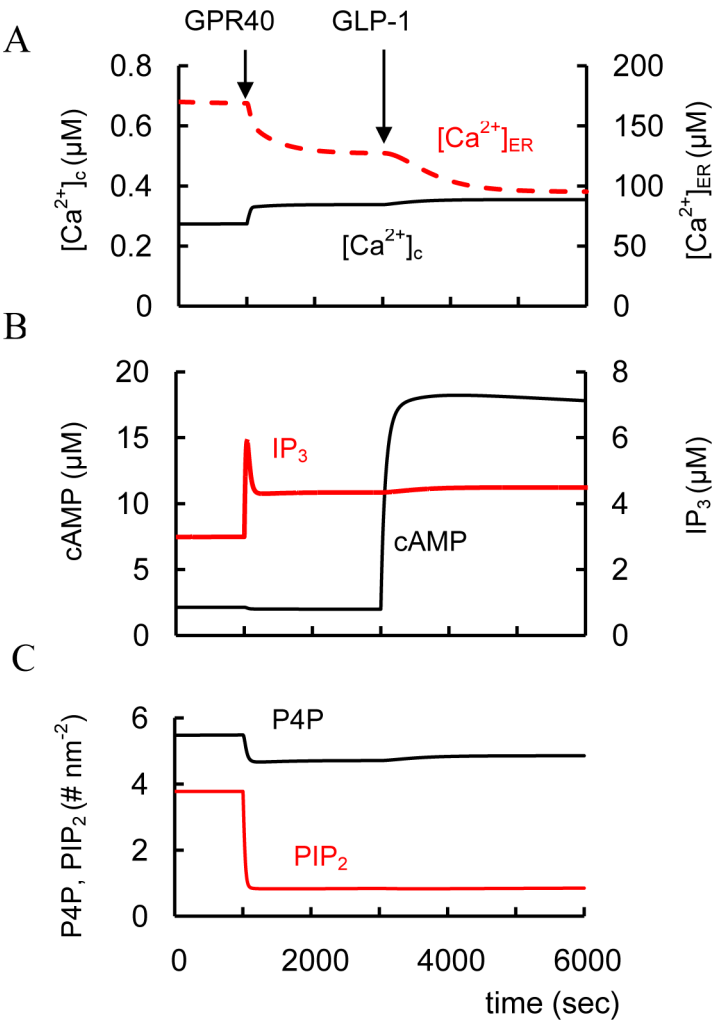

Fig 11. Simulated response to FFAR1/GPR40 activator with following addition GLP-1 at high glucose. (A) $[Ca^{2+}]_c$ and $[Ca^{2+}]_{ER}$; (B) Cytoplasmic cAMP and IP_3 concentrations; (C) Concentrations of P4P and PIP_2 on PM. Glucose (8 mM) induced changes of intracellular parameters were initially simulated as in Fig 3 up to steady state (left part). FFAR1/GPR40 activator was simulated at 1000 sec as an increased AR_7 from basal level (0.0506 μM) to 82 μM. After than GLP-1 action was simulated at 3000 sec (GLP-1 increased from basal level (3.1e-7 μM) to 6.2e-4 μM).

doi:10.1371/journal.pone.0152869.g011

However, our theoretical analysis shows the possible mechanisms and consequences of potential interactions.

In general, according to these simulations, simultaneous activation of the cAMP and PLC pathways should increase GSIS. This follows increased second messengers such as $[Ca^{2+}]_c$, cAMP and DAG that can activate an insulin secretion. In other words, receptor agonists for cAMP and PLC pathways can act cooperatively (for example see Figs 10 and 11). Indeed, the combination of GLP-1 and acetylcholine increased insulin release compared with each compound alone during an acute test in the β-cell line BRIN BD11 [190] and in the isolated perfused rat pancreas [191]. FFAR1/GPR40 and GLP-1 receptor agonists markedly increased GSIS and their combination led to GSIS that was significantly increased in comparison with each compound alone [166]. These data are in accord with our simulations. Interestingly, FFAR1/GPR40 and GLP-1 receptor agonists as well as their combination did not increase

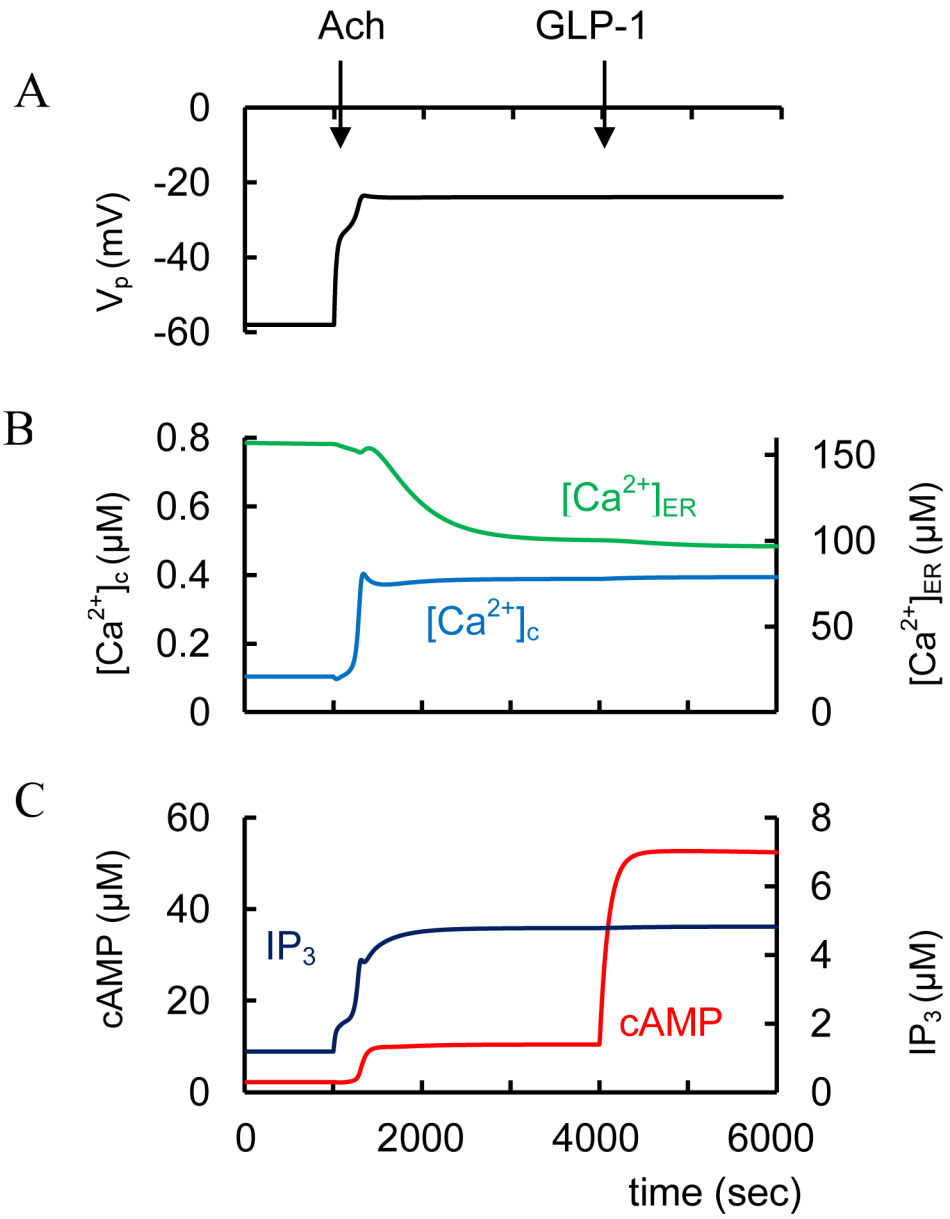

Fig 12. Simulated response to Ach at activated NALCN channels and decreased phosphodiesterase (PDE) activity in low glucose. (A) PM potentials (V_p); (B) $[Ca^{2+}]_c$ and $[Ca^{2+}]_{ER}$; (C) Cytoplasmic cAMP and IP_3 concentrations. For simulation of NALCN channel activity the maximal conductance (g_{mNM3}, Eq 25, CM) was initially increased from 0 nS (basal level) to 35 nS. PDE activity (Vcpde, Eq 66) was decreased from 1.4 μmol s^{-1} (basal level) to 0.3 μmol s^{-1}. All simulations were performed at low glucose level (3 mM).

doi:10.1371/journal.pone.0152869.g012

insulin secretion at low glucose in islets isolated from normal rats [166]. This could be the result of a inadequate activation of AC and PLC at low $[Ca^{2+}]_c$.

Limitations and Perspectives

Interpretation of the effects of G-protein blockers and activators on β-cells is difficult because a change of any messenger potentially alters several aspects of the messenger dynamics of other messenger pathways. For this reason, using a mathematical modeling approach opens up

significant new possibilities and allows a better understanding of potential messenger interactions. Our model represents significant improvements in a number of areas of β-cell computational simulation. It was possible to roughly determine the contribution of each messenger pathway to $[Ca^{2+}]_c$ and insulin secretion dynamics under specific conditions. Our simulations confirm that the specific messenger dynamics interactions can lead to an appropriate increase in insulin secretion.

The model we developed here must also be considered in the context of known limitations. Some limitations are unavoidable because of the limited current knowledge of basic biochemical and physiological data, the extensive variability among experimental data, the considerable variation in experimental conditions, and the potentially deleterious effects inherent in experiments with β-cells. For example, the actual variations in the number of receptors, G-proteins and target enzymes during signaling as well as the mechanisms of their interactions are not known.

These limitations required some formulations from other models based on animal experiments to be used. Therefore it would be unreasonable to expect the model to accurately reproduce all previously observed experimental results. However, we were able to show that the model we developed can reproduce a number of experimental observations ranging from G-protein coupled receptors to Ca^{2+} and insulin secretion dynamics. It can be used as the groundwork for *in silico* examination of the effects of agents that modulate insulin secretion via regulation of GPCRs. As other receptors are further characterized they can be readily incorporated into this basic model. This creates opportunities for *in silico* studies of possible functional influence of different agents on β–cell functional properties that it is difficult to evaluate at this time.

The data used to fit the parameters of our model were taken primarily from mouse islets and cell lines. For this reason the simulations of the experimental results obtained with rat and human β-cells can present difficulties. Some differences between species were stressed above. However, more data is clearly needed to analyze the human cells and islets.

Other limitations are related to mechanisms of insulin secretion. Insulin is secreted by exocytosis of large dense-core vesicles. Regulation of insulin–containing granule secretion in β-cells is a complex function of cytoplasmic Ca^{2+}, cAMP and the PLC pathways. Several mathematical models were developed for describing exocytosis of insulin granules (see for review [25, 192]). However, our knowledge of the molecular regulation of exocytosis in β-cells remains fragmentary. A detailed consideration and modeling of the effects of additional regulatory pathways on the rate of exocytosis of insulin–containing granules is needed.

Conclusion

The multiple receptors expressed by β-cell pass their signals through a common set of downstream effectors distinguished by multiple isoforms with different specificities and activities. The coupling among these pathways causes interactions among the signals sent by the different classes of receptors. We have developed a computational integrated model of the G-protein signal transduction system from the receptors to the intracellular second-messengers: Ca^{2+}, PIP_2, cAMP, DAG and IP_3. The model includes detailed descriptions of interactions between G-protein-coupled-receptors, $[Ca^{2+}]_c$, Ca^{2+}-bound calmodulin (Ca^{2+}/CaM), adenylyl cyclase, phosphodiesterase and PLC pathway regulation. We used this model to predict the signal processing of several G-protein-coupled-receptors.

By combining experimental data on G-protein and second messenger interactions with mathematical modeling, our systems approach is likely yield a detailed analysis of metabolic and signaling pathway interactions in the β-cell and help elucidate key regulatory mechanisms

involved in regulation of insulin secretion. The simulations provide a way to compare the time-course and consequence of changes in expression of mechanisms that regulate cytoplasmic Ca^{2+} relative to the activation of cAMP and PLC pathways and to evaluate hypotheses on regulatory mechanisms of insulin secretion.

The most important results of our system biology computational analysis are:

1. The concentration of incretin hormone receptors in the PM can be a key limiting factor in mechanisms leading to activation of insulin secretion by incretins.
2. There can considerable variability in the effects of acetylcholine and GLP-1, GIP or FFAR1/GPR40 agonists on insulin secretion. Our theoretical analysis shows that activators of GLP-1, GIP and FFAR1/GPR40 receptors may have a low risk of hypoglycemia because they need a concomitant increase in $[Ca^{2+}]_c$ for activation whereas an activator of muscarinic receptors can lead to hypoglycemia. This is a consequence of an activation of specific channels, leading to depolarization of the PM and $[Ca^{2+}]_c$ increase even at lower blood glucose levels.
3. G-coupled receptor activators can have additive effects on insulin secretion if they act on different messenger pathways (i.e. cAMP and PLC pathway in our case). The effectors may not have any additive interactions if they act on the same pathway (for example the pair GLP-1 and GIP or FFAR1/GPR40 activators and acetylcholine).
4. The modeling of messenger pathway interactions is important for determining the pharmacological targets for improving insulin secretion in T2D. The results of the model applications can guide clinical approaches to improvement of β-cell function by combinations of stimuli via GPCR agonists, helping to minimize side effects and maximize clinical benefit.

Computational Model (CM)

The purpose of this section is to develop the mathematical formalism for a β-cell model of receptors and second messenger interactions. A schematic diagram of the biochemical steps, channels, receptors, Ca^{2+} handling and messenger pathways in β-cell is presented in Fig 1. We will highlight some basic assumptions and general properties of the model reflecting the main mechanisms describing in text. We assume concentration of most species lies in the range that allows us to avoid the need to use complex stochastic algorithms that would be necessary if regulatory processes are dependent on minute quantities of molecules. The β-cell is modeled as a small spherical cell. Modeling [24] has shown that in such a cell, for example, cAMP is distributed rapidly and uniformly throughout the cytoplasm, even following GLP-1 receptor activation, in time intervals that we used in our simulations (minutes). On this base we suggested that species are distributed uniformly on PM, in cytoplasm or ER of β-cells in our models. Certainly some molecular events are critically dependent on localized gradients such as possible activation of insulin granule release by Ca^{2+} near specific Ca^{2+} channels [193], however these potentially important events are not considered in our model.

Approach

The present model is created as systems of ordinary differential equations with nonlinear terms. Numerical integration was carried out using standard numerical methods. Three compartments: plasma membrane, cytoplasm and ER were used. The units, except where indicated otherwise: cytosolic and ER species and ligand concentrations are represented by concentration in (μM) while membrane-bound species are given as area densities (number per unit of

membrane area) in (# μm^{-2}), time in seconds (s), voltage in millivolts (mV), current in femtoamperes (fA), conductance in picosiemens (pS), capacitance in femtofarads (fF) (per cell).

Experimental data are often represented only for concentration per volume and it is often nessesary to calculate a concentration on PM surface. Then the coefficient (f_{Nc}) to convert the concentration from # μm^{-2} to μM for β-cell can be calculated as

$$f_{Nc} = 10^6 \, S_c/(N_{av} \, V_c) \tag{1}$$

where S_c is the cell surface, V_c is the volume of the cell cytoplasm (in liter) and N_{av} is Avogadro's constant. f_{Nc} = 0.00211 μM μm^{-2} if the data from Table 1 were used.

Lifetimes are often only accessible from experimental articles. Assuming the first-order processes, the detected lifetimes ($t_{1/2}$) can be converted to rate constants according to equation $k = \ln 2/t_{1/2} = 0.693/\, t_{1/2}$.

The data used to fit the computational model in our study were taken primarily from isolated rodent β-cells and cell lines. Some parameters were taken from the literature. Remaining parameters were experimentally unreachable and we optimized their values by simulated the model and compare with experimental data (Tables 1–6). For simplicity, we use the concentrations the components inside a cell without brackets. Basal initial conditions were denoted as (-in).

Glucose metabolism

The influence of glucose (Glu) and FFA on GSIS was modeled as the dynamical changes in [ATP]/[ADP] ratio that determines K_{ATP} channel opening. We assume that the nucleotide ratio satisfies the first-order kinetic (see [203]).

$$d\ ATD\ /dt = (ATD_o - ATD)/t_{ATD} \tag{2}$$

where

$$ATD = ATP/ADP \tag{3}$$

$$ATD_o = \frac{ATD_m \, (Glu + k_{GFr} \, FFA)^{hgla}}{(Glu + k_{GFr} \, FFA)^{hgla} + K_{GF}{}^{hgla}} \tag{4}$$

$$AT = ATP + ADP_f \tag{5}$$

$$ADP_f = AT/(1 + ATD) \tag{6}$$

Table 1. Cell and physical parameters.

Parameter	Value (units)	Eq.	Ref.
f_{nc}	0.00211 μM μm^2	1	Ad
C_m	6158 fF	8	[33]
V_c	764 μm^3	1	[194]
S_c	973 μm^2	1	[194]
V_{ER}	280 μm^3	87	[194]
f_{cf}	0.01	86	[33]
f_{ER}	0.03	87	[33]
F	96.487 C μM^{-1}	86	
N_{av}	6.022 10^{23} mol^{-1}	1	

Ad, adjusted to fit the integrated experimental values for whole system.

doi:10.1371/journal.pone.0152869.t001

Table 2. Cell metabolism and membrane current parameters.

Parameter	Value (units)	Eq.	Ref.
ATD_in	1.5	2	Ad
t_{ATD}	100 s	2	Ad
ATD_m	32	4	Ad
K_{GF}	5200 μM	4	[195]
k_{GFr}	7.4	4	Ad
hgla	5	4	[195]
FFA	0 μM	4	Ad
AT	4000 μM	5	[33]
V_P_in	-62 mV	8	Ad
g_{mKATPi}	24,000 pS	9	[33]
E_K	-75 mV	9	[29]
K_{KPI2}	1125 # μm^{-2}	10	[38]
k_{dd}	17 μM	11	[29]
k_{td}	26 μM	11	[29]
k_{tt}	50 μM	11	[29]
k_{KPKa}	1.	13	Ad
g_{mKr}	45000 pS	15	[29]
V_{dKr}	-9 mV	16	[29]
k_{dKr}	5 mV	16	[29]
g_{mCa}	900 pS	18	Ad
E_{Ca}	100 mV	18	[29]
V_{dCa}	-19 mV	19	[33]
k_{dCa}	9.5 mV	19	[33]
K_{dCap}	0.01	19	Ad
V_{fCa}	-9 mV	20	[29]
k_{fCa}	8 mV	20	[29]
gmSOC	10 pS	21	Ad
K_{NS}	200 μM	22	[196]
P_{mCa}	6000 fA	23	Ad
K_{pCa}	0.2 μM	23	Ad
E_{Na}	70 mV	24	[29]
g_{mNb}	10 pS	25	Ad
gmNM3	0 pS	25	Ad

Ad, adjusted to fit the integrated experimental values for whole system.

doi:10.1371/journal.pone.0152869.t002

and

$$\mathrm{Glu} = \mathrm{Glu_i} + \mathrm{Glu1}\ (\mathrm{t} > \mathrm{t1}) \tag{7}$$

where ADP_f and ATP are concentrations of free ADP and ATP in cytoplasm, Glu and FFA are the concentrations of glucose and free fatty acid in surrounding medium. ATD_o is the steady-state ATP/ADP ratio. Glu_i is the initial Glu concentration. Glu1 is the change in Glu in time (t1).

The dependence of ATD_o on extracellular concentration of glucose and FFA (Eq 4) was suggested as a Hill function with saturated value (ATD_m), K_{GF} is the coefficient for half-saturated glucose and FFA concentrations, hgla is the the Hill coefficient, k_{GFr} is the coefficient for a conversion from FFA to glucose concentration, t_{ATD} is the time constant (Table 2).

Table 3. Initial values and coefficients for receptors and G-proteins.

Parameter (units)	Initial values and coefficients (Eq 46)		Initial values and coefficients (Eq 47)		Initial values and coefficients (Eq 48)	
Ligand (L_n, μM)	GLP1i	$3.1\ 10^{-7}$	GIPi	$1.37\ 10^{-6}$	AR3i	0.002
Re_{nd} (# μm^{-2})	ReGLd_in	0.1	ReGId_in	0.1	ReARd_in	0.1
L_nR_n (# μm^{-2})	LR1_in	0.01	LR2_in	0.01	LR3_in	0.01
$L_nR_nG_n$ (# μm^{-2})	LRG1_in	0.01	LRG2_in	0.01	LRG3_in	0.01
$G_{\alpha nGTP}$ (# μm^{-2})	GaT1_in	0.01	GaT2_in	0.01	GaT3_in	0.01
$G_{\alpha nGDP}$ (# μm^{-2})	GaD1_in	0.01	GaD2_in	0.01	GaD3_in	0.01
$G_{\alpha nGTP}E_n$ (#μm^2)	AC_{GLP}_in	0.3	AC_{GIP}_in	0.3	AC_{AR}_in	0.3
Re_{nt} (# μm^{-2})	Re_{GLt}	2	Re_{GIt}	2.5	Re_{ARt}	3
G_{nt} (# μm^{-2})	G1t	20	G2t	25	G3t	20
E_{nt} (#μm^{-2})	AC_{pt}	3	AC_{pt}	3	AC_{pt}	3
K_L (μM)	K_{GLP1}	$3.1\ 10^{-5}$	K_{GIP}	$1.71\ 10^{-4}$	K_{AR3}	0.3
k_{1n} ($\mu M^{-1}\ s^{-1}$)	R11	7	R21	7	R31	7
k_{2n} ($\#^{-1}\ \mu m^2\ s^{-1}$)	R12	1	R22	1	R32	1
k_{2nr} (s^{-1})	R12r	0.68	R22r	0.68	R32r	0.68
k_{3n} (s^{-1})	R13	0.7	R23	0.7	R33	0.7
k_{4n} ($\#^{-1}\ \mu m^2\ s^{-1}$)	R14	1	R24	1	R34	1
k_{5n} (s^{-1})	R15	0.026	R25	0.026	R35	0.026
k_{6n} (s^{-1})	R16	0.4	R26	0.4	R36	0.4
k_{7n} ($\#^{-1}\ \mu m^2\ s^{-1}$)	R17	1.	R27	1	R37	1
k_{8n} (s^{-1})	R18	0.00005	R28	0.00005	R38	0.00005
k_{9n} (s^{-1})	R19	$2.83\ 10^{-4}$	R29	$2.83\ 10^{-4}$	R39	$2.83\ 10^{-4}$

doi:10.1371/journal.pone.0152869.t003

Table 4. Initial values and coefficients for receptors and G-proteins (continuation).

Parameter (Units)	Initial value and coefficients (Eq 49)		Initial value and coefficients (Eq 50)	
Ligand (L_n) (μM)	AM3i	0.022	AR7i	0.0506
R_nG_n (#μm^{-2})	RG6_in	0.01	NA	NA
R_{nd} (# μm^{-2})	Re_{M3d}_in	0.1	Re_{R40d}_in	0.1
L_nR_n (# μm^{-2})	NA	NA	LR7_in	0.01
$L_nR_nG_n$ (# μm^{-2})	LRG6_in	0.01	LRG7_in	0.01
$G_{\alpha nGTP}$(# μm^{-2})	GaT6_in	0.01	GaT7_in	0.01
G_{anGDT} (# μm^{-2})	G_aD6_in	0.01	GaD7_in	0.01
$G_{\alpha nGTP}E_n$ (# μm^{-2})	PLC_{M3}_in	0.1	PLC_{R40}_in	0.1
R_{nt} (# μm^{-2})	Re_{M3t}	2	Re_{R40t}	2
G_{nt} (# μm^{-2})	G6t	20	$G7_t$	20
E_{nt} (# μm^{-2})	PLC_{pt}	3	PLC_{pt}	3
K_M (μM)	K_{AM3}	0.22	K_{AR7}	4.6
k_{1n} ($\mu M^{-1}\ s^{-1}$)	R61	10	R71	7
k_{2n} ($\#^{-1}\ \mu m^2 s^{-1}$)	R62	0.68	R72	1
k_{2nr} (s^{-1})	R62r	6.8	R72r	0.68
k_{3n} (s^{-1})	R63	0.65	R73	0.7
k_{4n} ($\#^{-1}\ \mu m^2\ s^{-1}$)	R64	1	R74	1
k_{5n} (s^{-1})	R65	0.026	R75	0.026
k_{6n} (s^{-1})	R66	0.4	R76	0.4
k_{7n} ($\#^{-1}\ \mu m^2\ s^{-1}$)	R67	1	R77	1
k_{8n} (s^{-1})	R68	0.007	R78	$5\ 10^{-5}$
k_{9n} (s^{-1})	R69	0.00105	R79	$2.83\ 10^{-4}$

doi:10.1371/journal.pone.0152869.t004

Table 5. Parameters and coefficients for calmodulin and cAMP pathways.

Parameter	Value (units)	Eq.	Ref.
CaCaM_in	0.42 μM	51	[25]
k_{1f}	2.3 10^3 μM s^{-1}	51	[23]
k_{1b}	2.4 10^3 s^{-1}	51	[23]
k_{2f}	2.3 10^3 μM s^{-1}	52	[23]
k_{2b}	2.4 $10^3 s^{-1}$	52	[23]
k_{3f}	160 10^3 μM s^{-1}	53	[23]
k_{3b}	405 10^3 s^{-1}	53	[23]
k_{4f}	160 10^3 μM s^{-1}	54	[23]
k_{4b}	405 10^3 s^{-1}	54	[23]
CaMo	11.25 μM	55	[23]
kda	0.01	57	Ad
AC_{pt}	3 # μm^{-2}	59	Ad
V_{mCaM}	2 μmol s^{-1}	63	Ad
K_{PCaM}	0.348 μM	64	[23]
K_{NCa}	75 μM	64	[23]
V_{mACc}	0.2 μmol s^{-1}	65	Ad
K_{mAACS}	1030 μM	65	[197]
K_{mCACS}	0.5 μM	65	Ad
k_{ACS}	0.01 μmol s^{-1}	65	Ad
k_{ipdei}	1	66	Ad
V_{gpde}	0.04 μmol s^{-1}	66	[23]
V_{cpde}	1.4 μmol s^{-1}	66	Ad
K_{dpe}	0.348 μM	66	[23]
K_{pde}	3 μM	66	[23]
PKAa_in	0.24	67	[25]
k_{ak}	1	67	Ad
t_{pka}	900 s	67	[198]
K_{pcm}	2.9 μM	69	[24]
hpca	1.4	69	[24]
EPa_in	0.01	70	Ad
t_{ep}	900 s	70	[25]
K_{mep}	20.2 μM	72	[199]
hce	2	72	Ad

doi:10.1371/journal.pone.0152869.t005

The coefficients K_{GF} and hgla were taken from work [195] where these data were evaluated for human β-cell. The scaling coefficient k_{GFr} was evaluated using data for FFAR1/GPR40 knockout mice because FFA can also activate FFAR1/GPR40 receptor affecting on GSIS. According to Fig 5A from [204] insulin secretion at 8.3 mM glucose and 0.5 mM palmitate is about the same as for 12 mM glucose in FFAR1/GPR40 knockout mice islets. In this case k_{GFr} = 7.4 (example calculated for palmitate concentration).

Membrane potential, channels and pumps

Plasma membrane potential. Increased extracellular glucose promotes membrane depolarization. Several ionic channels regulate this process. A diagram of the main β-cell specific channels considered here is presented in Fig 1. We used our models of electrophysiological processes in the β-cell [29, 30, 33] as a framework. However, only the most important currents

Table 6. Parameters and coefficients for PLC pathway and Ca^{2+} handling.

Parameter	Value (units)	Eq.	Ref.
P4P_in	4000 # μm^{-2}	73	[200]
k_{PI}	0.0015s^{-1}	73	Ad
k_{PIr}	0.006 s^{-1}	73	[200]
k_{P4P}	0.02 s^{-1}	73	[200]
k_{P4Pr}	0.014 s^{-1}	73	[200]
PI	140,000 # μm^{-2}	73	[201]
K_{CaPI}	0.3	74	Ad
K_{P4PK}	0.5	74	Ad
k_{cpi}	0.2	74	Ad
PIP2_in	4200 # μm^{-2}	75	Ad
K_{PIP2}	2370 # μm^{-2}	76	Ad
k_{pPL}	15 μmol s^{-1}	77	Ad
V_{mPLPi}	700 μmol s^{-1}	78	Ad
K_{CaPL}	0.4 μM	78	[33]
V_{mPLC}	50 μmol s^{-1}	81	Ad
K_{CCaPL}	0.2 μM	81	Ad
IP_3_in	1 μM	82	Ad
k_{dIP3}	0.04 s^{-1}	82	[33]
DAG_in	23 # μm^{-2}	83	[200]
k_{dDAG}	0.05 s^{-1}	83	[200]
PKCa_in	0.1	84	Ad
k_{PKC}	3E-6 s^{-1}	84	Ad
k_{PKCr}	0.0034 $\mathbf{s^{-1}}$	84	[202]
Cac_in	0.09 μM	86	Ad
k_{sg}	0.00001 s^{-1}	86	Ad
Ca_{ER}_in	160 μM	87	Ad
P_{CaER}	6 μmol s^{-1}	88	Ad
K_{ser}	0.4 μM	88	Ad
k_{mIP}	7 μM s^{-1}	89	Ad
k_{leak}	0.002 s^{-1}	89	Ad
K_{RPCa}	0.35 μM	90	Ad
K_{IP3}	3.2 μM	90	[33]
K_{IP3R}	0.5	90	Ad

doi:10.1371/journal.pone.0152869.t006

were taken into account to achieve the desired granularity. For simplification Boltzman-type equations in steady-state were employed for activation (d_i) and inactivation functions (f_i) to avoid a simulation of spike activity.

We modeled the electrophysiological events for one cell. The plasma membrane (PM) potential in a single β-cell can be described with the following current balance differential equation

$$V_p/dt = -(I_{KATP} + I_{Kr} + I_{Ca} + I_{SOC} + I_{PCa} + I_{Nab})/C_m \quad (8)$$

where V_p is the PM potential, t is the time, C_m is the whole-cell membrane capacitance, I_{KATP} is the ATP-sensitive K^+ channel current, I_{Kr} is the voltage-dependent K^+ current, I_{Ca} is the high-voltage-activated Ca^{2+} current, I_{SOC} is the store-operated current activated by decrease of

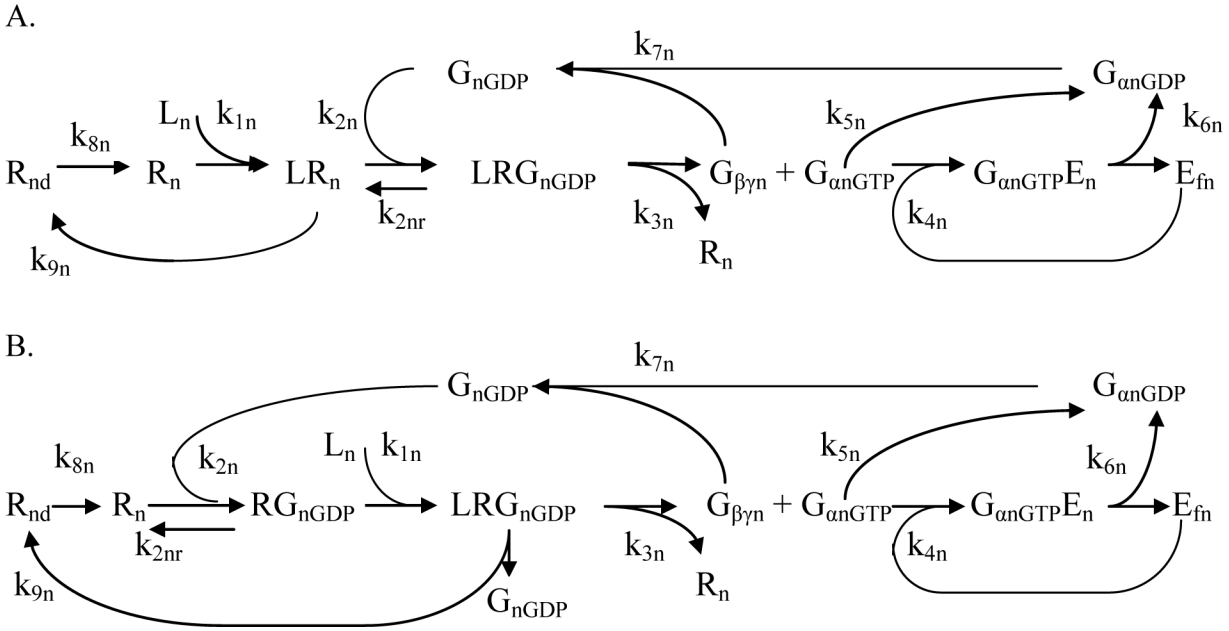

Fig 13. Diagram of the kinetic model of ligand, G protein and target enzyme interactions. R_{nd} is the desensitized receptor, R_n is the free receptor, L_n is the ligand, LR_n is the receptor bound with ligand, LRG_{nGDP} is the receptor bound with ligand and G protein, G_{nGDP} is the G proteins consisting of subunits α, β and γ. In this ground state the α-subunit is bound to GDP. $G_{\alpha nGTP}$ is the GTP-bound α subunit of G protein, $G_{\beta\gamma n}$ is the β and γ subunit of G protein, $G_{\alpha nGDP}$ is GDP-bound α subunit of G protein, $G_{\alpha nGTP}E_n$ is the complex of the α-subunit carries the GTP and effectors enzyme (E_n). E_{fn} is the enzyme that is not bound with G protein. The constants can be identified by their subcripts, where n the forward transition and nr is the reverse transition. For reversible reactions (double arrows), forward reactions are in the direction of association. (A) Collision coupling model. (B). Pre-coupling of receptor and G-protein model.

doi:10.1371/journal.pone.0152869.g013

Ca^{2+} in ER, I_{PCa} is the plasma membrane Ca^{2+}-pump current, I_{Nab} is the Na^+ background current, that can be activated also by muscarinic acetylcholine M_3 receptor.

ATP-sensitive K^+ channels current (I_{KATP})

We adopted a kinetic model [29, 33] for whole-cell ATP-sensitive K^+ channels current (I_{KATP}). However, a dependence of this current on PIP_2 and PKA activation was also found and we introduced the corresponding factors. The influence of PIP_2 was represented as Michaelis-Menten function (f_{KPI}, Eq 10) where PIP_2 increase can enchance I_{KATP}.

Both SUR1 and $K_{ir6.2}$ subunits contain consensus PKA phophorylation sites and, for example, GLP-1 dependent activation of PKA leads to phosphorylation of SUR1 subunits lowering their affinity for ADP [205, 206]. For simplicity we introduced this dependence as a function (f_{KPKa}, Eq 13) where an activated PKA (PKA_a) decreases the calculated $[MgADP_f]_c$ leading to additional I_{KATP} decrease.

$$I_{KATP} = g_{mKATP}\, f_{KPI}\, O_{KATP}\, (V_P - E_K) \tag{9}$$

where

$$f_{KPI} = PIP_2/(PIP_2 + K_{KPI2}) \tag{10}$$

$$O_{KATP} = \frac{0.08\,(1 + 2\,MgADP_f/k_{dd}) + 0.89\,(MgADP_f/k_{dd})^2}{(1 + MgADP_f/k_{dd})^2\,(1 + 0.45\,MgADP_f/k_{td} + ATP_f/k_{tt})} \tag{11}$$

$$MgADP_f = 0.055\, f_{KPKa}\, ADP_f \quad (12)$$

$$f_{KPKa} = 1/\,(1 + k_{KPKa}\, PKA_a) \quad (13)$$

$$g_{mKATP} = g_{mKATPi} + g_{mKATP1}\ (t > t9) \quad (14)$$

where g_{mKATP} is is the maximum conductance for I_{KATP}, g_{mKATPi} is the initial conductance, g_{mKATP1} is the increase in conductance in time (t9). E_K is the reversal potential for K^+ current, PIP_2 is the PIP_2 content on PM, K_{KPI2} is the activation constant, O_{KATP} is the fraction of open K_{ATP} channels, k_{dd}, k_{td} and k_{tt} are the dissotiation coefficients, $MgADP_f$ is free Mg-bound ADP, ATP_f and ADP_f are free ATP and ADP concentrations in cytoplasm; k_{KPKa} is the inhibition constant.

To determine K_{KPI2} (Eq 10) we suggest that f_{KPI} dependence corresponds to PIP_2 dose-dependent activation of K_{ATP} channels (in absence GST-Syn-1A) where EC_{50} values for PIP2 was calculated as 2.38±0.81 μM [38] or 1125 #/μm^{-2} in our definition (see Eq 1).

Voltage-gated K^+ current (I_{Kr})

Different voltage gated K^+ currents (I_{Kr}) were also registrated in β-cell. For example, delayed rectifier K^+ current is main voltage-dependent K^+ current in rodents [207]. This current activates at membrane potential near -30 mV and then increased with the applied voltage, an inactivation was negligible during at least 200 ms depolarization [208]. The Hodgkin-Huxley-type with stationary dependences for delayed rectifier K^+ current and some corresponding coefficients were used from our previous mouse and human β-cell model to describe I_{Kr} [29, 30].

$$I_{Kr} = g_{mKr}\, d_{Kri}^{\ 2}\, f_{Kri}\, (V_P - E_K), \quad (15)$$

where

$$d_{Kri} = 1/(1 + \exp[(V_{dKr} - V_P)/\, k_{dKr}]) \quad (16)$$

$$f_{Kri} = 1 \quad (17)$$

g_{mKr} is the maximum conductance for I_{Kr}, V_{dKr} is the half-activation potential, k_{dKr} is the slope of half-activation potential.

Ca^{2+} current (I_{Ca})

I_{Ca} was modeled as L-type Ca^{2+} channel with one inactivation gating variables [29] without time dependent parameters

$$I_{Ca} = g_{mCa}\, d_{Cai}\, f_{Cai}\, (V_P - E_{Ca}) \quad (18)$$

where

$$d_{Cai} = 1/(1 + \exp[(V_{dCa} - V_P)/k_{dCa}])\ + k_{dCap} \quad (19)$$

$$f_{Cai} = 1/\,(1 + \exp[-(V_{fCa} - V_P)/\, k_{fCa}] \quad (20)$$

where g_{mCa} is the maximum conductance for I_{Ca}, E_{Ca} is the reversal potential for Ca^{2+} current, V_{dCa} is the half-activation potential, k_{dCa} is the slope of half-activation potential, k_{dCap} is the coefficient of the constitutive channel activity, V_{fCa} is the half-inactivation potential, k_{fCa} is the slope of half-inactivation potential.

Store-operated Ca^{2+} current (I_{SOC})

$[Ca^{2+}]_{ER}$ decrease activates the Ca^{2+} release-activated Ca^{2+} current through PM. Interestingly, in human Jurkat leukaemic T cells expressing an ER-targeted Ca^{2+} indicator, SOC channel activation follows the function of $[Ca^{2+}]_{ER}$, reaching half-maximum at ~200 μM with a Hill coefficient of ~4 [196]. We use these dependence and coefficients in our model (Table 2). We consider I_{SOC} as a voltage-independent Ca^{2+} inward current

$$I_{SOC} = g_{mSOC}\, f_{SOC}\, (V_p - E_{Ca}) \tag{21}$$

where

$$f_{SOC} = K_{NS}{}^4 / (K_{NS}{}^4 + [Ca^{2+}]_{ER}{}^4) \tag{22}$$

g_{mSOC} is the maximum whole-cell conductance, f_{SOC} is the $[Ca^{2+}]_{ER}$ dependent function, K_{NS} is the $[Ca^{2+}]_{ER}$ inhibition constant.

Plasma membrane Ca^{2+} pump current (I_{PCa})

Ca^{2+} pumps provide an outward current and also contribute to V_p. The corresponding equation was adapted from previous model [33]

$$I_{PCa} = P_{mCa}[Ca^{2+}]_c{}^2 / (K_{pCa}{}^2 + [Ca^{2+}]_c{}^2) \tag{23}$$

where P_{mCa} is the maximum I_{PCa} current, K_{pCa} is the $[Ca^{2+}]_c$ activation constant.

Na^+ background current (I_{Nab})

The model contains a voltage-independent Na^+ background current. This current can depolarize the resting PM potential and modifies mouse and human β-cell electrical activity (see for details [29, 30, 33]). We have also included the specific NALCN channels, that activatable by the muscarinic acetylcholine M_3 receptor. Than

$$I_{Nab} = g_{Nab}\, (V_p - E_{Na}) \tag{24}$$

where

$$g_{Nab} = g_{mNb} + g_{mNM3}\, LRG_6 \tag{25}$$

E_{Na} is the reversal potential for Na^+, g_{mNb} is the permanent conductance for I_{Nab}, g_{mNM3} is the maximum conductivity of NALCN channels and LRG_6 is the M_3 receptor bound with ligand and G-protein (see below).

Receptors, G-proteins and target enzymes

Plasma membrane receptors and G proteins usually possess a high number of distinct binding domains inducing the formation of large multiprotein signaling complexes. In quantitative models of GPCR signaling that incorporate these varied states, parameter values are often uncharacterized or varied over large ranges, making identification of important parameters and signaling outcomes difficult [53]. However, despite their diversity, signaling pathways in β-cells employ a set of common components that we have used for modeling. Fig 13 shows the reaction scheme for the minimal model of a receptor cascade. We modeled two different proposals about ligand-receptor interactions that were suggested in literature: 1. Collision coupling model, where a ligand binds to the free receptor and then the ligand-receptor complex "collides" with the free G-protein (Fig 13A). 2. Pre-coupling model where stable receptor/G-protein complex exists in the absence of ligand and ligand bounds with this complex (Fig 13B).

In the collision coupling model the initial steps in GPCR signaling take place in the plasma membrane and involve the binding of a ligand (L_n) to a receptor that rapidly shifts an inactive receptor (R_n) to an active state (L_nR_n). In the following steps the activated receptor couples to

heterotrimeric G proteins ($G_{\alpha\beta\gamma nGDP}$). In pre-coupling model the initial steps in GPCR signaling take place also in the plasma membrane. In this case a ligand binds with a receptor/G-protein complex.

The following steps are identical for both models. Heterotrimeric G proteins coupled with receptor activates through the release of a bound guanosine diphosphate (GDP) and the capture of guanosine triphosphate (GTP) on the G protein α-subunit. A series of intra and intermolecular events in the heterotrimer Gαβγ leads to a dissociation of this complex resulting in active Gα·GTP and Gβγ subunits.

Although both Gα·GTP and Gβγ can then activate different signaling pathways and effector proteins, we focus only on the reactions downstream of Gα·GTP activation since it is principal process for receptors, that we considerate in this article. In this case, as laterally diffusing Gα·GTP subunits bind isoforms of inactive (presumably freely diffusing) target enzymes (E_{fn}) on the inner leaflet of the plasma membrane and forming a complex ($G_{\alpha nGTP}$ E_n) (coefficient k_{4n}), that activates or inhibits biochemical processes. Activated G proteins ($G_{\alpha nGTP}$) deactivate through their own GTPase activity (coefficient k_{5n}) (or much faster when bound to E_{fn}, coefficient k_{6n}). This allows $G_{\alpha nGDP}$ to recombine with $G_{\beta\gamma n}$ (coefficient k_{7n}) starting a new cycle.

Cells can fine-tune their excitability by changing the susceptibility of receptors, e.g. switch between active (L_nR_n–in collision coupling model or $L_nR_nG_{nGDP}$ in pre-coupling model) forms and desensitized form (R_{nd}) by regulating the number of receptors via internalization. We have modeled process of desensitization of activated receptor (rate constant—k_{9n}). Internalized receptors can then undergo activation and return to the surface in our model (rate constant—k_{8n}).

Receptor dynamics and G protein cascade. Our model of receptor dynamics is based on several earlier studies [209, 210]. However, we were not able to find a model that matches well to our aims. The majority of these models do not include a G-protein bound with target enzyme. For this reason we constructed a minimal model of the receptor signaling transduction and corresponding target enzymes activations.

Several suggestions were made. Our model assumes that initial concentration of ligand is sufficiently high so that it is not significantly depleted by binding to the receptors and therefore the ligands can be presumed as a fixed concentration. The process of receptors and G-proteins synthesis is assumed to compensate for intracellular receptor and G protein degradation, so that the total area density of receptors and G proteins in different states (free, active, and internalized) remains constant.

We have assumed that the processes occur in the plasma membrane and all the species, except for the agonist, are membrane bound and are diffuse freely. We simplify the model by ignoring the processes, such as the nucleotide exchange on G-proteins that are not bound to the receptor or bound to the receptor that is not bound to the ligand and others. Receptor desensitization was included as a process that can deactivate the receptor-ligand complex. The multiple deactivation and reactivation steps were shortened in single irreversible reactions (see Fig 13).

We modeled two different models of ligand-receptor interactions: 1. Collision coupling model and 2. Pre-coupling model (see Fig 13). Based on the above assumptions and using the law of mass action the collision coupling model suggests that ligands, receptors and G-proteins collide and binds to the corresponding enzyme transiently to produce target enzyme activation. For simplicity, we use concentrations on PM without brackets. Than a collision coupling model is represented as a system of ordinary differential equations:

$$d\,LR_n / dt = k_{1n}\,R_n\,([L_n]/(K_L + ([L_n])) + k_{2nr}\,LRG_n\,LRG_{2n}\,G_n{}^{*}LR_n - LR_{9n}\,LR_n \qquad (26)$$

$$d\ LRG_n\ /\ dt = k_{2n}\ G_n{}^{*}LR_n - k_{2nr}\ LRG_n - k_{3n}\ LRG_n \tag{27}$$

$$d\ R_{nd}\ /\ dt = k_{9n}\ LR_n - k_{8n}\ R_{nd} \tag{28}$$

The following conservation constrain also holds (R_{nt})

$$R_{nt} = R_{nd} + R_n + LR_n + LRG_n \tag{29}$$

or

$$R_n = R_{nt} - R_{nd} - LR_n - LRG_n \tag{30}$$

where $[L_n]$ is the free ligand concentration; K_L is the Michaelis-Menten constant, R_n, LR_n, LRG_n and R_{nd} are, respectively, the area density of free, bound with ligand, bound with ligand and G-protein and internalized (desensitized) receptors and R_{nt} is the total receptor area density in μm^{-2}. (Definition $L_nR_nG_n$ instead $L_nR_nG_{nGDP}$ was used for simplification). k_{1n}, k_{2n}, k_{3n}, k_{8n} and k_{9n} are the forward rate constants and k_{2nr} is the backward rate constant (see Fig 13A).

The first binding step reflects a simple bimolecular interaction between the ligand (L_n) and the receptor (R_n) (coefficient k_{1n}) that is strictly dependent on ligand concentration. According to mass action kinetics, we have assumed that $G_{\alpha nGTP}E_n$ are produced at a rate proportional to the area density of GTP-bound α subunit of G-protein, $G_{\alpha nGTP}$, and the inactive target protein area density (E_{fn}) (coefficient k_{4n}).

$$d\ G_{\alpha nGTP}\ /dt = k_{3n}\ LRG_n - k_{4n}\cdot G_{\alpha nGTP}{}^{*}E_{fn} - k_{5n}\cdot G_{\alpha nGTP} \tag{31}$$

$$d\ G_{\alpha nGTP}E_n/dt = k_{4n}\ G_{\alpha nGTP}{}^{*}E_{fn} - k_{6n}\ G_{\alpha nGTP}E_n \tag{32}$$

$$d\ G_{\alpha nGDP}\ /dt = k_{5n}\ G_{\alpha nGTP} + k_{6n}\ G_{\alpha nGTP}E_n - k_{7n}\ G_{\alpha nGDP}{}^{*}G_{\beta\gamma n} \tag{33}$$

where k_{4n} - k_{7n} are the forward rate constants.

We suggest that the content of the endogenous G-proteins (G_{nt}) and target enzymes (E_{nt}) remain constant

$$G_{nt} = G_{nGDT} + LRG_n + G_{\alpha nGTP} + G_{\alpha nGDP} + G_{\alpha nGTP}E_n \tag{34}$$

or

$$G_{nGDP} = G_{nt} - L_nR_nG_n - G_{\alpha nGTP} - G_{\alpha nGDP} - G_{\alpha nGTP}E_n \tag{35}$$

$$G_{\beta\gamma n} = G_{\alpha nGTP} + G_{\alpha nGDP} + G_{\alpha nGTP}E_n \tag{36}$$

$$E_{nt} = E_{fn} + G_{\alpha nGTP}E_n \tag{37}$$

or

$$E_{fn} = E_{nt} - G_{\alpha nGTP}E_n \tag{38}$$

where G_{nGDP}, LRG_n, $G_{\alpha nGTP}$, $G_{\alpha nGDP}$ and $G_{\alpha nGTP}E_n$ are the area density of free, bound with ligand and receptor, active, inactive and bound with the target enzyme G-proteins, respectively. G_{nt} is the total area density of G_n proteins per unit of PM, both activated and inactivated. E_{fn} is the free target enzyme and E_{nt} is the total area density of the target enzyme.

Pre-coupling mechanism of ligand-receptor interaction suggestes that the stable receptor/G-protein complex exists in the absence of ligand and ligand bounds with this complex (see Fig 13B). Equations for a pre-coupling model can also be obtained similarly Eqs 26–30 as a system of ordinary differential equations:

$$d\ RG_n / dt = k_{2n}\ R_n^* G_n - k_{1n}\ ([L_n]/(K_L + ([L_n])))\ LR_n - k_{2nr}\ R_n^* G_n \quad (39)$$

$$d\ LRG_n / dt = k_{1n}\ [L_n]^* RG_n - k_{3n}\ LRG_n - k_{9n}\ LRG_n \quad (40)$$

$$d\ R_{nd} / dt = k_{9n}\ LRG_n - k_{8n}\ R_{nd} \quad (41)$$

The following conservation constrains also hold

$$R_{nt} = R_{nd} + R_n + RG_n + LRG_n \quad (42)$$

$$R_n = R_{nt} - R_{nd} - RG_n - LRG_n \quad (43)$$

$$G_{nt} = G_{nGDP} + RG_n + LRG_n + G_{\alpha nGTP} + G_{\alpha nGDP} + G_{\alpha nGTP}E_n \quad (44)$$

or

$$G_{nGDP} = G_{nt} - RG_n - LRG_n - G_{\alpha nGTP} - G_{\alpha nGDP} - G_{\alpha nGTP}E_n \quad (45)$$

Other equations for pre-coupling model are similar to the collision coupling model (Eqs 31–38).

Several suggestions were accepted in order to determine of coefficients of both models:

The number of βγ subunits is the same as the number of α subunits, because each G-protein splits into one α and one βγ. Estimated ratio of G-protein to receptors was accepted as ~ 10:1 [211, 212].

Kinetics of ligand binding are usually fast relative to the other processes in the model (see [213]). The fast speed observed for receptor activation in response to saturated concentrations of small agonist molecules (coefficient k_{1n}, Fig 13A) has half-life ($t_{1/2}$) ranges between ≈ 40 and 100 ms in the case of α_{2A}- and β_1-adrenergic receptors, muscarinic M_1- and M_2-receptors [214] ($k = \ln 2/t_{1/2}$). We used a coefficient of receptor ligand binding ($k_{1n} \approx 7\ \mu M^{-1}\ s^{-1}$) for the collision coupled model that corresponds to the half-life about 100 ms.

Coefficient for binding of LR_n with target G protein in the collision coupling model (k_{2n} in Fig 13A) depends on the area density of molecules on PM and was evaluated as $1\ \#^{-1}\mu m^2\ s^{-1}$ [215]. Coefficient for receptor–G-protein unbinding (k_{2nr}) was calculated for collision coupling model as $0.68\ s^{-1}$ and for pre-coupling model as $6.8\ s^{-1}$ [216].

Speed of G-protein activation (coefficient k_{3n} Fig 13A and 13B) is slow (half-life $t_{1/2} \approx 1$ sec) [214]. This values corresponds $k_{3n} \approx 0.7\ s^{-1}$. It is close to $0.8\ s^{-1}$ evaluated by [217] or $1\ s^{-1}$ [218].

Binding of $G_{\alpha nGTP}$ with target enzyme E_{fn} (coefficient k_{4n} in Fig 13A and 13B) was evaluated by [216] as $1\ \#^{-1}\mu m^2\ s^{-1}$. Deactivation of $G_{\alpha nGTP}$ through its own GTPase activity (coefficient k_{5n} Fig 13A and 13B) was evaluated by [216] as $0.026\ s^{-1}$. Dissociation of complex of G protein and target enzyme (coefficient k_{6n} Fig 13A and 13B) was evaluated by us as $0.4\ s^{-1}$. The recombination of α and βγ subunits (coefficient k_{7n} in Fig 13A) is thought not to be limiting and was evaluated as $1\ \mu m^2\ s^{-1}$ [216, 218]. Typical rate constants for desensitization of activated receptor (k_{9n}) and its return to the surface (k_{8n}) in our model was taken from model for slow GLP-1 receptor kinetics [24] ($k_{8n} = 5\ 10^{-5}\ s^{-1}$ and $k_{9n} = 0.000283\ s^{-1}$). We used these

parameters and coefficients if no additional experimental data can be found in literature for some receptors, corresponding G proteins or target enzymes.

Tonic receptor effects are simulated by including the presence of low concentrations of corresponding receptor ligands even when the experiments were simulated without specific agonists.

GLP-1R (R_1). We used the collision coupling model for this receptor. The processes were described similar to Eqs 26–40)

$$d\ LR1\ /\ dt = R_{11}\ Re_{GL}\ (GLP1/(K_{GLP1} + GLP1) + R_{12r}\ LRG1 - R_{12}\ G1^{*}LR1 - R_{19}\ LR1 \quad (46)$$

$$d\ LRG1\ /\ dt = R_{12}\ G1^{*}LR1 - R_{12r}\ LRG1 - R_{13}\ LRG1$$

$$d\ Re_{GLd}\ /\ dt = R_{19}\ LR1 - R_{18}\ Re_{GLd}$$

$$d\ G_{aT1}\ /\ dt = R_{13}\ LRG1 - R_{14}\ G_{aT1}{}^{*}AC_{pf} - R_{15}\ G_{aT1}$$

$$d\ AC_{GLP}\ /\ dt = R_{14}\ G_{aT1}{}^{*}AC_{pf} - R_{16}\ AC_{GLP}$$

$$d\ G_{aD1}\ /\ dt = R_{15}\ G_{aT1} + R_{16}\ AC_{GLP} - R_{17}\ G_{aD1}{}^{*}G_{bg1}$$

$$Re_{GL} = Re_{GLt} - Re_{GLd} - LR1 - LRG1$$

$$G_{1} = G_{1t} - LRG_{1} - G_{aT1} - G_{aD1} - AC_{GLP}$$

$$G_{bg1} = G_{aT1} + G_{aD1} + AC_{GLP}$$

$$GLP1 = GLP1i + GLP11\ (t > t2)$$

GLP1 was used instead $[L_n]$, GLP1i is the initial GLP-1 concentration. GLP11 is the increase in GLP1 in time (t2), K_{GLP1} was used instead K_L and R_{1X} instead the corresponding coefficients (see Table 3). AC_{GLP} is the PM bound AC activated by GLP-1 receptor. The parameters and coefficients can be identified by their subscripts, where 1 was used instead n (Table 3).

Specific concentrations and coefficients: According [219] the amount of GLP-1R (Re_{GLt}) in one INS-1 cell is about 2,000, i.e. it can be evaluated as about 2 # μm^{-2} (if cell surface is about 1000 μm^{-2}). Half saturation ($\log_{10}M$ = -10.5) for GLP1 was measured as an increase in cAMP production in the pancreatic β-cell line (Fig 5 from [220]), that we used for evaluation of K_{GLP1} (0.000031 μM, Table 3). Other coefficients were chosen as general coefficients.

GIPR (R_2). Regulated mechanisms for GIP receptor are assumed to be similar to those of GLP-1R.

$$d\ LR2 / dt = R_{21}\ R_{eGI}\ GIP/(K_{GIP} + GIP) + R_{22r}\ LRG2 - R_{22}\ G2^{*}LR2 - R_{29}\ LR2 \qquad (47)$$

$$d\ LRG2 / dt = R_{22}\ G2^{*}LR2 - R_{22r}\ LRG2 - R_{23}\ LRG2$$

$$d\ Re_{GId} / dt = R_{29} \cdot LR2 - R_{28} \cdot Re_{GId}$$

$$d\ G_{\alpha T2} / dt = R_{23}\ LRG_2 - R_{24}\ G_{\alpha T2}{}^{*}AC_{pf} - R_{25}\ G_{\alpha T2}$$

$$d\ AC_{GIP} / dt = R_{24}\ G_{\alpha T2}{}^{*}AC_{pf} - R_{26}\ AC_{GIP}$$

$$d\ G_{\alpha D2} / dt = R_{25}\ G_{\alpha T2} + R_{26}\ AC_{GIP} - R_{27}\ G_{\alpha D2}{}^{*}G_{bg2}$$

$$Re_{GI} = Re_{GIt} - Re_{GId} - LR_2 - LRG_2$$

$$G2 = G_{2t} - LRG_2 - G_{aT2} - G_{aD2} - AC_{GIP}$$

$$G_{bg2} = G_{aT2} + G_{aD2} + AC_{GIP}$$

$$GIP = GIP_i + GIP1\ (t > t3)$$

GIP was used instead $[L_n]$, K_{GIP} instead K_L and R_{2X} instead the corresponding coefficients (see Table 3). AC_{GIP} is the PM bound AC_p activated by GIP receptor. GIP_i is the initial GIP concentration. GIP1 is the increase in GIP in time (t3). The parameters and coefficients can be identified by their subscripts, where 2 was used instead n (Table 3).

Specific concentrations and coefficients: INS-1 cells expressed an average of 2443μ400 GIP receptors (G_{2t}) on the cell surface or ~ 2.5 # μm^{-2} [221]. EC_{50} for GIP was evaluated as 171 pM for activation cAMP production [222], i.e. K_{GIP} = 0.000171 μM. Other coefficients were chosen as the general coefficients.

α2A-adrenergic receptor (R3). A model of α_{2A} adrenergic receptor activation in β-cell was constructed as a collision coupling model. In this case an active $G_{\alpha}GTP$ messenger ($G_{\alpha T3}$)

released from stimulated receptor binds to the enzyme AC_{pf}.

$$d\ LR3\ /\ dt = R_{31}\ Re_{AR}\ AR_3/(K_{AR3} + AR_3) + R_{32r}\ LRG3 - R_{32}\ G_3{}^{*}LR_3 - R_{39}\ LR_3 \qquad (48)$$

$$d\ LRG3\ /\ dt = R_{32}\ G3^{*}LR3 - R_{32r}\ LRG3 - R_{33}\ LRG3$$

$$d\ Re_{ARd}\ /\ dt = R_{39}{\cdot}LR3 - R_{38}{\cdot}Re_{ARd}$$

$$d\ G_{\alpha T3}\ /\ dt = R_{33}\ LRG_3 - R_{34}\ G_{\alpha T3}{}^{*}AC_{pf} - R_{35}\ G_{\alpha T3}$$

$$d\ AC_{AR}\ /dt = R_{34}\ G_{\alpha T3}{}^{*}AC_{pf} - R_{36}\ AC_{AR}$$

$$d\ G_{\alpha D3}\ /dt = R_{35}\ G_{\alpha T3} + R_{36}\ AC_{AR} - R_{37}\ G_{\alpha D3}\ G_{bg3}$$

$$Re_{AR} = Re_{ARt} - Re_{ARd} - LR_3 - LRG_3$$

$$G_3 = G_{3t} - LRG_3 - G_{aT3} - G_{aD3} - AC_{AR}$$

$$G_{bg3} = G_{aT3} + G_{aD3} + AC_{AR}$$

$$AR_3 = AR_{3i} + AR_31\ (t > t4)$$

AR_3 was used instead $[L_n]$, K_{AR3} instead K_L and R_{3X} instead the corresponding coefficients (see Table 3). AR_{3i} is the initial AR_3 concentration. AR_{31} is the increase in AR_3 in time (t4), AC_{AR} is the PM bound AC activated by α_{2A}-adrenergic receptor. The parameters and coefficients can be identified by their subscripts, where 3 was used instead n (Table 3).

Specific concentrations and coefficients: Noradrenaline (norepinephrine) was shown to be a potent inhibitor of GSIS from rat pancreatic islets, with half-maximal inhibition of the secretory response to 20 mM-glucose occurring at approx. 0.3 μM [223], and we accepted this value for the coefficient K_{AR3}. Other coefficients were chosen as the general coefficients.

Basal concentrations of GLP-1R, GIPR and AdR, that determinate constitutive receptor activity, were taken in such manner that 0.1 AC_P was bound for each receptor (see Eq 59).

M3 muscarinic receptor (R_6). We used the pre-coupled model for this receptor.

$$d\ RG_6 / dt = R_{62}\ Re_{M3}{}^{*}G_6 - R_{61}\ RG_6\ AM_3 / (K_{AM3} + AM_3) - R_{62r}\ RG_6 \quad (49)$$

$$d\ LRG_6 / dt = R_{61}\ RG_6\ AM_3 / (K_{AM3} + AM_3) - R_{63}\ LRG_6 - R_{69}\ LRG_6$$

$$d\ Re_{M3d} / dt = R_{69} \cdot LRG_6 - R_{68} \cdot Re_{M3d}$$

$$d\ G_{\alpha T6} / dt = R_{63}\ LRG_6 - R_{64}\ G_{\alpha T6}{}^{*}PLC_{pf} - R_{65}\ G_{\alpha T6}$$

$$d\ PLC_{M3} / dt = R_{64}\ G_{\alpha T6}{}^{*}\ PLC_{pf} - R_{66}\ PLC_{M3}$$

$$d\ G_{\alpha D6} / dt = R_{65}\ G_{\alpha T6} + R_{66}\ PLC_{M3} - R_{67}\ G_{\alpha D6}{}^{*}G_{bg6}$$

$$Re_{M3} = Re_{M3t} - Re_{M3d} - RG_6 - LRG_6$$

$$G_6 = G_{6t} - RG6 - LRG6 - G_{aT6} - G_{aD6} - PLC_{M3}$$

$$G_{bg6} = G_{aT6} + G_{aD6} + PLC_{M3}$$

$$AM_3 = AM_{3i} + AM_{31}\ (t > t6)$$

AM_3 was used instead $[L_n]$, K_{AM3} instead K_L and R_{6X} instead the corresponding coefficients (see Table 4). PLC_{M3} is the PM bound PLC activated by M_3 muscarinic receptor; PLC_{pf} is the free PLC on PM (see Eq 88). AM_{3i} is the initial AM_3 concentration. AM_{31} is the increase in AM_3 in time (t6). The parameters and coefficients can be identified by their subscripts, where 6 or M_3 were used instead n.

Specific concentrations and coefficients: acetylcholine and carbachol (MR agonist) have different K_{AM3}. We used the coefficients by Hoffman et al [224] for acetylcholine in human M_3 muscarinic receptor (see Table 4). Agonists such as acetylcholine, carbachol or muscarine activate each receptor construct with half-maximal activation times between 60 and 70ms for human M3 muscarinic receptor [225] (coefficient R_{61}) (or $R_{61} = 10\ s^{-1}$).

Receptor deactivation kinetics was found to be slow and independent of agonist concentrations [224] (coefficient R_{62r} was taken according [216]). R_{68} (coef k_{8n} in Fig 13B) was evaluated as the coefficient of M_3 receptor dephosphorylation in work [226]. Human M_3 receptors were internalized with a half life of 11 min (660 s) for M_3 receptors expressed in COS-7 cells and in the presence of 10^{-3} M carbamylcholine (for receptor activation) [227] and we determined the coefficient R_{69} from these data. Other coefficients were chosen as general coefficients (Table 4).

FFAR1/GPR40 (R_7). A model for FFAR1/GPR40 was made as for collision coupling model receptors.

$$d\ LR7 / dt = R_{71}\ Re_{R40}\ AR_7 / (K_{AR7} + AR_7) + R_{72r}\ LRG_7 - R_{72}\ G7^*LR_7 - R_{79}\ LR_7 \quad (50)$$

$$d\ LRG7 / dt = R_{72}\ G_7{}^*LR_7\ R_{72r}\ LRG_7 - R_{73}\ LRG_7$$

$$d\ Re_{R40d} / dt = R_{79} \cdot LR_7 - R_{78} \cdot Re_{R40d}$$

$$d\ G_{\alpha T7} / dt = R_{73}\ LRG_7 - R_{74}\ G_{\alpha T7}{}^*PLC_{Pf} - R_{75}\ G_{\alpha T7}$$

$$d\ PLC_{R40} / dt = R_{74}\ G_{\alpha T7}{}^*\ PLC_{pf} - R_{76}\ PLC_{R40}$$

$$d\ G_{\alpha D7} / dt = R_{75}\ G_{\alpha T7} + R_{76}\ PLC_{R40} - R_{77}\ G_{\alpha D7}{}^*G_{bg7}$$

$$Re_{R40} = Re_{R40t} - Re_{R40d} - LRG_7 - LR_7$$

$$G_7 = G_{7t} - LRG_7 - G_{aT7} - G_{aD7} - PLC_{R40}$$

$$G_{bg7} = G_{aT7} + G_{aD7} + PLC_{R40}$$

$$AR_7 = AR_{7i} + AR_{71}\ (t > t7)$$

AR_7 was used instead $[L_n]$, K_{AR7} instead K_L and R_{7X} instead the corresponding coefficients (see Table 4). PLC_{R40} is the PM bound PLC activated by FFAR1/GPR40 receptor. AR_{7i} is the initial AR_7 concentration. AR_{71} is the increase in AR_7 in time (t7). The parameters and coefficients can be identified by their subscripts, where 7 or R40 were used instead of n.

Specific concentrations and coefficients: K_{AR7} for AR7 was evaluated as palmitic acid potency (EC_{50}) to induce $[Ca^{2+}]_c$ rise in mouse CHO cells expressing FFAR1/GPR40 [167]. Other coefficients were chosen as the general coefficients.

Basal concentrations of FFAR1/GPR40 and AR_7, that determinate constitutive receptor activity, were taken in such manner that 0.1 PLC_{Pt} was bound for each receptor (see Eq 79).

Calmodulin

Ca^{2+} binds to calmodulin (CaM) in four steps and generates four species of Ca^{2+}-bound calmodulin: CaCaM, Ca_2CaM, Ca_3CaM, and Ca_4CaM. However, CaM needs to bind at least 3 Ca^{2+} to be active. We accepted the model for CaM dynamic from [23] (Table 5).

$$dCaCaM/dt = k_{1f}\ [Ca^{2+}]_c\ CAM - k_{1b}\ CaCaM \quad (51)$$

where

$$Ca_2CaM = (k_{2f}/k_{2b})\,[Ca^{2+}]_c\,CaCaM \quad (52)$$

$$Ca_3CaM = (k_{3f}/k_{3b})\,[Ca^{2+}]_c\,Ca_2CaM \quad (53)$$

$$Ca_4CaM = (k_{4f}/k_{4b})\,[Ca^{2+}]_c\,Ca_3CaM \quad (54)$$

$$CaM = CaM_o - CaCaM - Ca_2CaM - Ca_3CaM - Ca_4CaM \quad (55)$$

$$CaM_a = Ca_3CaM + Ca_4CaM \quad (56)$$

where k_{1f}–k_{4f} are the forward rate constants and k_{1b}–k_{4b} are the backward rate constants in the four steps of Ca^{2+} binding to CaM, CaM_o is the total amount calmodulin, CaM_a is the active form of CaM.

Modeling of cAMP pathway

Activated adenylyl cyclase synthesizes cAMP from the substrate Mg^{2+}ATP. Our recent mathematical model of the cAMP pathway in pancreatic β-cells includes detailed descriptions of interactions between $[Ca^{2+}]_c$, Ca^{2+}-bound calmodulin (Ca^{2+}/CaM), adenylyl cyclase (AC), phosphodiesterase (PDE) and dynamics of cAMP concentration in the cytoplasm [23]. We have extended this model to include a description of cAMP-dependent modulation of PKA and Ecap and an activation of exocytosis processes [25]. In this article we added the equation for cAMP production by soluble Ca^{2+}-activated AC isoform. As cAMP molecules are known to diffuse through the cytosol, we refer to cAMP production and degradation in terms of concentration (in μM) instead of the area density of molecules on PM. The dynamic of intracellular concentration of cAMP is determined by the rates of cAMP synthesis and degradationcan (see [23]):

$$d\ cAMP/dt = V_{AC} - V_{PDE} - k_{da}\ cAMP \quad (57)$$

where V_{AC} is AC activity, V_{PDE} is the PDE activity, k_{da} is the coefficient of PDE-independent cAMP degradation.

AC activities were divided into two functionally distinct categories:

$$V_{AC} = V_{ACp} + V_{ACc} \quad (58)$$

where V_{ACp} is G-protein and Ca^{2+} dependent AC activity on PM, V_{ACc} is the glucose and Ca^{2+}-activated cytoplasmic AC activity that is independent on G-proteins.

GLP-1 and GIP activate and catecholamines inhibite the same CaM and Ca^{2+}-dependent isoform of AC on PM that bound corresponding G protens for activation. Equation for the area density of this activated AC isoform on PM is based on our previous analysis (see Eqs 46–48)

$$AC_{pt} = AC_{GLP} + AC_{GIP} + AC_{AR} + AC_{pf} \quad (59)$$

or

$$AC_{pf} = AC_{pt} - AC_{GLP} - AC_{GIP} - AC_{AR} \quad (60)$$

where

$$AC_{pa} = AC_{GLP} + AC_{GIP} \quad (61)$$

$$AC_{par} = AC_{pa}/AC_{pt} \quad (62)$$

AC_{pt} is the total concentration of AC isoform on PM, AC_{pf} is the concentration of free AC isoform on PM, AC_{GLP}, AC_{GIP} and AC_{AR} are the concentrations of AC_p bound with corresponding G-proteins activated by GLP-1R, GIPR and α_{2A} adrenergic receptors (see above). AC_{pa} is the area density of active AC molecules that can be stimulated by G-proteins, AC_{par} is the relative concentration of AC_{pa}. CaM/Ca^{2+} dependence of AC_p activity was accepted similarly to work [23],

$$V_{ACp} = V_{mCaM} f_{acca} AC_{par} \quad (63)$$

where

$$f_{acca} = \frac{CaM_a}{CaM_a + K_{PCaM}} \frac{K_{NCa}}{K_{NCa} + [Ca^{2+}]_c} \quad (64)$$

V_{mCaM} is the maximum AC_p activity, f_{acca} is CaM activation factor, K_{PCaM} is the CaM_a activation constant, K_{NCa} is the $[Ca^{2+}]_c$ inhibition constant.

It was found that in S49 lymphoma cells, a widely used model system, each cell contains only a few thousand functional copies of the catalytic subunit of AC for binding forskolin (3000 molecules per cell) that can be consider as evaluation of PM bound AC (as 3 # μm^{-2}) and G-protein appears to exist in stoichiometric excess relative to AC [228]. We used this data for evaluation of the content of PM bound AC isoform in β cell (Table 5).

Another isoform is cytoplasmic AC (AC_c) that can be activated by ATP and Ca^{2+}. We used a the Michaelis-Menten function for an dependence AC_c on ATP and $[Ca^{2+}]_c$ concentrations that were found for this AC isoform [229]

$$V_{ACS} = \frac{V_{mACc} ATP}{ATP + K_{mAACS}} \frac{[Ca^{2+}]_c}{[Ca^{2+}]_c + K_{mCACS}} + k_{ACS} \quad (65)$$

where V_{mACc} is the maximum AC_c activity, K_{mAACS} is the of ATP activation constant, K_{mCACS} is the $[Ca^{2+}]_c$ activation constant, k_{ACS} is the coefficient of the constitutive AC_c activity.

The equation for the function of PDE was accepted from [23] in simplificated form. We added also the coefficient (k_{ipde}) for a simulation of the specific inhibition.

$$V_{pde} = k_{ipde} \left(V_{gpde} + V_{cpde} \frac{CaM_a}{CaM_a + K_{dpe}} \right) \frac{cAMP}{cAMP + K_{pde}} \quad (66)$$

$$k_{ipde} = k_{ipdei} + k_{ipde1} \ (t > t_{pde})$$

where V_{gpde} is the activity of Ca^{2+}/CaM-independent PDE, V_{cpde} is the basal level of Ca^{2+}/CaM dependent PDE activity, K_{dpe} is the CaM_a activation constant, K_{pde} is the cAMP activation constant, k_{ipde} is the the activation or inhibition coefficient. k_{ipdei} is the basal coefficient. k_{ipde1} is the change in k_{ipde} in time (t_{pde}).

cAMP dependent PKA and Epac activation. Binding of cAMP to the regulatory units of PKA or Epac results in release of the catalytic units and an activation of PKA or Epac. We used the mathematical models of PKA activation [198]. Relative steady-state level of PKA activation

by cAMP (f_{pca}) was described by an empirical Hill-type equation [25].

$$d\ PKAa\ /\ dt = k_{ak}\ (f_{pca}\ PKA_i - PKA_a)/t_{pka}\ , \tag{67}$$

where

$$PKAi\ =\ 1\ -\ PKAa, \tag{68}$$

$$f_{pca} = cAMP^{hpca}/(K_{pcm}{}^{hpca} + cAMP^{hpca}) \tag{69}$$

where PKA_a is the relative concentration of active PKA, PKA_i is the relative concentration of inactive PKA, the total relative concentration of active and inactive PKA was accepted as 1, t_{pka} is the time constant; k_{ak} is the scaling factor, f_{pca} is cAMP potential factor, where K_{pcm} is the cAMP activation coefficient [230] and hpca is the Hill coefficient.

The pathway, that includes Epac activation, was modeled similarly to the PKA dynamics

$$d\ EP_a/\ dt = (f_{EcA}\ EP_i - EP_a)/\ t_{ep} \tag{70}$$

where

$$EP_i = 1 - EP_a; \tag{71}$$

$$f_{EcA} = cAMP^{\,hce}/(K_{mep}{}^{hce} + cAMP^{hce}) \tag{72}$$

where EP_a is the relative concentration of active Epac, EP_i is the relative concentration of inactive Epac, the total relative concentration of active and inactive Epac was accepted as 1; f_{EcA} is the cAMP potential factor, where K_{mep} is the cAMP activation constant for Epac, hce is the Hill coefficient, t_{ep} is the time constant.

Epac has a lower binding capacity for cAMP to compare with PKA [94] (see Table 5).

Phosphoinositides

Phosphoinositides regulate numerous processes in pancreatic β-cells. We modeled phosphoinositides dynamics using the models and coefficients for sA201 cells [200, 201, 231] because a few quantitative kinetic measurements were made for pancreatic β-cells. According to [96] P4P synthesis activates by PKCa and Ca^{2+} that we have also taken into account introducing the specific term (f_{PI}). Than the equation for P4P dynamic can be written as:

$$d\ P4P\ /\ dt\ = k_{PI}\ f_{PI}\ PI + k_{P4Pr}\ PIP_2 - k_{PIr}\ P4P - k_{P4P}\ P4P \tag{73}$$

where

$$f_{PI}\ =\ \frac{[Ca^{2+}]_c{}^2}{[Ca^{2+}]_c{}^2\ +\ K_{CaPI}{}^2}\ \frac{PKC_a{}^2}{PKC_a{}^2 + K_{P4PK}{}^2} + k_{cpi} \tag{74}$$

where PI is the intracellular pool of phospholipids on PM, PIP_2 is the concentration of plasma membrane-bound phosphatidylinositol bisphosphate, k_{PI} is the P4P production coefficient, k_{PIr} is the backward rate constant for P4P, k_{P4Pr} is the backward rate constant for PIP_2, k_{P4P} is the the PIP_2 production coefficient, K_{CaPI} is the $[Ca^{2+}]_c$ activation coefficient, K_{P4PK} is the PKC_a activation coefficient.

PIP_2 dynamics. According to [183] ATP dose-dependently stimulated PIP_2 synthesis has the half-maximally stimulation at 300 μM ATP that significantly lower than ATP concentration in cytoplasm (see [31]). For this reason we did not take into account ATP concentration dependence at PIP_2 synthesis. On the other hand PLC hydrolyzes plasma PIP_2 molecules into

inositol trisphosphate (IP_3) and DAG. The rate of this reaction depends on activity of PLC.

$$d\ PIP_2\ /\ dt\ = k_{P4P}\ P4P - f_{PIP2}\ V_{PL} - k_{P4Pr}\ PIP_2 \tag{75}$$

where

$$f_{PIP2} = PIP_2/(K_{PIP2} + PIP_2) \tag{76}$$

where V_{PL} is the PLC activity (see below, Eq 77), K_{PIP2} is the PIP_2 activation coefficient.

Density of phosphoinositides at the plasma membrane in β-cell remains uncertain. We assumed that free PIP_2 is about 5000 # μM^{-2} in our modeling similarly evaluation for tsA201 cells in work [201].

PLC signaling pathway

Activation of PLC by M3 muscarinic receptors and FFAR1/GPR40 receptors was modeled above (Eqs 49–50). However, PLC activity is also regulated by G-protein independent (but $[Ca^{2+}]_c$ dependent) ways in insulin-secreting cells. We consider two different PLC isoforms: 1. MR and FFAR1/GPR40 activated (PLC_p). 2. Ca^{2+} activated G-protein independent PLC form (PLC_c). A schematic of these two PLC isoforms is shown in Fig 1.

$$V_{PL} = V_{PLP} + V_{PLC} + k_{pPL} \tag{77}$$

where

$$V_{PLP} = V_{mPLP}\frac{PLC_{pa}}{PLC_{pt}}\ \frac{[Ca^{2+}]_c^{\ 2}}{K_{CaPL}^{\ 2} + [Ca^{2+}]_c^{\ 2}} \tag{78}$$

$$\begin{gathered} V_{mPLP} = V_{mPLPi} + V_{mPLP1}\ (t > t10) \\ PLC_{pa} = PLC_{M3} + PLC_{R40} \end{gathered} \tag{79}$$

$$PLC_{pf} = PLC_{pt} - PLC_{pa} \tag{80}$$

$$V_{PLC} = V_{mPLC}\ [Ca^{2+}]_c^{\ 2}/(K_{CCaPL}^{\ 2} + [Ca^{2+}]_c^{\ 2}\ ) \tag{81}$$

where V_{PL} is the total PLC activity, V_{PLP} is the G-protein dependent and V_{PLC} is the G-protein independent (but Ca^{2+} dependent) PLC activity, k_{pPL} is the coefficient of the PLC constitutive activity. V_{mPLP} is the maximum of V_{PLP} activity, K_{CaPL} is the $[Ca^{2+}]_c$ activation constant, V_{mPLPi} is the initial (basal) activity. V_{mPLP1} is the increase in V_{mPLC} in time (t10), PLC_{pt} is the is the total concentration of PLC_p isoform on PM, PLC_{pa} is the concentration of PLC_p bound with MR and FFAR1/GPR40 receptors, PLC_{pf} is the concentration of free PLC_p, V_{mPLC} is the the maximum V_{PLC} activity, K_{CCaPL} is the $[Ca^{2+}]_c$ activation constant.

Endogenous PLC on PM (3 # μm^{-2}) was evaluated for a transformed human kidney cell line (tsA-201) whose dimensions are close to that of the β-cell [200, 216] and we used this value for PLC_{pt} evaluation (Table 4).

IP_3 dynamics. The generation of IP_3 is determined by the hydrolysis rate of PIP_2. Because IP_3 molecules diffuse through the cytosol, we refer to IP_3 production and degradation in terms of concentration (in μM) instead of the area density of molecules on PM. Different mechanisms seem to be available in the β-cells for degradation of IP_3, however, we assume that IP_3 is degraded at a rate proportional to the concentration of IP_3. Then we used the simplest model of IP_3 dynamics from [33]) but it was modified to consider the processes of IP_3 production on

PM.

$$d\ IP_3 / dt = V_{PL}\ f_{Nc}\ f_{PIP2} - k_{dIP3}\ IP_3 \quad (82)$$

where f_{Nc} is the coefficient to convert from μm^{-2} to μM (Eq 1), k_{dIP3} is the rate constant of IP_3 degradation.

DAG dynamics. DAG is the product of PLC-catalyzed breakdown of phosphoinositides, stimulates by PLC where it is produced stoichiometrically with IP_3. However, DAG is bound with PM. Model of the DAG dynamics was developed similarly to the IP3 model. Coefficients from model [201] for native tsA201 cells were used (Table 6).

$$d\ DAG / dt = V_{PL}\ f_{PIP2} - k_{dDAG}\ DAG \quad (83)$$

where k_{dDAG} is the coefficient of DAG degradation

DAG dependent PKC activation. Binding of DAG to the regulatory units of PKC results in release of the catalytic units from PKC and its activation. Relative PKC activation by DAG was described similarly to work [202] as equation:

$$d\ PKC_a / dt = k_{PKC}\ DAG\ ^{*}\ PKC_i - k_{PKCr}\ PKC_a, \quad (84)$$

$$PKC_i = PKC_t - PKC_a, \quad (85)$$

where $PKC_t = 1$

PKC_a is the relative concentration of active PKC, PKC_i is the relative concentration of inactive PKC, PKC_t is the total relative concentration of active and inactive PKC, k_{PKC} and k_{PKCr} are the forward backward rate constants. $t_{1/2}$ was evaluated as 204 s^{-1} [202] ($k_{PKCr} = 0.0034\ s^{-1}$).

Ca^{2+} dynamics

Cytoplasmic Ca^{2+} dynamics was modeled at the whole cell level. We included only fluxes through Ca^{2+} channels on PM, Ca^{2+} pumps on PM and ER and Ca^{2+} flux from ER. Then the free cytoplasmic Ca^{2+} ($[Ca^{2+}]_c$ or Cac in computational program) dynamics can be modeled by the following equations:

$$\frac{d[Ca^{2+}]_c}{dt} = \frac{f_{cf}}{V_c}\left(\frac{-I_{Ca} - I_{SOC} - 2I_{PCa}}{2\ F} + J_{rel} - J_{ser}\right) - k_{sg}\,[Ca^{2+}]_c \quad (86)$$

where f_{cf} is the fraction of free Ca^{2+} in cytoplasm, F is Faraday's constant, V_c is the effective volume of the cytosolic compartment, and k_{sg} is the coefficient of Ca^{2+} sequestration rate. Total Ca^{2+} current on PM include the current through the voltage-dependent Ca^{2+} channels—I_{Ca} (Eq 18); the store-operated current—I_{SOC} (Eq 21) and the PM Ca^{2+} ATP-ase pumps—I_{PCa} (Eq 23). J_{ser} is the Ca^{2+} flux from the cytosol into the ER activated by Ca^{2+} ATP-ases (SERCA) (per cell); J_{rel} is the Ca^{2+} flux from the ER into the cytosol (per cell).

Ca^{2+} dynamics in ER ($[Ca^{2+}]_{Er}$ or CaER in computational program) can be modeled by the following equation:

$$d[Ca^{2+}]_{Er} / dt = f_{er}\,(J_{ser} - J_{rel}) / V_{ER} \quad (87)$$

where f_{er} is the is the fraction of free Ca^{2+} in ER, V_{ER} is the effective volume of the ER compartment. A function of the Ca^{2+} ATP-ase on ER (per cell) was modeled using the usual expression

[33]:

$$J_{ser} = P_{CaER}[Ca^{2+}]_c^{\,2} / (K_{ser}^{\,2} + [Ca^{2+}]_c^{\,2}) \quad (88)$$

where P_{CaEr} is the maximum SERCA pump rate, K_{ser} is the $[Ca^{2+}]_c$ activation constant.

The total Ca^{2+} flux from the ER into the cytosol is given by

$$J_{rel} = (k_{mIP}\, P_{RIP3} + k_{leak})\, ([Ca^{2+}]_{Er} - [Ca^{2+}]_c) \quad (89)$$

where k_{mIP} is the maximum permeability for IP_3-activated channel, P_{RIP3} is the IP_3 receptor channel open probability, k_{leak} is the coefficient of Ca^{2+} passive leak from the ER through unspecified channels.

IP_3 Receptor. The simplest model of IP_3 receptor (IP_3R) activated by IP_3 and Ca^{2+} was taken from Bertram and Sherman [203]. Additional possibility is an activation of IP_3R by PKA. PKA-mediated phosphorylation leads to a direct increase in the sensitivity of the IP_3 receptor toward IP_3 without shifting its Ca^{2+} sensitivity. We modeled this effect as a decreased IP_3R activation constant with PKA activation (function f_{IPKA}).

$$P_{RIP3} = \left(\frac{[Ca^{2+}]_c}{K_{RPCa} + [Ca^{2+}]_c}\right)^3 \left(\frac{IP_3}{f_{IPKA}\, K_{IP3} + IP_3}\right)^3 \left(\frac{d_{inact}}{d_{inact} + [Ca^{2+}]_c}\right)^3 \quad (90)$$

where

$$f_{IPKA} = 1/(PKAa + K_{IP3})$$

P_{RIP3} is the channel open probability, K_{RPCa} is the $[Ca^{2+}]_c$ activation constant, K_{IP3} is the IP_3 activation constant, d_{inac} is the $[Ca^{2+}]_c$ inhibition constant at higher concentrations of Ca^{2+}, k_{IP3R} is the PKAa activation coefficient. The first factor represents an activation by Ca^{2+}, the second an activation by IP_3, and the third an inactivation at high concentration of $[Ca^{2+}]_c$.

Simulations

The model consists of a system of nonlinear ordinary differential equations describing the time rate of change in parameters. Parameter values and initial conditions (Tables 1–6) contain all the information necessary to carry out the simulations. These values were used in all simulations except where indicated otherwise. To calculate the steady-state cellular parameters, the model was allowed to run for at least 1000 s with no external stimulation.

Simulations were performed as noted previously using standard numerical methods and the software environment from "Virtual Cell" (see for example [25, 33]).

Acknowledgments

This work was supported by grants from the National Institutes of Health to LHP (DK063493 and DK092616), and by University of Chicago Diabetes Research and Training Center funding from the NIH (DK020595) to LHP. The Virtual Cell is supported by NIH Grant Number P41 GM103313 from the National Institute for General Medical Sciences.

Author Contributions

Analyzed the data: LEF LHP. Wrote the paper: LEF LHP. Mathematical simulation: LEF.

References

1. Kahn SE. The relative contributions of insulin resistance and beta-cell dysfunction to the pathophysiology of Type 2 diabetes. Diabetologia. 2003; 46(1):3–19. Epub 2003/03/15. doi: 10.1007/s00125-002-1009-0 PMID: 12637977.
2. Ashcroft FM, Rorsman P. Electrophysiology of the pancreatic beta-cell. Prog Biophys Mol Biol. 1989; 54(2):87–143. PMID: 2484976.
3. Gilon P, Henquin JC. Mechanisms and physiological significance of the cholinergic control of pancreatic beta-cell function. Endocr Rev. 2001; 22(5):565–604. PMID: 11588141.
4. Jacobson D, Philipson L. Ion Channels and Insulin secretion. In: Seino S, Bell G, editors. Pancreatic Beta Cell in Health and Desease. Japan,: Springer; 2008. p. 91–110.
5. Amisten S, Salehi A, Rorsman P, Jones PM, Persaud SJ. An atlas and functional analysis of G-protein coupled receptors in human islets of Langerhans. Pharmacol Ther. 2013; 139(3):359–91. Epub 2013/05/23. doi: S0163-7258(13)00119-8 [pii] doi: 10.1016/j.pharmthera.2013.05.004 PMID: 23694765.
6. Ahren B, Holst JJ. The cephalic insulin response to meal ingestion in humans is dependent on both cholinergic and noncholinergic mechanisms and is important for postprandial glycemia. Diabetes. 2001; 50(5):1030–8. Epub 2001/05/04. PMID: 11334405.
7. Just T, Pau HW, Engel U, Hummel T. Cephalic phase insulin release in healthy humans after taste stimulation? Appetite. 2008; 51(3):622–7. Epub 2008/06/17. doi: S0195-6663(08)00411-X [pii] doi: 10.1016/j.appet.2008.04.271 PMID: 18556090.
8. Storlien L, Oakes ND, Kelley DE. Metabolic flexibility. Proc Nutr Soc. 2004; 63(2):363–8. Epub 2004/08/06. doi: 10.1079/PNS2004349 S0029665104000497 [pii]. PMID: 15294056.
9. Drucker DJ. Incretin action in the pancreas: potential promise, possible perils, and pathological pitfalls. Diabetes. 2013; 62(10):3316–23. Epub 2013/07/03. doi: db13-0822 [pii] doi: 10.2337/db13-0822 PMID: 23818527; PubMed Central PMCID: PMC3781450.
10. Straub SG, Sharp GW. Evolving insights regarding mechanisms for the inhibition of insulin release by norepinephrine and heterotrimeric G proteins. Am J Physiol Cell Physiol. 2012; 302(12):C1687–98. Epub 2012/04/12. doi: ajpcell.00282.2011 [pii] doi: 10.1152/ajpcell.00282.2011 PMID: 22492651; PubMed Central PMCID: PMC3378079.
11. Winzell MS, Ahren B. G-protein-coupled receptors and islet function-implications for treatment of type 2 diabetes. Pharmacol Ther. 2007; 116(3):437–48. Epub 2007/09/29. doi: S0163-7258(07)00159-3 [pii] doi: 10.1016/j.pharmthera.2007.08.002 PMID: 17900700.
12. Doyle ME, Egan JM. Mechanisms of action of glucagon-like peptide 1 in the pancreas. Pharmacol Ther. 2007; 113(3):546–93. Epub 2007/02/20. doi: S0163-7258(06)00203-8 [pii] doi: 10.1016/j.pharmthera.2006.11.007 PMID: 17306374; PubMed Central PMCID: PMC1934514.
13. Seino S, Shibasaki T, Minami K. Dynamics of insulin secretion and the clinical implications for obesity and diabetes. J Clin Invest. 2011; 121(6):2118–25. Epub 2011/06/03. doi: 45680 [pii] doi: 10.1172/JCI45680 PMID: 21633180; PubMed Central PMCID: PMC3104758.
14. Hamann J, Aust G, Arac D, Engel FB, Formstone C, Fredriksson R, et al. International Union of Basic and Clinical Pharmacology. XCIV. Adhesion G protein-coupled receptors. Pharmacol Rev. 2015; 67(2):338–67. Epub 2015/02/26. doi: 67/2/338 [pii] doi: 10.1124/pr.114.009647 PMID: 25713288; PubMed Central PMCID: PMC4394687.
15. Holzhutter HG, Drasdo D, Preusser T, Lippert J, Henney AM. The virtual liver: a multidisciplinary, multilevel challenge for systems biology. Wiley Interdiscip Rev Syst Biol Med. 2012; 4(3):221–35. Epub 2012/01/17. doi: 10.1002/wsbm.1158 PMID: 22246674.
16. Moraru II, Loew LM. Intracellular signaling: spatial and temporal control. Physiology (Bethesda). 2005; 20:169–79. Epub 2005/05/13. doi: 20/3/169 [pii] doi: 10.1152/physiol.00052.2004 PMID: 15888574.
17. Sreenath SN, Cho KH, Wellstead P. Modelling the dynamics of signalling pathways. Essays Biochem. 2008; 45:1–28. Epub 2008/09/17. doi: BSE0450001 [pii] doi: 10.1042/BSE0450001 PMID: 18793120.
18. Cazzaniga P, Damiani C, Besozzi D, Colombo R, Nobile MS, Gaglio D, et al. Computational strategies for a system-level understanding of metabolism. Metabolites. 2014; 4(4):1034–87. Epub 2014/11/27. doi: metabo4041034 [pii] doi: 10.3390/metabo4041034 PMID: 25427076; PubMed Central PMCID: PMC4279158.
19. Sauro HM, Kholodenko BN. Quantitative analysis of signaling networks. Prog Biophys Mol Biol. 2004; 86(1):5–43. Epub 2004/07/21. doi: 10.1016/j.pbiomolbio.2004.03.002 S0079610704000446 [pii]. PMID: 15261524.
20. Manninen T, Hituri K, Kotaleski JH, Blackwell KT, Linne ML. Postsynaptic signal transduction models for long-term potentiation and depression. Front Comput Neurosci. 2010; 4:152. Epub 2010/12/29. doi: 10.3389/fncom.2010.00152 PMID: 21188161; PubMed Central PMCID: PMC3006457.

21. Klingmuller U, Bauer A, Bohl S, Nickel PJ, Breitkopf K, Dooley S, et al. Primary mouse hepatocytes for systems biology approaches: a standardized in vitro system for modelling of signal transduction pathways. Syst Biol (Stevenage). 2006; 153(6):433–47. Epub 2006/12/26. PMID: 17186705.

22. Iancu RV, Jones SW, Harvey RD. Compartmentation of cAMP signaling in cardiac myocytes: a computational study. Biophys J. 2007; 92(9):3317–31. Epub 2007/02/13. doi: S0006-3495(07)71137-2 [pii] doi: 10.1529/biophysj.106.095356 PMID: 17293406; PubMed Central PMCID: PMC1852367.

23. Fridlyand LE, Harbeck MC, Roe MW, Philipson LH. Regulation of cAMP dynamics by Ca2+ and G protein-coupled receptors in the pancreatic beta-cell: a computational approach. Am J Physiol Cell Physiol. 2007; 293(6):C1924–33. PMID: 17928534.

24. Takeda Y, Amano A, Noma A, Nakamura Y, Fujimoto S, Inagaki N. Systems analysis of GLP-1 receptor signaling in pancreatic beta-cells. Am J Physiol Cell Physiol. 2011; 301(4):C792–803. Epub 2011/07/08. doi: ajpcell.00057.2011 [pii] doi: 10.1152/ajpcell.00057.2011 PMID: 21734192.

25. Fridlyand LE, Philipson LH. Coupling of metabolic, second messenger pathways and insulin granule dynamics in pancreatic beta-cells: a computational analysis. Prog Biophys Mol Biol. 2011; 107 (2):293–303. Epub 2011/09/17. doi: S0079-6107(11)00100-3 [pii] doi: 10.1016/j.pbiomolbio.2011.09.001 PMID: 21920379.

26. Peercy BE, Sherman AS. How pancreatic beta-cells discriminate long and short timescale cAMP signals. Biophys J. 2010; 99(2):398–406. Epub 2010/07/21. doi: S0006-3495(10)00541-2 [pii] doi: 10.1016/j.bpj.2010.04.043 PMID: 20643057; PubMed Central PMCID: PMC2905120.

27. Peercy BE, Sherman AS, Bertram R. Modeling of glucose-induced cAMP oscillations in pancreatic beta cells: cAMP rocks when metabolism rolls. Biophys J. 2015; 109(2):439–49. Epub 2015/07/23. doi: S0006-3495(15)00607-4 [pii] doi: 10.1016/j.bpj.2015.06.024 PMID: 26200880.

28. Benninger RK, Piston DW. Cellular communication and heterogeneity in pancreatic islet insulin secretion dynamics. Trends Endocrinol Metab. 2014; 25(8):399–406. Epub 2014/04/01. doi: S1043-2760 (14)00041-1 [pii] doi: 10.1016/j.tem.2014.02.005 PMID: 24679927; PubMed Central PMCID: PMC4112137.

29. Fridlyand LE, Jacobson DA, Kuznetsov A, Philipson LH. A model of action potentials and fast Ca2+ dynamics in pancreatic beta-cells. Biophys J. 2009; 96(8):3126–39. PMID: 19383458. doi: 10.1016/j.bpj.2009.01.029

30. Fridlyand LE, Jacobson DA, Philipson LH. Ion channels and regulation of insulin secretion in human beta-cells: A computational systems analysis. Islets. 2013; 5(1):1–15. Epub 2013/04/30. doi: 24166 [pii] doi: 10.4161/isl.24166 PMID: 23624892.

31. Fridlyand LE, Ma L, Philipson LH. Adenine nucleotide regulation in pancreatic beta-cells: modeling of ATP/ADP-Ca2+ interactions. Am J Physiol Endocrinol Metab. 2005; 289(5):E839–48. PMID: 15985450.

32. Fridlyand LE, Philipson LH. Glucose sensing in the pancreatic beta cell: a computational systems analysis. Theor Biol Med Model. 2010; 7(1):15. Epub 2010/05/26. doi: 1742-4682-7-15 [pii] doi: 10.1186/1742-4682-7-15 PMID: 20497556.

33. Fridlyand LE, Tamarina N, Philipson LH. Modeling of Ca2+ flux in pancreatic beta-cells: role of the plasma membrane and intracellular stores. Am J Physiol Endocrinol Metab. 2003; 285(1):E138–54. PMID: 12644446.

34. Fridlyand LE, Tamarina N, Philipson LH. Bursting and calcium oscillations in pancreatic beta-cells: specific pacemakers for specific mechanisms. Am J Physiol Endocrinol Metab. 2010; 299(4):E517–32. Epub 2010/07/16. doi: ajpendo.00177.2010 [pii] doi: 10.1152/ajpendo.00177.2010 PMID: 20628025.

35. Henquin JC. Regulation of insulin secretion: a matter of phase control and amplitude modulation. Diabetologia. 2009; 52(5):739–51. PMID: 19288076. doi: 10.1007/s00125-009-1314-y

36. Prentki M, Matschinsky FM, Madiraju SR. Metabolic signaling in fuel-induced insulin secretion. Cell Metab. 2013; 18(2):162–85. Epub 2013/06/25. doi: S1550-4131(13)00208-8 [pii] doi: 10.1016/j.cmet.2013.05.018 PMID: 23791483.

37. Doliba NM, Qin W, Vinogradov SA, Wilson DF, Matschinsky FM. Palmitic acid acutely inhibits acetylcholine- but not GLP-1-stimulated insulin secretion in mouse pancreatic islets. Am J Physiol Endocrinol Metab. 2010; 299(3):E475–85. Epub 2010/07/08. doi: ajpendo.00072.2010 [pii] doi: 10.1152/ajpendo.00072.2010 PMID: 20606076; PubMed Central PMCID: PMC2944283.

38. Liang T, Xie L, Chao C, Kang Y, Lin X, Qin T, et al. Phosphatidylinositol 4,5-biphosphate (PIP2) Modulates Interaction of Syntaxin-1A with Sulfonylurea Receptor 1 to Regulate Pancreatic Beta-Cell ATP-Sensitive Potassium Channels. J Biol Chem. 2014. Epub 2014/01/17. doi: M113.511808 [pii] doi: 10.1074/jbc.M113.511808 PMID: 24429282.

39. Swayne LA, Mezghrani A, Varrault A, Chemin J, Bertrand G, Dalle S, et al. The NALCN ion channel is activated by M3 muscarinic receptors in a pancreatic beta-cell line. EMBO Rep. 2009; 10(8):873–80.

Epub 2009/07/04. doi: embor2009125 [pii] doi: 10.1038/embor.2009.125 PMID: 19575010; PubMed Central PMCID: PMC2710536.

40. Bertram R, Sherman A, Satin LS. Electrical bursting, calcium oscillations, and synchronization of pancreatic islets. Adv Exp Med Biol. 2010; 654:261–79. PMID: 20217502. doi: 10.1007/978-90-481-3271-3_12

41. Selway JL, Moore CE, Mistry R, John Challiss RA, Herbert TP. Molecular mechanisms of muscarinic acetylcholine receptor-stimulated increase in cytosolic free Ca(2+) concentration and ERK1/2 activation in the MIN6 pancreatic beta-cell line. Acta Diabetol. 2012; 49(4):277–89. Epub 2011/08/13. doi: 10.1007/s00592-011-0314-9 PMID: 21833779; PubMed Central PMCID: PMC3407357.

42. Xie LH, Horie M, Takano M. Phospholipase C-linked receptors regulate the ATP-sensitive potassium channel by means of phosphatidylinositol 4,5-bisphosphate metabolism. Proc Natl Acad Sci U S A. 1999; 96(26):15292–7. Epub 1999/12/28. PMID: 10611378; PubMed Central PMCID: PMC24813.

43. Kruse M, Hammond GR, Hille B. Regulation of voltage-gated potassium channels by PI(4,5)P2. J Gen Physiol. 2012; 140(2):189–205. Epub 2012/08/02. doi: jgp.201210806 [pii] doi: 10.1085/jgp.201210806 PMID: 22851677; PubMed Central PMCID: PMC3409096.

44. Logothetis DE, Petrou VI, Adney SK, Mahajan R. Channelopathies linked to plasma membrane phosphoinositides. Pflugers Arch. 2010; 460(2):321–41. Epub 2010/04/17. doi: 10.1007/s00424-010-0828-y PMID: 20396900.

45. Putney JW. Capacitative calcium entry: from concept to molecules. Immunol Rev. 2009; 231(1):10–22. PMID: 19754887. doi: 10.1111/j.1600-065X.2009.00810.x

46. Tamarina NA, Kuznetsov A, Philipson LH. Reversible translocation of EYFP-tagged STIM1 is coupled to calcium influx in insulin secreting beta-cells. Cell Calcium. 2008; 44(6):533–44. Epub 2008/05/03. doi: S0143-4160(08)00053-5 [pii] doi: 10.1016/j.ceca.2008.03.007 PMID: 18452988.

47. Gopel S, Kanno T, Barg S, Galvanovskis J, Rorsman P. Voltage-gated and resting membrane currents recorded from B-cells in intact mouse pancreatic islets. J Physiol. 1999; 521 Pt 3:717–28. PMID: 10601501.

48. Colsoul B, Vennekens R, Nilius B. Transient receptor potential cation channels in pancreatic beta cells. Rev Physiol Biochem Pharmacol. 2011; 161:87–110. Epub 2011/07/12. doi: 10.1007/112_2011_2 PMID: 21744203.

49. Jacobson DA, Philipson LH. TRP channels of the pancreatic beta cell. Handb Exp Pharmacol. 2007; (179:):409–24. PMID: 17217070.

50. Gilon P, Rorsman P. NALCN: a regulated leak channel. EMBO Rep. 2009; 10(9):963–4. Epub 2009/08/08. doi: embor2009185 [pii] doi: 10.1038/embor.2009.185 PMID: 19662077; PubMed Central PMCID: PMC2750048.

51. Jakubik J, Janickova H, Randakova A, El-Fakahany EE, Dolezal V. Subtype differences in pre-coupling of muscarinic acetylcholine receptors. PLoS One. 2011; 6(11):e27732. Epub 2011/11/24. doi: 10.1371/journal.pone.0027732 PONE-D-11-17463 [pii]. PMID: 22110745; PubMed Central PMCID: PMC3218020.

52. Hein P, Bunemann M. Coupling mode of receptors and G proteins. Naunyn Schmiedebergs Arch Pharmacol. 2009; 379(5):435–43. Epub 2008/12/03. doi: 10.1007/s00210-008-0383-7 PMID: 19048232.

53. Vilardaga JP, Romero G, Feinstein TN, Wehbi VL. Kinetics and dynamics in the G protein-coupled receptor signaling cascade. Methods Enzymol. 2013; 522:337–63. Epub 2013/02/05. doi: B978-0-12-407865-9.00016–9 [pii] doi: 10.1016/B978-0-12-407865-9.00016–9 PMID: 23374192.

54. Hausdorff WP, Caron MG, Lefkowitz RJ. Turning off the signal: desensitization of beta-adrenergic receptor function. FASEB J. 1990; 4(11):2881–9. Epub 1990/08/01. PMID: 2165947.

55. Haga T. Molecular properties of muscarinic acetylcholine receptors. Proc Jpn Acad Ser B Phys Biol Sci. 2013; 89(6):226–56. Epub 2013/06/14. doi: DN/JST.JSTAGE/pjab/89.226 [pii]. PMID: 23759942; PubMed Central PMCID: PMC3749793.

56. Rajan S, Torres J, Thompson MS, Philipson LH. SUMO downregulates GLP-1-stimulated cAMP generation and insulin secretion. Am J Physiol Endocrinol Metab. 2012; 302(6):E714–23. Epub 2012/01/12. doi: ajpendo.00486.2011 [pii] doi: 10.1152/ajpendo.00486.2011 PMID: 22234371; PubMed Central PMCID: PMC3311292.

57. Rajan S, Dickson LM, Mathew E, Orr CM, Ellenbroek JH, Philipson LH, et al. Chronic hyperglycemia downregulates GLP-1 receptor signaling in pancreatic beta-cells via protein kinase A. Mol Metab. 2015; 4(4):265–76. Epub 2015/04/02. doi: 10.1016/j.molmet.2015.01.010 S2212-8778(15)00023-X [pii]. PMID: 25830090; PubMed Central PMCID: PMC4354925.

58. Seifert R, Wenzel-Seifert K. Constitutive activity of G-protein-coupled receptors: cause of disease and common property of wild-type receptors. Naunyn Schmiedebergs Arch Pharmacol. 2002; 366 (5):381–416. Epub 2002/10/17. doi: 10.1007/s00210-002-0588-0 PMID: 12382069.

59. Woodroffe PJ, Bridge LJ, King JR, Chen CY, Hill SJ. Modelling of the activation of G-protein coupled receptors: drug free constitutive receptor activity. J Math Biol. 2010; 60(3):313–46. Epub 2009/04/07. doi: 10.1007/s00285-009-0268-5 PMID: 19347339.

60. Srinivasan S, Lubrano-Berthelier C, Govaerts C, Picard F, Santiago P, Conklin BR, et al. Constitutive activity of the melanocortin-4 receptor is maintained by its N-terminal domain and plays a role in energy homeostasis in humans. J Clin Invest. 2004; 114(8):1158–64. Epub 2004/10/19. doi: 10.1172/JCI21927 PMID: 15489963; PubMed Central PMCID: PMC522250.

61. Whalley NM, Pritchard LE, Smith DM, White A. Processing of proglucagon to GLP-1 in pancreatic alpha-cells: is this a paracrine mechanism enabling GLP-1 to act on beta-cells? J Endocrinol. 2011; 211(1):99–106. Epub 2011/07/29. doi: JOE-11-0094 [pii] doi: 10.1530/JOE-11-0094 PMID: 21795304.

62. Molina J, Rodriguez-Diaz R, Fachado A, Jacques-Silva MC, Berggren PO, Caicedo A. Control of insulin secretion by cholinergic signaling in the human pancreatic islet. Diabetes. 2014; 63(8):2714–26. Epub 2014/03/25. doi: db13-1371 [pii] doi: 10.2337/db13-1371 PMID: 24658304; PubMed Central PMCID: PMC4113066.

63. Willard FS, Sloop KW. Physiology and emerging biochemistry of the glucagon-like peptide-1 receptor. Exp Diabetes Res. 2012; 2012:470851. Epub 2012/06/06. doi: 10.1155/2012/470851 PMID: 22666230; PubMed Central PMCID: PMC3359799.

64. Nadkarni P, Chepurny OG, Holz GG. Regulation of Glucose Homeostasis by GLP-1. Prog Mol Biol Transl Sci. 2014; 121:23–65. Epub 2014/01/01. doi: B978-0-12-800101-1.00002–8 [pii] doi: 10.1016/B978-0-12-800101-1.00002–8 PMID: 24373234.

65. Syme CA, Zhang L, Bisello A. Caveolin-1 regulates cellular trafficking and function of the glucagon-like Peptide 1 receptor. Mol Endocrinol. 2006; 20(12):3400–11. Epub 2006/08/26. doi: me.2006-0178 [pii] doi: 10.1210/me.2006-0178 PMID: 16931572.

66. Tornehave D, Kristensen P, Romer J, Knudsen LB, Heller RS. Expression of the GLP-1 receptor in mouse, rat, and human pancreas. J Histochem Cytochem. 2008; 56(9):841–51. Epub 2008/06/11. doi: jhc.2008.951319 [pii] doi: 10.1369/jhc.2008.951319 PMID: 18541709; PubMed Central PMCID: PMC2516959.

67. Ahren B. Islet G protein-coupled receptors as potential targets for treatment of type 2 diabetes. Nat Rev Drug Discov. 2009; 8(5):369–85. Epub 2009/04/15. doi: nrd2782 [pii] doi: 10.1038/nrd2782 PMID: 19365392.

68. McIntosh CH, Widenmaier S, Kim SJ. Glucose-dependent insulinotropic polypeptide (Gastric Inhibitory Polypeptide; GIP). Vitam Horm. 2009; 80:409–71. Epub 2009/03/03. doi: S0083-6729(08)00615-8 [pii] doi: 10.1016/S0083-6729(08)00615-8 PMID: 19251046.

69. Yabe D, Seino Y. Two incretin hormones GLP-1 and GIP: comparison of their actions in insulin secretion and beta cell preservation. Prog Biophys Mol Biol. 2011; 107(2):248–56. Epub 2011/08/09. doi: S0079-6107(11)00081-2 [pii] doi: 10.1016/j.pbiomolbio.2011.07.010 PMID: 21820006.

70. Schelshorn D, Joly F, Mutel S, Hampe C, Breton B, Mutel V, et al. Lateral allosterism in the glucagon receptor family: glucagon-like peptide 1 induces G-protein-coupled receptor heteromer formation. Mol Pharmacol. 2012; 81(3):309–18. Epub 2011/11/24. doi: mol.111.074757 [pii] doi: 10.1124/mol.111.074757 PMID: 22108912.

71. Wheeler MB, Gelling RW, Hinke SA, Tu B, Pederson RA, Lynn F, et al. Characterization of the carboxyl-terminal domain of the rat glucose-dependent insulinotropic polypeptide (GIP) receptor. A role for serines 426 and 427 in regulating the rate of internalization. J Biol Chem. 1999; 274(35):24593–601. Epub 1999/08/24. PMID: 10455124.

72. Hoare SR. Mechanisms of peptide and nonpeptide ligand binding to Class B G-protein-coupled receptors. Drug Discov Today. 2005; 10(6):417–27. Epub 2005/04/06. doi: S1359644605033702 [pii] doi: 10.1016/S1359-6446(05)03370-2 PMID: 15808821.

73. Fagerholm V, Haaparanta M, Scheinin M. alpha2-adrenoceptor regulation of blood glucose homeostasis. Basic Clin Pharmacol Toxicol. 2011; 108(6):365–70. Epub 2011/03/23. doi: 10.1111/j.1742-7843.2011.00699.x PMID: 21418144.

74. Porte D Jr, Graber AL, Kuzuya T, Williams RH. The effect of epinephrine on immunoreactive insulin levels in man. J Clin Invest. 1966; 45(2):228–36. Epub 1966/02/01. doi: 10.1172/JCI105335 PMID: 5901508; PubMed Central PMCID: PMC292687.

75. Okuma Y, Reisine T. Immunoprecipitation of alpha 2a-adrenergic receptor-GTP-binding protein complexes using GTP-binding protein selective antisera. Changes in receptor/GTP-binding protein

interaction following agonist binding. J Biol Chem. 1992; 267(21):14826–31. Epub 1992/07/25. PMID: 1353077.

76. Hein P, Frank M, Hoffmann C, Lohse MJ, Bunemann M. Dynamics of receptor/G protein coupling in living cells. Embo J. 2005; 24(23):4106–14. Epub 2005/11/18. doi: 7600870 [pii] doi: 10.1038/sj.emboj.7600870 PMID: 16292347; PubMed Central PMCID: PMC1356310.

77. Shenoy SK, Lefkowitz RJ. Trafficking patterns of beta-arrestin and G protein-coupled receptors determined by the kinetics of beta-arrestin deubiquitination. J Biol Chem. 2003; 278(16):14498–506. Epub 2003/02/08. doi: 10.1074/jbc.M209626200 M209626200 [pii]. PMID: 12574160.

78. Delmeire D, Flamez D, Hinke SA, Cali JJ, Pipeleers D, Schuit F. Type VIII adenylyl cyclase in rat beta cells: coincidence signal detector/generator for glucose and GLP-1. Diabetologia. 2003; 46 (10):1383–93. Epub 2003/09/19. doi: 10.1007/s00125-003-1203-8 PMID: 13680124.

79. Roger B, Papin J, Vacher P, Raoux M, Mulot A, Dubois M, et al. Adenylyl cyclase 8 is central to glucagon-like peptide 1 signalling and effects of chronically elevated glucose in rat and human pancreatic beta cells. Diabetologia. 2011; 54(2):390–402. Epub 2010/11/04. doi: 10.1007/s00125-010-1955-x PMID: 21046358.

80. Kitaguchi T, Oya M, Wada Y, Tsuboi T, Miyawaki A. Extracellular calcium influx activates adenylate cyclase 1 and potentiates insulin secretion in MIN6 cells. Biochem J. 2013; 450(2):365–73. Epub 2013/01/04. doi: BJ20121022 [pii] doi: 10.1042/BJ20121022 PMID: 23282092.

81. Seed Ahmed M, Kovoor A, Nordman S, Abu Seman N, Gu T, Efendic S, et al. Increased expression of adenylyl cyclase 3 in pancreatic islets and central nervous system of diabetic Goto-Kakizaki rats: a possible regulatory role in glucose homeostasis. Islets. 2012; 4(5):343–8. Epub 2012/09/29. doi: 22283 [pii] doi: 10.4161/isl.22283 PMID: 23018249; PubMed Central PMCID: PMC3524141.

82. Xia Z, Storm DR. Calmodulin-regulated adenylyl cyclases and neuromodulation. Curr Opin Neurobiol. 1997; 7(3):391–6. Epub 1997/06/01. doi: S0959-4388(97)80068-2 [pii]. PMID: 9232797.

83. Cooper DM, Karpen JW, Fagan KA, Mons NE. Ca(2+)-sensitive adenylyl cyclases. Adv Second Messenger Phosphoprotein Res. 1998; 32:23–51. Epub 1998/01/09. PMID: 9421584.

84. Seino S, Shibasaki T. PKA-dependent and PKA-independent pathways for cAMP-regulated exocytosis. Physiol Rev. 2005; 85(4):1303–42. PMID: 16183914.

85. Sunahara RK, Dessauer CW, Whisnant RE, Kleuss C, Gilman AG. Interaction of Gsalpha with the cytosolic domains of mammalian adenylyl cyclase. J Biol Chem. 1997; 272(35):22265–71. Epub 1997/08/29. PMID: 9268375.

86. Milligan G. The stoichiometry of expression of protein components of the stimulatory adenylyl cyclase cascade and the regulation of information transfer. Cell Signal. 1996; 8(2):87–95. Epub 1996/02/01. doi: 0898656895020349 [pii]. PMID: 8730510.

87. Raoux M, Vacher P, Papin J, Picard A, Kostrzewa E, Devin A, et al. Multilevel control of glucose homeostasis by adenylyl cyclase 8. Diabetologia. 2014. Epub 2014/11/19. doi: 10.1007/s00125-014-3445-z PMID: 25403481.

88. Steiner D, Avidor-Reiss T, Schallmach E, Butovsky E, Lev N, Vogel Z. Regulation of adenylate cyclase type VIII splice variants by acute and chronic Gi/o-coupled receptor activation. Biochem J. 2005; 386(Pt 2):341–8. Epub 2004/11/13. doi: BJ20041670 [pii] doi: 10.1042/BJ20041670 PMID: 15537392; PubMed Central PMCID: PMC1134799.

89. Holz GG, Leech CA, Chepurny OG. New insights concerning the molecular basis for defective glucoregulation in soluble adenylyl cyclase knockout mice. Biochim Biophys Acta. 2014. Epub 2014/07/02. doi: S0925-4439(14)00200-2 [pii] doi: 10.1016/j.bbadis.2014.06.023 PMID: 24980705.

90. Heimann E, Jones HA, Resjo S, Manganiello VC, Stenson L, Degerman E. Expression and regulation of cyclic nucleotide phosphodiesterases in human and rat pancreatic islets. PLoS One. 2010; 5(12): e14191. Epub 2010/12/15. doi: 10.1371/journal.pone.0014191 PMID: 21152070; PubMed Central PMCID: PMC2995729.

91. Pyne NJ, Furman BL. Cyclic nucleotide phosphodiesterases in pancreatic islets. Diabetologia. 2003; 46(9):1179–89. Epub 2003/08/09. doi: 10.1007/s00125-003-1176-7 PMID: 12904862.

92. Dov A, Abramovitch E, Warwar N, Nesher R. Diminished phosphodiesterase-8B potentiates biphasic insulin response to glucose. Endocrinology. 2008; 149(2):741–8. Epub 2007/11/10. doi: en.2007-0968 [pii] doi: 10.1210/en.2007-0968 PMID: 17991719.

93. Seino S, Takahashi H, Fujimoto W, Shibasaki T. Roles of cAMP signalling in insulin granule exocytosis. Diabetes Obes Metab. 2009; 11 Suppl 4:180–8. PMID: 19817800. doi: 10.1111/j.1463-1326.2009.01108.x

94. Holz GG, Kang G, Harbeck M, Roe MW, Chepurny OG. Cell physiology of cAMP sensor Epac. J Physiol. 2006; 577(Pt 1):5–15. Epub 2006/09/16. doi: jphysiol.2006.119644 [pii] doi: 10.1113/jphysiol.2006.119644 PMID: 16973695; PubMed Central PMCID: PMC2000694.

95. Barker CJ, Berggren PO. New horizons in cellular regulation by inositol polyphosphates: insights from the pancreatic beta-cell. Pharmacol Rev. 2013; 65(2):641–69. Epub 2013/02/23. doi: 65/2/641 [pii] doi: 10.1124/pr.112.006775 PMID: 23429059.

96. Wuttke A, Sagetorp J, Tengholm A. Distinct plasma-membrane PtdIns(4)P and PtdIns(4,5)P2 dynamics in secretagogue-stimulated beta-cells. J Cell Sci. 2010; 123(Pt 9):1492–502. Epub 2010/04/09. doi: jcs.060525 [pii] doi: 10.1242/jcs.060525 PMID: 20375060.

97. Fruman DA, Meyers RE, Cantley LC. Phosphoinositide kinases. Annu Rev Biochem. 1998; 67:481–507. Epub 1998/10/06. doi: 10.1146/annurev.biochem.67.1.481 PMID: 9759495.

98. Baukrowitz T, Fakler B. K(ATP) channels: linker between phospholipid metabolism and excitability. Biochem Pharmacol. 2000; 60(6):735–40. Epub 2000/08/10. doi: S0006-2952(00)00267-7 [pii]. PMID: 10930527.

99. Shyng SL, Nichols CG. Membrane phospholipid control of nucleotide sensitivity of KATP channels. Science. 1998; 282(5391):1138–41. Epub 1998/11/06. PMID: 9804554.

100. Ahren B. Autonomic regulation of islet hormone secretion—implications for health and disease. Diabetologia. 2000; 43(4):393–410. Epub 2000/05/20. PMID: 10819232.

101. Berridge MJ. Inositol trisphosphate and calcium signalling mechanisms. Biochim Biophys Acta. 2009; 1793(6):933–40. PMID: 19010359. doi: 10.1016/j.bbamcr.2008.10.005

102. Ruiz de Azua I, Gautam D, Guettier JM, Wess J. Novel insights into the function of beta-cell M3 muscarinic acetylcholine receptors: therapeutic implications. Trends Endocrinol Metab. 2011; 22(2):74–80. Epub 2010/11/26. doi: S1043-2760(10)00174-8 [pii] doi: 10.1016/j.tem.2010.10.004 PMID: 21106385; PubMed Central PMCID: PMC3053051.

103. Smrcka AV, Brown JH, Holz GG. Role of phospholipase Cepsilon in physiological phosphoinositide signaling networks. Cell Signal. 2012; 24(6):1333–43. Epub 2012/01/31. doi: S0898-6568(12)00014-9 [pii] doi: 10.1016/j.cellsig.2012.01.009 PMID: 22286105; PubMed Central PMCID: PMC3325758.

104. Nakajima K, Jain S, Ruiz de Azua I, McMillin SM, Rossi M, Wess J. Minireview: Novel aspects of M3 muscarinic receptor signaling in pancreatic beta-cells. Mol Endocrinol. 2013; 27(8):1208–16. Epub 2013/07/04. doi: me.2013-1084 [pii] doi: 10.1210/me.2013-1084 PMID: 23820900; PubMed Central PMCID: PMC3725345.

105. Azpiazu I, Gautam N. A fluorescence resonance energy transfer-based sensor indicates that receptor access to a G protein is unrestricted in a living mammalian cell. J Biol Chem. 2004; 279(26):27709–18. Epub 2004/04/14. doi: 10.1074/jbc.M403712200 M403712200 [pii]. PMID: 15078878.

106. Mancini AD, Poitout V. The fatty acid receptor FFA1/GPR40 a decade later: how much do we know? Trends Endocrinol Metab. 2013; 24(8):398–407. Epub 2013/05/02. doi: S1043-2760(13)00050-7 [pii] doi: 10.1016/j.tem.2013.03.003 PMID: 23631851.

107. Sanchez-Fernandez G, Cabezudo S, Garcia-Hoz C, Beninca C, Aragay AM, Mayor F Jr, et al. Galphaq signalling: the new and the old. Cell Signal. 2014; 26(5):833–48. Epub 2014/01/21. doi: S0898-6568(14)00021-7 [pii] doi: 10.1016/j.cellsig.2014.01.010 PMID: 24440667.

108. Sassmann A, Gier B, Grone HJ, Drews G, Offermanns S, Wettschureck N. The Gq/G11-mediated signaling pathway is critical for autocrine potentiation of insulin secretion in mice. J Clin Invest. 2010; 120(6):2184–93. Epub 2010/05/05. doi: 41541 [pii] doi: 10.1172/JCI41541 PMID: 20440069; PubMed Central PMCID: PMC2877950.

109. Qian J, Wu C, Chen X, Li X, Ying G, Jin L, et al. Differential requirements of arrestin-3 and clathrin for ligand-dependent and -independent internalization of human G protein-coupled receptor 40. Cell Signal. 2014; 26(11):2412–23. Epub 2014/07/20. doi: S0898-6568(14)00241-1 [pii] doi: 10.1016/j.cellsig.2014.07.019 PMID: 25038452.

110. Gresset A, Sondek J, Harden TK. The phospholipase C isozymes and their regulation. Subcell Biochem. 2012; 58:61–94. Epub 2012/03/10. doi: 10.1007/978-94-007-3012-0_3 PMID: 22403074; PubMed Central PMCID: PMC3638883.

111. Vines CM. Phospholipase C. Adv Exp Med Biol. 2012; 740:235–54. Epub 2012/03/29. doi: 10.1007/978-94-007-2888-2_10 PMID: 22453945.

112. Kim MJ, Lee KH, Min DS, Yoon SH, Hahn SJ, Kim MS, et al. Distributional patterns of phospholipase C isozymes in rat pancreas. Pancreas. 2001; 22(1):47–52. Epub 2001/01/04. PMID: 11138970.

113. Zawalich WS, Bonnet-Eymard M, Zawalich KC. Insulin secretion, inositol phosphate levels, and phospholipase C isozymes in rodent pancreatic islets. Metabolism. 2000; 49(9):1156–63. Epub 2000/10/04. doi: S0026-0495(00)84888-X [pii] doi: 10.1053/meta.2000.8613 PMID: 11016897.

114. Harden TK, Waldo GL, Hicks SN, Sondek J. Mechanism of activation and inactivation of Gq/phospholipase C-beta signaling nodes. Chem Rev. 2011; 111(10):6120–9. Epub 2011/10/13. doi: 10.1021/cr200209p PMID: 21988240; PubMed Central PMCID: PMC3626114.

115. Yamazaki H, Zawalich KC, Zawalich WS. Physiologic implications of phosphoinositides and phospholipase C in the regulation of insulin secretion. J Nutr Sci Vitaminol (Tokyo). 2010; 56(1):1–8. Epub 2010/04/01. doi: JST.JSTAGE/jnsv/56.1 [pii]. PMID: 20354339.

116. Fiume R, Ramazzotti G, Faenza I, Piazzi M, Bavelloni A, Billi AM, et al. Nuclear PLCs affect insulin secretion by targeting PPARgamma in pancreatic beta cells. FASEB J. 2012; 26(1):203–10. Epub 2011/10/07. doi: fj.11-186510 [pii] doi: 10.1096/fj.11-186510 PMID: 21974932.

117. Garcia MC, Hermans MP, Henquin JC. Glucose-, calcium- and concentration-dependence of acetylcholine stimulation of insulin release and ionic fluxes in mouse islets. Biochem J. 1988; 254(1):211–8. Epub 1988/08/15. PMID: 3052430; PubMed Central PMCID: PMC1135058.

118. Berridge MJ, Bootman MD, Roderick HL. Calcium signalling: dynamics, homeostasis and remodelling. Nat Rev Mol Cell Biol. 2003; 4(7):517–29. PMID: 12838335.

119. Gonelle-Gispert C, Costa M, Takahashi M, Sadoul K, Halban P. Phosphorylation of SNAP-25 on serine-187 is induced by secretagogues in insulin-secreting cells, but is not correlated with insulin secretion. Biochem J. 2002; 368(Pt 1):223–32. Epub 2002/08/08. doi: 10.1042/BJ20020896 BJ20020896 [pii]. PMID: 12164783; PubMed Central PMCID: PMC1222969.

120. Ferdaoussi M, Bergeron V, Zarrouki B, Kolic J, Cantley J, Fielitz J, et al. G protein-coupled receptor (GPR)40-dependent potentiation of insulin secretion in mouse islets is mediated by protein kinase D1. Diabetologia. 2012; 55(10):2682–92. Epub 2012/07/24. doi: 10.1007/s00125-012-2650-x PMID: 22820510.

121. Kong KC, Butcher AJ, McWilliams P, Jones D, Wess J, Hamdan FF, et al. M3-muscarinic receptor promotes insulin release via receptor phosphorylation/arrestin-dependent activation of protein kinase D1. Proc Natl Acad Sci U S A. 2010; 107(49):21181–6. Epub 2010/11/17. doi: 1011651107 [pii] doi: 10.1073/pnas.1011651107 PMID: 21078968; PubMed Central PMCID: PMC3000281.

122. Islam MS. Calcium signaling in the islets. Adv Exp Med Biol. 2010; 654:235–59. Epub 2010/03/11. doi: 10.1007/978-90-481-3271-3_11 PMID: 20217501.

123. Rorsman P, Braun M, Zhang Q. Regulation of calcium in pancreatic alpha- and beta-cells in health and disease. Cell Calcium. 2012; 51(3–4):300–8. Epub 2011/12/20. doi: S0143-4160(11)00223-5 [pii] doi: 10.1016/j.ceca.2011.11.006 PMID: 22177710; PubMed Central PMCID: PMC3334273.

124. Tamarina NA, Kuznetsov A, Rhodes CJ, Bindokas VP, Philipson LH. Inositol (1,4,5)-trisphosphate dynamics and intracellular calcium oscillations in pancreatic beta-cells. Diabetes. 2005; 54(11):3073–81. PMID: 16249428.

125. Dyachok O, Gylfe E. Ca(2+)-induced Ca(2+) release via inositol 1,4,5-trisphosphate receptors is amplified by protein kinase A and triggers exocytosis in pancreatic beta-cells. J Biol Chem. 2004; 279 (44):45455–61. Epub 2004/08/19. doi: 10.1074/jbc.M407673200 M407673200 [pii]. PMID: 15316011.

126. Dyer JL, Mobasheri H, Lea EJ, Dawson AP, Michelangeli F. Differential effect of PKA on the Ca2+ release kinetics of the type I and III InsP3 receptors. Biochem Biophys Res Commun. 2003; 302 (1):121–6. Epub 2003/02/21. doi: S0006291X03001207 [pii]. PMID: 12593857.

127. Vanderheyden V, Devogelaere B, Missiaen L, De Smedt H, Bultynck G, Parys JB. Regulation of inositol 1,4,5-trisphosphate-induced Ca2+ release by reversible phosphorylation and dephosphorylation. Biochim Biophys Acta. 2009; 1793(6):959–70. Epub 2009/01/10. doi: S0167-4889(08)00419-9 [pii] doi: 10.1016/j.bbamcr.2008.12.003 PMID: 19133301; PubMed Central PMCID: PMC2693466.

128. Rorsman P, Eliasson L, Kanno T, Zhang Q, Gopel S. Electrophysiology of pancreatic beta-cells in intact mouse islets of Langerhans. Prog Biophys Mol Biol. 2011; 107(2):224–35. Epub 2011/07/19. doi: S0079-6107(11)00056-3 [pii] doi: 10.1016/j.pbiomolbio.2011.06.009 PMID: 21762719.

129. Ravier MA, Daro D, Roma LP, Jonas JC, Cheng-Xue R, Schuit FC, et al. Mechanisms of control of the free Ca2+ concentration in the endoplasmic reticulum of mouse pancreatic beta-cells: interplay with cell metabolism and [Ca2+]c and role of SERCA2b and SERCA3. Diabetes. 2011; 60(10):2533–45. Epub 2011/09/03. doi: db10-1543 [pii] doi: 10.2337/db10-1543 PMID: 21885870; PubMed Central PMCID: PMC3178295.

130. Varadi A, Rutter GA. Dynamic imaging of endoplasmic reticulum Ca2+ concentration in insulin-secreting MIN6 Cells using recombinant targeted cameleons: roles of sarco(endo)plasmic reticulum Ca2 +-ATPase (SERCA)-2 and ryanodine receptors. Diabetes. 2002; 51 Suppl 1:S190–201. Epub 2002/ 01/30. PMID: 11815480.

131. Gilon P, Chae HY, Rutter GA, Ravier MA. Calcium signaling in pancreatic beta-cells in health and in Type 2 diabetes. Cell Calcium. 2014. Epub 2014/09/23. doi: S0143-4160(14)00136-5 [pii] doi: 10.1016/j.ceca.2014.09.001 PMID: 25239387.

132. Del Guerra S, Lupi R, Marselli L, Masini M, Bugliani M, Sbrana S, et al. Functional and molecular defects of pancreatic islets in human type 2 diabetes. Diabetes. 2005; 54(3):727–35. PMID: 15734849.

133. Doliba NM, Qin W, Najafi H, Liu C, Buettger CW, Sotiris J, et al. Glucokinase activation repairs defective bioenergetics of islets of Langerhans isolated from type 2 diabetics. Am J Physiol Endocrinol Metab. 2012; 302(1):E87–E102. Epub 2011/09/29. doi: ajpendo.00218.2011 [pii] doi: 10.1152/ajpendo.00218.2011 PMID: 21952036; PubMed Central PMCID: PMC3328091.

134. Gerencser AA. Bioenergetic Analysis of Single Pancreatic Beta-Cells Indicates an Impaired Metabolic Signature in Type 2 Diabetic Subjects. Endocrinology. 2015:en20151552. Epub 2015/07/24. doi: 10.1210/en.2015-1552 PMID: 26204464.

135. Ashcroft FM, Rorsman P. K(ATP) channels and islet hormone secretion: new insights and controversies. Nat Rev Endocrinol. 2013; 9(11):660–9. Epub 2013/09/18. doi: nrendo.2013.166 [pii] doi: 10.1038/nrendo.2013.166 PMID: 24042324.

136. Dyachok O, Isakov Y, Sagetorp J, Tengholm A. Oscillations of cyclic AMP in hormone-stimulated insulin-secreting beta-cells. Nature. 2006; 439(7074):349–52. PMID: 16421574.

137. Cognard E, Dargaville CG, Hay DL, Shepherd PR. Identification of a pathway by which glucose regulates beta-catenin signalling via the cAMP/protein kinase A pathway in beta-cell models. Biochem J. 2012. Epub 2012/12/04. doi: BJ20121454 [pii] doi: 10.1042/BJ20121454 PMID: 23198873.

138. Landa LR Jr, Harbeck M, Kaihara K, Chepurny O, Kitiphongspattana K, Graf O, et al. Interplay of Ca2+ and cAMP signaling in the insulin-secreting MIN6 beta-cell line. J Biol Chem. 2005; 280(35):31294–302. PMID: 15987680.

139. Tengholm A. Cyclic AMP dynamics in the pancreatic beta-cell. Ups J Med Sci. 2012; 117(4):355–69. Epub 2012/09/14. doi: 10.3109/03009734.2012.724732 PMID: 22970724; PubMed Central PMCID: PMC3497220.

140. Degerman E, Ahmad F, Chung YW, Guirguis E, Omar B, Stenson L, et al. From PDE3B to the regulation of energy homeostasis. Curr Opin Pharmacol. 2011; 11(6):676–82. Epub 2011/10/18. doi: S1471-4892(11)00182-2 [pii] doi: 10.1016/j.coph.2011.09.015 PMID: 22001403; PubMed Central PMCID: PMC3225700.

141. Nauck MA, Baller B, Meier JJ. Gastric inhibitory polypeptide and glucagon-like peptide-1 in the pathogenesis of type 2 diabetes. Diabetes. 2004; 53 Suppl 3:S190–6. Epub 2004/11/25. doi: 53/suppl_3/S190 [pii]. PMID: 15561910.

142. Calanna S, Christensen M, Holst JJ, Laferrere B, Gluud LL, Vilsboll T, et al. Secretion of glucose-dependent insulinotropic polypeptide in patients with type 2 diabetes: systematic review and meta-analysis of clinical studies. Diabetes Care. 2013; 36(10):3346–52. Epub 2013/09/26. doi: 36/10/3346 [pii] doi: 10.2337/dc13-0465 PMID: 24065842; PubMed Central PMCID: PMC3781498.

143. Holst JJ, Gromada J. Role of incretin hormones in the regulation of insulin secretion in diabetic and nondiabetic humans. Am J Physiol Endocrinol Metab. 2004; 287(2):E199–206. Epub 2004/07/24. doi: 10.1152/ajpendo.00545.2003 287/2/E199 [pii]. PMID: 15271645.

144. Baggio LL, Drucker DJ. Biology of incretins: GLP-1 and GIP. Gastroenterology. 2007; 132(6):2131–57. Epub 2007/05/15. doi: S0016-5085(07)00580-X [pii] doi: 10.1053/j.gastro.2007.03.054 PMID: 17498508.

145. Gault VA, Kerr BD, Harriott P, Flatt P. Administration of an acylated GLP-1 and GIP preparation provides added beneficial glucose-lowering and insulinotropic actions over single incretins in mice with type 2 diabetes and obesity. Clin Sci (Lond). 2011. Epub 2011/02/22. doi: CS20110006 [pii] doi: 10.1042/CS20110006 PMID: 21332446.

146. Gromada J, Holst JJ, Rorsman P. Cellular regulation of islet hormone secretion by the incretin hormone glucagon-like peptide 1. Pflugers Arch. 1998; 435(5):583–94. Epub 1998/04/16. PMID: 9479010.

147. Jia X, Brown JC, Ma P, Pederson RA, McIntosh CH. Effects of glucose-dependent insulinotropic polypeptide and glucagon-like peptide-I-(7–36) on insulin secretion. Am J Physiol. 1995; 268(4 Pt 1):E645–51. Epub 1995/04/01. PMID: 7733263.

148. Meloni AR, DeYoung MB, Lowe C, Parkes DG. GLP-1 receptor activated insulin secretion from pancreatic beta-cells: mechanism and glucose dependence. Diabetes Obes Metab. 2013; 15(1):15–27. Epub 2012/07/11. doi: 10.1111/j.1463-1326.2012.01663.x PMID: 22776039; PubMed Central PMCID: PMC3556522.

149. de Heer J, Holst JJ. Sulfonylurea compounds uncouple the glucose dependence of the insulinotropic effect of glucagon-like peptide 1. Diabetes. 2007; 56(2):438–43. Epub 2007/01/30. doi: 56/2/438 [pii] doi: 10.2337/db06-0738 PMID: 17259389.

150. Pacini G, Thomaseth K, Ahren B. Dissociated effects of glucose-dependent insulinotropic polypeptide vs glucagon-like peptide-1 on beta-cell secretion and insulin clearance in mice. Metabolism. 2010; 59(7):988–92. Epub 2010/02/16. doi: S0026-0495(09)00452-1 [pii] doi: 10.1016/j.metabol.2009.10.021 PMID: 20153002.

151. Gainetdinov RR, Premont RT, Bohn LM, Lefkowitz RJ, Caron MG. Desensitization of G protein-coupled receptors and neuronal functions. Annu Rev Neurosci. 2004; 27:107–44. Epub 2004/06/26. doi: 10.1146/annurev.neuro.27.070203.144206 PMID: 15217328.

152. Mohammad S, Patel RT, Bruno J, Panhwar MS, Wen J, McGraw TE. A Naturally Occurring GIP Receptor Variant Undergoes Enhanced Agonist-Induced Desensitization, Which Impairs GIP Control of Adipose Insulin Sensitivity. Mol Cell Biol. 2014; 34(19):3618–29. Epub 2014/07/23. doi: MCB.00256-14 [pii] doi: 10.1128/MCB.00256-14 PMID: 25047836.

153. Nauck MA, Vardarli I, Deacon CF, Holst JJ, Meier JJ. Secretion of glucagon-like peptide-1 (GLP-1) in type 2 diabetes: what is up, what is down? Diabetologia. 2011; 54(1):10–8. Epub 2010/09/28. doi: 10.1007/s00125-010-1896-4 PMID: 20871975.

154. Kaneto H, Matsuoka TA. Down-regulation of pancreatic transcription factors and incretin receptors in type 2 diabetes. World J Diabetes. 2013; 4(6):263–9. Epub 2014/01/01. doi: 10.4239/wjd.v4.i6.263 PMID: 24379916; PubMed Central PMCID: PMC3874485.

155. Shu L, Matveyenko AV, Kerr-Conte J, Cho JH, McIntosh CH, Maedler K. Decreased TCF7L2 protein levels in type 2 diabetes mellitus correlate with downregulation of GIP- and GLP-1 receptors and impaired beta-cell function. Hum Mol Genet. 2009; 18(13):2388–99. Epub 2009/04/24. doi: ddp178 [pii] doi: 10.1093/hmg/ddp178 PMID: 19386626; PubMed Central PMCID: PMC2722186.

156. Kang ZF, Deng Y, Zhou Y, Fan RR, Chan JC, Laybutt DR, et al. Pharmacological reduction of NEFA restores the efficacy of incretin-based therapies through GLP-1 receptor signalling in the beta cell in mouse models of diabetes. Diabetologia. 2013; 56(2):423–33. Epub 2012/11/29. doi: 10.1007/s00125-012-2776-x PMID: 23188390; PubMed Central PMCID: PMC3536946.

157. Lamont BJ, Li Y, Kwan E, Brown TJ, Gaisano H, Drucker DJ. Pancreatic GLP-1 receptor activation is sufficient for incretin control of glucose metabolism in mice. J Clin Invest. 2012; 122(1):388–402. Epub 2011/12/21. doi: 42497 [pii] doi: 10.1172/JCI42497 PMID: 22182839; PubMed Central PMCID: PMC3248276.

158. Pan M, Yang G, Cui X, Yang SN. Subthreshold alpha(2)-adrenergic activation counteracts glucagon-like peptide-1 potentiation of glucose-stimulated insulin secretion. Exp Diabetes Res. 2011; 2011:604989. Epub 2011/01/22. doi: 10.1155/2011/604989 PMID: 21253359; PubMed Central PMCID: PMC3021849.

159. Kimple ME, Neuman JC, Linnemann AK, Casey PJ. Inhibitory G proteins and their receptors: emerging therapeutic targets for obesity and diabetes. Exp Mol Med. 2014; 46:e102. Epub 2014/06/21. doi: emm201440 [pii] doi: 10.1038/emm.2014.40 PMID: 24946790; PubMed Central PMCID: PMC4081554.

160. Rosengren AH, Jokubka R, Tojjar D, Granhall C, Hansson O, Li DQ, et al. Overexpression of alpha2A-adrenergic receptors contributes to type 2 diabetes. Science. 2010; 327(5962):217–20. Epub 2009/12/08. doi: science.1176827 [pii] doi: 10.1126/science.1176827 PMID: 19965390.

161. Vollert S, Kaessner N, Heuser A, Hanauer G, Dieckmann A, Knaack D, et al. The glucose-lowering effects of the PDE4 inhibitors roflumilast and roflumilast-N-oxide in db/db mice. Diabetologia. 2012; 55(10):2779–88. Epub 2012/07/14. doi: 10.1007/s00125-012-2632-z PMID: 22790061.

162. Jain R, Lammert E. Cell-cell interactions in the endocrine pancreas. Diabetes Obes Metab. 2009; 11 Suppl 4:159–67. Epub 2009/10/13. doi: DOM1102 [pii] doi: 10.1111/j.1463-1326.2009.01102.x PMID: 19817798.

163. Gromada J, Frokjaer-Jensen J, Dissing S. Glucose stimulates voltage- and calcium-dependent inositol trisphosphate production and intracellular calcium mobilization in insulin-secreting beta TC3 cells. Biochem J. 1996; 314 (Pt 1):339–45. Epub 1996/02/15. PMID: 8660305; PubMed Central PMCID: PMC1217047.

164. Sunil V, Verma MK, Oommen AM, Sadasivuni M, Singh J, Vijayraghav DN, et al. CNX-011-67, a novel GPR40 agonist, enhances glucose responsiveness, insulin secretion and islet insulin content in n-STZ rats and in islets from type 2 diabetic patients. BMC Pharmacol Toxicol. 2014; 15:19. Epub 2014/03/29. doi: 2050-6511-15-19 [pii] doi: 10.1186/2050-6511-15-19 PMID: 24666736; PubMed Central PMCID: PMC3994293.

165. Nagasumi K, Esaki R, Iwachidow K, Yasuhara Y, Ogi K, Tanaka H, et al. Overexpression of GPR40 in pancreatic beta-cells augments glucose-stimulated insulin secretion and improves glucose tolerance in normal and diabetic mice. Diabetes. 2009; 58(5):1067–76. Epub 2009/04/30. doi: 58/5/1067 [pii] doi: 10.2337/db08-1233 PMID: 19401434; PubMed Central PMCID: PMC2671040.

166. Nakashima R, Yano T, Ogawa J, Tanaka N, Toda N, Yoshida M, et al. Potentiation of insulin secretion and improvement of glucose intolerance by combining a novel G protein-coupled receptor 40 agonist DS-1558 with glucagon-like peptide-1 receptor agonists. Eur J Pharmacol. 2014; 737:194–201. Epub 2014/05/27. doi: S0014-2999(14)00376-8 [pii] doi: 10.1016/j.ejphar.2014.05.014 PMID: 24858371.

167. Itoh Y, Kawamata Y, Harada M, Kobayashi M, Fujii R, Fukusumi S, et al. Free fatty acids regulate insulin secretion from pancreatic beta cells through GPR40. Nature. 2003; 422(6928):173–6. Epub 2003/03/12. doi: 10.1038/nature01478 nature01478 [pii]. PMID: 12629551.

168. Schnell S, Schaefer M, Schofl C. Free fatty acids increase cytosolic free calcium and stimulate insulin secretion from beta-cells through activation of GPR40. Mol Cell Endocrinol. 2007; 263(1–2):173–80. Epub 2006/11/15. doi: S0303-7207(06)00475-8 [pii] doi: 10.1016/j.mce.2006.09.013 PMID: 17101212.

169. Zhou YJ, Song YL, Zhou H, Li Y. Linoleic acid activates GPR40/FFA1 and phospholipase C to increase [Ca2+]i release and insulin secretion in islet beta-cells. Chin Med Sci J. 2012; 27(1):18–23. Epub 2012/06/28. PMID: 22734209.

170. Fujiwara K, Maekawa F, Yada T. Oleic acid interacts with GPR40 to induce Ca2+ signaling in rat islet beta-cells: mediation by PLC and L-type Ca2+ channel and link to insulin release. Am J Physiol Endocrinol Metab. 2005; 289(4):E670–7. Epub 2005/05/26. doi: 00035.2005 [pii] doi: 10.1152/ajpendo.00035.2005 PMID: 15914509.

171. Burant CF, Viswanathan P, Marcinak J, Cao C, Vakilynejad M, Xie B, et al. TAK-875 versus placebo or glimepiride in type 2 diabetes mellitus: a phase 2, randomised, double-blind, placebo-controlled trial. Lancet. 2012; 379(9824):1403–11. Epub 2012/03/01. doi: S0140-6736(11)61879-5 [pii] doi: 10.1016/S0140-6736(11)61879-5 PMID: 22374408.

172. Hashimoto T MH, Morioka T, Tsuriya D, Morita H., Oki Y. Sulfonylurea (SU) and GLP-1-cAMP related agent. Diabetes. 2014.

173. Defossa E, Wagner M. Recent developments in the discovery of FFA1 receptor agonists as novel oral treatment for type 2 diabetes mellitus. Bioorg Med Chem Lett. 2014; 24(14):2991–3000. Epub 2014/06/03. doi: S0960-894X(14)00506-X [pii] doi: 10.1016/j.bmcl.2014.05.019 PMID: 24881568.

174. Thore S, Dyachok O, Gylfe E, Tengholm A. Feedback activation of phospholipase C via intracellular mobilization and store-operated influx of Ca2+ in insulin-secreting beta-cells. J Cell Sci. 2005; 118(Pt 19):4463–71. Epub 2005/09/15. doi: jcs.02577 [pii] doi: 10.1242/jcs.02577 PMID: 16159958.

175. Mears D, Zimliki CL, Atwater I, Rojas E, Glassman M, Leighton X, et al. The Anx7(+/-) knockout mutation alters electrical and secretory responses to Ca(2+)-mobilizing agents in pancreatic beta-cells. Cell Physiol Biochem. 2012; 29(5–6):697–704. Epub 2012/05/23. doi: 000186926 [pii] doi: 10.1159/000186926 PMID: 22613970.

176. Schofl C, Borger J, Lange S, von zur Muhlen A, Brabant G. Energetic requirement of carbachol-induced Ca2+ signaling in single mouse beta-cells. Endocrinology. 2000; 141(11):4065–71. Epub 2000/11/23. doi: 10.1210/endo.141.11.7741 PMID: 11089537.

177. Doliba NM, Qin W, Vatamaniuk MZ, Li C, Zelent D, Najafi H, et al. Restitution of defective glucose-stimulated insulin release of sulfonylurea type 1 receptor knockout mice by acetylcholine. Am J Physiol Endocrinol Metab. 2004; 286(5):E834–43. Epub 2004/01/23. doi: 10.1152/ajpendo.00292.2003 00292.2003 [pii]. PMID: 14736703.

178. Henquin JC, Garcia MC, Bozem M, Hermans MP, Nenquin M. Muscarinic control of pancreatic B cell function involves sodium-dependent depolarization and calcium influx. Endocrinology. 1988; 122(5):2134–42. Epub 1988/05/01. doi: 10.1210/endo-122-5-2134 PMID: 3282876.

179. Yada T, Hamakawa N, Yaekura K. Two distinct modes of Ca2+ signalling by ACh in rat pancreatic beta-cells: concentration, glucose dependence and Ca2+ origin. J Physiol. 1995; 488 (Pt 1):13–24. Epub 1995/10/01. PMID: 8568649; PubMed Central PMCID: PMC1156697.

180. Seino Y, Miki T, Fujimoto W, Lee EY, Takahashi Y, Minami K, et al. Cephalic phase insulin secretion is KATP channel-independent. J Endocrinol. 2013. Epub 2013/04/24. doi: JOE-12-0579 [pii] doi: 10.1530/JOE-12-0579 PMID: 23608222.

181. Gautam D, Han SJ, Hamdan FF, Jeon J, Li B, Li JH, et al. A critical role for beta cell M3 muscarinic acetylcholine receptors in regulating insulin release and blood glucose homeostasis in vivo. Cell Metab. 2006; 3(6):449–61. Epub 2006/06/07. doi: S1550-4131(06)00128-8 [pii] doi: 10.1016/j.cmet.2006.04.009 PMID: 16753580.

182. Kruse AC, Li J, Hu J, Kobilka BK, Wess J. Novel Insights into M Muscarinic Acetylcholine Receptor Physiology and Structure. J Mol Neurosci. 2013. Epub 2013/09/27. doi: 10.1007/s12031-013-0127-0 PMID: 24068573.

183. Thore S, Wuttke A, Tengholm A. Rapid turnover of phosphatidylinositol-4,5-bisphosphate in insulin-secreting cells mediated by Ca2+ and the ATP-to-ADP ratio. Diabetes. 2007; 56(3):818–26. Epub 2007/03/01. doi: 56/3/818 [pii] doi: 10.2337/db06-0843 PMID: 17327453.

184. Lin CW, Yan F, Shimamura S, Barg S, Shyng SL. Membrane phosphoinositides control insulin secretion through their effects on ATP-sensitive K+ channel activity. Diabetes. 2005; 54(10):2852–8. Epub 2005/09/28. doi: 54/10/2852 [pii]. PMID: 16186385; PubMed Central PMCID: PMC1350465.

185. Suzuki Y, Zhang H, Saito N, Kojima I, Urano T, Mogami H. Glucagon-like peptide 1 activates protein kinase C through Ca2+-dependent activation of phospholipase C in insulin-secreting cells. J Biol Chem. 2006; 281(39):28499–507. Epub 2006/07/28. doi: M604291200 [pii] doi: 10.1074/jbc.M604291200 PMID: 16870611.

186. Guettier JM, Gautam D, Scarselli M, Ruiz de Azua I, Li JH, Rosemond E, et al. A chemical-genetic approach to study G protein regulation of beta cell function in vivo. Proc Natl Acad Sci U S A. 2009; 106(45):19197–202. Epub 2009/10/28. doi: 0906593106 [pii] doi: 10.1073/pnas.0906593106 PMID: 19858481; PubMed Central PMCID: PMC2767362.

187. Jain S, Ruiz de Azua I, Lu H, White MF, Guettier JM, Wess J. Chronic activation of a designer G(q)-coupled receptor improves beta cell function. J Clin Invest. 2013; 123(4):1750–62. Epub 2013/03/13. doi: 66432 [pii] doi: 10.1172/JCI66432 PMID: 23478411; PubMed Central PMCID: PMC3613926.

188. Tian Y, Laychock SG. Protein kinase C and calcium regulation of adenylyl cyclase in isolated rat pancreatic islets. Diabetes. 2001; 50(11):2505–13. Epub 2001/10/27. PMID: 11679428.

189. Dolz M, Bailbe D, Giroix MH, Calderari S, Gangnerau MN, Serradas P, et al. Restitution of defective glucose-stimulated insulin secretion in diabetic GK rat by acetylcholine uncovers paradoxical stimulatory effect of beta-cell muscarinic receptor activation on cAMP production. Diabetes. 2005; 54 (11):3229–37. Epub 2005/10/27. doi: 54/11/3229 [pii]. PMID: 16249449.

190. Miguel JC, Abdel-Wahab YH, Green BD, Mathias PC, Flatt PR. Cooperative enhancement of insulinotropic action of GLP-1 by acetylcholine uncovers paradoxical inhibitory effect of beta cell muscarinic receptor activation on adenylate cyclase activity. Biochem Pharmacol. 2003; 65(2):283–92. Epub 2002/12/31. doi: S000629520201482X [pii]. PMID: 12504804.

191. Fehmann HC, Goke R, Goke B, Arnold R. Carbachol priming increases glucose- and glucagon-like peptide-1 (7–36)amide-, but not arginine-induced insulin secretion from the isolated perfused rat pancreas. Z Gastroenterol. 1990; 28(7):348–52. Epub 1990/07/01. PMID: 2238765.

192. Pedersen MG, Cortese G, Eliasson L. Mathematical modeling and statistical analysis of calcium-regulated insulin granule exocytosis in beta-cells from mice and humans. Prog Biophys Mol Biol. 2011; 107(2):257–64. Epub 2011/08/16. doi: S0079-6107(11)00083-6 [pii] doi: 10.1016/j.pbiomolbio.2011.07.012 PMID: 21839108.

193. Selway J, Rigatti R, Storey N, Lu J, Willars GB, Herbert TP. Evidence that Ca2+ within the microdomain of the L-type voltage gated Ca2+ channel activates ERK in MIN6 cells in response to glucagon-like peptide-1. PLoS One. 2012; 7(3):e33004. Epub 2012/03/14. doi: 10.1371/journal.pone.0033004 PONE-D-11-04940 [pii]. PMID: 22412973; PubMed Central PMCID: PMC3296766.

194. Dean PM. Ultrastructural morphometry of the pancreatic -cell. Diabetologia. 1973; 9(2):115–9. Epub 1973/04/01. PMID: 4577291.

195. Felix-Martinez GJ, Azpiroz-Leehan J, Avila-Poroz R, Godinez-Fernandez JR. Effect of Impared ATP Production and Glucose Sensitivity on Human beta-cell Function: A Simulation Study. Revista Mexicana de Ingenieria Biomedica. 2014; 35(2):1–13. Epub 2014.

196. Luik RM, Wang B, Prakriya M, Wu MM, Lewis RS. Oligomerization of STIM1 couples ER calcium depletion to CRAC channel activation. Nature. 2008; 454(7203):538–42. Epub 2008/07/04. doi: nature07065 [pii] doi: 10.1038/nature07065 PMID: 18596693; PubMed Central PMCID: PMC2712442.

197. Dessauer CW, Scully TT, Gilman AG. Interactions of forskolin and ATP with the cytosolic domains of mammalian adenylyl cyclase. J Biol Chem. 1997; 272(35):22272–7. Epub 1997/08/29. PMID: 9268376.

198. Smolen P, Baxter DA, Byrne JH. A model of the roles of essential kinases in the induction and expression of late long-term potentiation. Biophys J. 2006; 90(8):2760–75. Epub 2006/01/18. doi: S0006-3495(06)72458-4 [pii] doi: 10.1529/biophysj.105.072470 PMID: 16415049; PubMed Central PMCID: PMC1414565.

199. Tsalkova T, Blumenthal DK, Mei FC, White MA, Cheng X. Mechanism of Epac activation: structural and functional analyses of Epac2 hinge mutants with constitutive and reduced activities. J Biol Chem. 2009; 284(35):23644–51. Epub 2009/06/26. doi: M109.024950 [pii] doi: 10.1074/jbc.M109.024950 PMID: 19553663; PubMed Central PMCID: PMC2749139.

200. Falkenburger BH, Dickson EJ, Hille B. Quantitative properties and receptor reserve of the DAG and PKC branch of G(q)-coupled receptor signaling. J Gen Physiol. 2013; 141(5):537–55. Epub 2013/05/01. doi: jgp.201210887 [pii] doi: 10.1085/jgp.201210887 PMID: 23630338; PubMed Central PMCID: PMC3639584.

201. Falkenburger BH, Jensen JB, Hille B. Kinetics of PIP2 metabolism and KCNQ2/3 channel regulation studied with a voltage-sensitive phosphatase in living cells. J Gen Physiol. 2010; 135(2):99–114. Epub 2010/01/27. doi: jgp.200910345 [pii] doi: 10.1085/jgp.200910345 PMID: 20100891; PubMed Central PMCID: PMC2812502.

202. Heitzler D, Durand G, Gallay N, Rizk A, Ahn S, Kim J, et al. Competing G protein-coupled receptor kinases balance G protein and beta-arrestin signaling. Mol Syst Biol. 2012; 8:590. Epub 2012/06/28. doi: msb201222 [pii] doi: 10.1038/msb.2012.22 PMID: 22735336; PubMed Central PMCID: PMC3397412.

203. Bertram R, Sherman A. A calcium-based phantom bursting model for pancreatic islets. Bull Math Biol. 2004; 66(5):1313–44. Epub 2004/08/06. doi: 10.1016/j.bulm.2003.12.005 S0092824004000096 [pii]. PMID: 15294427.

204. Latour MG, Alquier T, Oseid E, Tremblay C, Jetton TL, Luo J, et al. GPR40 is necessary but not sufficient for fatty acid stimulation of insulin secretion in vivo. Diabetes. 2007; 56(4):1087–94. Epub 2007/03/31. doi: 56/4/1087 [pii] doi: 10.2337/db06-1532 PMID: 17395749; PubMed Central PMCID: PMC1853382.

205. Light PE, Manning Fox JE, Riedel MJ, Wheeler MB. Glucagon-like peptide-1 inhibits pancreatic ATP-sensitive potassium channels via a protein kinase A- and ADP-dependent mechanism. Mol Endocrinol. 2002; 16(9):2135–44. Epub 2002/08/29. PMID: 12198249.

206. Beguin P, Nagashima K, Nishimura M, Gonoi T, Seino S. PKA-mediated phosphorylation of the human K(ATP) channel: separate roles of Kir6.2 and SUR1 subunit phosphorylation. Embo J. 1999; 18(17):4722–32. Epub 1999/09/02. doi: 10.1093/emboj/18.17.4722 PMID: 10469651; PubMed Central PMCID: PMC1171545.

207. Tamarina NA, Kuznetsov A, Fridlyand LE, Philipson LH. Delayed-rectifier (KV2.1) regulation of pancreatic beta-cell calcium responses to glucose: inhibitor specificity and modeling. Am J Physiol Endocrinol Metab. 2005; 289(4):E578–85. Epub 2005/07/15. doi: 00054.2005 [pii] doi: 10.1152/ajpendo.00054.2005 PMID: 16014354.

208. Dai XQ, Manning Fox JE, Chikvashvili D, Casimir M, Plummer G, Hajmrle C, et al. The voltage-dependent potassium channel subunit Kv2.1 regulates insulin secretion from rodent and human islets independently of its electrical function. Diabetologia. 2012; 55(6):1709–20. Epub 2012/03/14. doi: 10.1007/s00125-012-2512-6 PMID: 22411134.

209. Lemon G, Gibson WG, Bennett MR. Metabotropic receptor activation, desensitization and sequestration-I: modelling calcium and inositol 1,4,5-trisphosphate dynamics following receptor activation. J Theor Biol. 2003; 223(1):93–111. Epub 2003/06/05. doi: S0022519303000791 [pii]. PMID: 12782119.

210. Kim M, Huang T, Abel T, Blackwell KT. Temporal sensitivity of protein kinase a activation in late-phase long term potentiation. PLoS Comput Biol. 2010; 6(2):e1000691. Epub 2010/03/03. doi: 10.1371/journal.pcbi.1000691 PMID: 20195498; PubMed Central PMCID: PMC2829045.

211. Woolf PJ, Kenakin TP, Linderman JJ. Uncovering biases in high throughput screens of G-protein coupled receptors. J Theor Biol. 2001; 208(4):403–18. Epub 2001/02/27. doi: 10.1006/jtbi.2000.2227 S0022-5193(00)92227-6 [pii]. PMID: 11222046.

212. Bokoch GM, Bickford K, Bohl BP. Subcellular localization and quantitation of the major neutrophil pertussis toxin substrate, Gn. J Cell Biol. 1988; 106(6):1927–36. Epub 1988/06/01. PMID: 3133377; PubMed Central PMCID: PMC2115155.

213. Wagner J, Keizer J. Effects of rapid buffers on Ca2+ diffusion and Ca2+ oscillations. Biophys J. 1994; 67(1):447–56. Epub 1994/07/01. doi: S0006-3495(94)80500-4 [pii] doi: 10.1016/S0006-3495(94)80500-4 PMID: 7919018; PubMed Central PMCID: PMC1225377.

214. Vilardaga JP. Theme and variations on kinetics of GPCR activation/deactivation. J Recept Signal Transduct Res. 2010; 30(5):304–12. Epub 2010/09/15. doi: 10.3109/10799893.2010.509728 PMID: 20836728; PubMed Central PMCID: PMC3380358.

215. Shea LD, Neubig RR, Linderman JJ. Timing is everything the role of kinetics in G protein activation. Life Sci. 2000; 68(6):647–58. Epub 2001/02/24. doi: S0024320500009772 [pii]. PMID: 11205879.

216. Falkenburger BH, Jensen JB, Hille B. Kinetics of M1 muscarinic receptor and G protein signaling to phospholipase C in living cells. J Gen Physiol. 2010; 135(2):81–97. Epub 2010/01/27. doi: jgp.200910344 [pii] doi: 10.1085/jgp.200910344 PMID: 20100890; PubMed Central PMCID: PMC2812500.

217. Saucerman JJ, Brunton LL, Michailova AP, McCulloch AD. Modeling beta-adrenergic control of cardiac myocyte contractility in silico. J Biol Chem. 2003; 278(48):47997–8003. Epub 2003/09/16. doi: 10.1074/jbc.M308362200 M308362200 [pii]. PMID: 12972422.

218. Brinkerhoff CJ, Traynor JR, Linderman JJ. Collision coupling, crosstalk, and compartmentalization in G-protein coupled receptor systems: can a single model explain disparate results? J Theor Biol. 2008; 255(3):278–86. Epub 2008/09/02. doi: S0022-5193(08)00413-X [pii] doi: 10.1016/j.jtbi.2008.08.003 PMID: 18761019; PubMed Central PMCID: PMC2917770.

219. Widmann C, Burki E, Dolci W, Thorens B. Signal transduction by the cloned glucagon-like peptide-1 receptor: comparison with signaling by the endogenous receptors of beta cell lines. Mol Pharmacol. 1994; 45(5):1029–35. Epub 1994/05/01. PMID: 8190093.

220. Li N, Lu J, Willars GB. Allosteric modulation of the activity of the glucagon-like peptide-1 (GLP-1) metabolite GLP-1 9–36 amide at the GLP-1 receptor. PLoS One. 2012; 7(10):e47936. Epub 2012/10/25. doi: 10.1371/journal.pone.0047936 PONE-D-12-23191 [pii]. PMID: 23094100; PubMed Central PMCID: PMC3477139.

221. Whitaker GM, Lynn FC, McIntosh CH, Accili EA. Regulation of GIP and GLP1 receptor cell surface expression by N-glycosylation and receptor heteromerization. PLoS One. 2012; 7(3):e32675. Epub 2012/03/14. doi: 10.1371/journal.pone.0032675 PONE-D-11-23159 [pii]. PMID: 22412906; PubMed Central PMCID: PMC3296735.

222. Hinke SA, Gelling RW, Pederson RA, Manhart S, Nian C, Demuth HU, et al. Dipeptidyl peptidase IV-resistant [D-Ala(2)]glucose-dependent insulinotropic polypeptide (GIP) improves glucose tolerance in normal and obese diabetic rats. Diabetes. 2002; 51(3):652–61. Epub 2002/03/02. PMID: 11872663.

223. Morgan NG, Montague W. Studies on the mechanism of inhibition of glucose-stimulated insulin secretion by noradrenaline in rat islets of Langerhans. Biochem J. 1985; 226(2):571–6. Epub 1985/03/01. PMID: 2986600; PubMed Central PMCID: PMC1144746.

224. Hoffmann C, Nuber S, Zabel U, Ziegler N, Winkler C, Hein P, et al. Comparison of the activation kinetics of the M3 acetylcholine receptor and a constitutively active mutant receptor in living cells. Mol Pharmacol. 2012; 82(2):236–45. Epub 2012/05/09. doi: mol.112.077578 [pii] doi: 10.1124/mol.112.077578 PMID: 22564786.

225. Ziegler N, Batz J, Zabel U, Lohse MJ, Hoffmann C. FRET-based sensors for the human M1-, M3-, and M5-acetylcholine receptors. Bioorg Med Chem. 2011; 19(3):1048–54. Epub 2010/08/19. doi: S0968-0896(10)00713-3 [pii] doi: 10.1016/j.bmc.2010.07.060 PMID: 20716489.

226. Jovic A, Wade SM, Neubig RR, Linderman JJ, Takayama S. Microfluidic interrogation and mathematical modeling of multi-regime calcium signaling dynamics. Integr Biol (Camb). 2013; 5(7):932–9. Epub 2013/06/05. doi: 10.1039/c3ib40032h PMID: 23732791; PubMed Central PMCID: PMC3704220.

227. Tsuga H, Okuno E, Kameyama K, Haga T. Sequestration of human muscarinic acetylcholine receptor hm1-hm5 subtypes: effect of G protein-coupled receptor kinases GRK2, GRK4, GRK5 and GRK6. J Pharmacol Exp Ther. 1998; 284(3):1218–26. Epub 1998/03/13. PMID: 9495886.

228. Alousi AA, Jasper JR, Insel PA, Motulsky HJ. Stoichiometry of receptor-Gs-adenylate cyclase interactions. FASEB J. 1991; 5(9):2300–3. Epub 1991/06/01. PMID: 1650314.

229. Litvin TN, Kamenetsky M, Zarifyan A, Buck J, Levin LR. Kinetic properties of "soluble" adenylyl cyclase. Synergism between calcium and bicarbonate. J Biol Chem. 2003; 278(18):15922–6. Epub 2003/03/01. doi: 10.1074/jbc.M212475200 M212475200 [pii]. PMID: 12609998.

230. Ekanger R, Sand TE, Ogreid D, Christoffersen T, Doskeland SO. The separate estimation of cAMP intracellularly bound to the regulatory subunits of protein kinase I and II in glucagon-stimulated rat hepatocytes. J Biol Chem. 1985; 260(6):3393–401. Epub 1985/03/25. PMID: 2982859.

231. Hille B, Dickson E, Kruse M, Falkenburger B. Dynamic metabolic control of an ion channel. Prog Mol Biol Transl Sci. 2014; 123:219–47. Epub 2014/02/25. doi: B978-0-12-397897-4.00008–5 [pii] doi: 10.1016/B978-0-12-397897-4.00008–5 PMID: 24560147.